

博士論文

Driving behavior analysis at basic segment bottleneck
on expressways

(高速道路単路部ボトルネックとする
追従挙動の分析)

楊 燕

Yang Yan

Abstract

This research presents a simulation study of probabilistic congestion occurrence at expressway basic segment bottlenecks well known as sag section in Japan with individual variations in car-following behavior obtained from an actual sag section. A sag section is a road segment on an expressway in which the vertical slope increases at a small but constant rate. It is impossible to predict congestion from detector data because the only observable flow condition changes happen right at the time congestion occurs. The propagation of unnoticed deceleration due to the vertical slope increase has long been researched as the cause of congestion. Perturbation amplifies in dense vehicle platoon consisted with drivers of varying car-following behavior. In this research, a car-following behavior model considering both the intra-driver variations and inter-driver variations is utilized and calibrated with field observation data. The variations are described with parameter distribution of car-following model. A simulation to reproduce traffic condition with the estimated parameters is thus proposed and validated in order to predict the probability of congestion occurrence at basic segment bottlenecks as well as test possible countermeasures to prevent and alleviate bottleneck congestion.

Two datasets containing all together 875 trajectories during congestion formation at the tomei yamato sag section are used in car-following behavior modeling. One is a dataset of 393 trajectory data observed in 4 days including position, speed and acceleration recorded every 1/30s along a 1.2 km sag section with 11 fixed road side cameras is analyzed for individual variations in car-following behavior. The other is a dataset of 482 trajectories observed for around 1km at the same sag section with different starting point. Trajectories of independent vehicles which do not react to the driving behavior of preceding vehicle and vehicles already involved in congestion are excluded from analysis. A car-following model considering both the intra-driver variations and inter-driver variations is utilized. The car-following model is consisted of speed difference and spacing difference to its desired spacing with a time lag as well as an unnoticed deceleration caused by the vertical grade change at sag section. After thorough examination of parameter estimation approaches from observed data, the combined use of regression analysis for the desired speed, correlation analysis for the boundaries of reaction time and heuristic search algorithm cross-entropy method for other parameters, is found to have the best performance. Apart from the objective function of relative spacing error, performance indicators of the root mean square error of spacing, speed and acceleration are also examined to ensure the performance of estimated parameter values. The relationships between different parameters are studied and no cross correlations excepted for the two parameters to determine desired speed are found.

A simulation platform which describes individual trajectory reflecting the variations in the

distributed parameter values is proposed. The platform is designed to reproduce the probabilistic nature of traffic congestion occurrence at a bottleneck of sag section including the effect of vertical slope increase. It was carefully validated with different initial settings to make sure its capability of accurately reproducing the real condition. It provides a platform for analyze how different key components of the driving behavior, leading car behavior affecting the probability of congestion occurrence as well as a tool to quantify the effect of countermeasure like Adaptive Cruise Control (ACC) system. An interactive user interface was made to visualize the congestion formation progress. It reproduces congestion occurrence by changing the order of vehicles within the same platoon, which will help us to analyze the parameters of vehicles tending to cause congestion. It enables us to study the range of car-following parameters that causes propagation and amplification of speed reduction. Three kinds of drivers are observed in simulation: aggressive, negligent and nimble drivers. Collision and sudden stop occurs in 5-min platoon of aggressive drivers. Congestion occurs in 5-min platoon of negligent drivers, while no congestion occurs in 5-min platoon of nimble drivers at sag section. The simulation successfully reproduces the tendency that the congestion occurrence probability grows with traffic demand. The congestion occurrence probability is obtained through simulation with estimated parameters. A higher traffic demand will cause higher probability of congestion occurrence at sag section, which is the same in reality. With this platform, the effect of introducing ACC system was also studied. Apart from the ACC penetration rate, two different ACC introduction schemes of 1) Random introduction and 2) Intentional introduction by replacing vehicles with certain features, e.g. aggressive, negligent and nimble drivers, is simulated and compared.

Contents

Contents	4
1 Introduction.....	10
1.1 Background and key issues.....	10
1.2 Research aim and scope	13
1.3 Structure of this research.....	14
2 Literature review	16
2.1 Research approaches on congestion and bottleneck capacity at sag sections	16
2.2 Car-following behavior modeling	18
2.3 Parameter estimation methods	23
2.4 Simulating of driver's behavior.....	24
2.5 Prevent congestion with driving assistant system	25
3 Field observation	28
3.1 Data.....	28
3.2 Methodology.....	30
3.3 Assumptions and analysis boundaries.....	32
3.4 3.4 Analysis Framework.....	33
4 Driving behavior parameter estimation	34
4.1 Estimate desired spacing	34
4.2 Estimate reaction time.....	39
4.3 Cross-Entropy method	43
4.4 Estimation results	49
4.5 Performance analysis of car-following parameters estimation	55
4.6 Independent vehicle behavior	59
4.7 Parameter distribution.....	60
5 Simulation.....	79
5.1 Simulation modeling structure	79
5.2 Basic settings and input scenarios	80
5.3 Leading car behavior	83
5.4 Congestion occurrence probability	110
5.5 Car-following parameters distribution	116
5.6 Simulation findings.....	117
6 Discussion.....	119
6.1 Car-following behavior of ACC system.....	119
6.2 ACC system introduction to prevent congestion occurrence at sag section	124
7 Conclusion and future work.....	130
Acknowledgement	133
References.....	134

List of Figures

Figure 1.1.1 Driver's reaction to vertical grade effect	11
Figure 1.1.2 Countermeasures to prevent congestion occurrence.....	12
Figure 1.3.1 structure of this research	15
Figure 2.2.1 Calibration result of car-following models in Shibuya's research.....	22
Figure 2.5.1 Congestion duration observed on Japanese expressway bottleneck.....	25
Figure 2.5.2 Countermeasures to prevent congestion occurrence.....	26
Figure 3.1.1 Vertical layout of observation location of dataset1	29
Figure 3.1.2 Observation location of dataset 2.....	30
Figure 3.4.1 Estimation approach.....	34
Figure 4.1.1 Desired spacing estimation with all vehicle trajectories	36
Figure 4.1.2 Desired spacing estimation with individual trajectory (several stable states)	37
Figure 4.1.3 Desired spacing estimation with individual trajectory (single stable state).....	38
Figure 4.1.4 Estimated result of desired spacing	39
Figure 4.2.1 Correlation analysis area of Δt	40
Figure 4.2.2 Analysis range for reaction time	41
Figure 4.2.3 Reaction time range with correlation analysis.....	42
Figure 4.3.1 Cross-entropy method for searching best combination of parameters.....	47
Figure 4.3.2 The fitted behavior of vehicle with car-following model.....	48
Figure 4.3.3 The trajectory with car-following model	49
Figure 4.4.1 The extraction of study area	50
Figure 4.4.2 The desired spacing function estimated with linear regression	51
Figure 4.4.3 Correlaiton of acceleration with relative speed and spacing difference within reaction time range	51
Figure 4.4.4 Behavior of vehicle estimated with car-following model	52
Figure 4.4.5 Trajectory of vehicle estimated with car-following model.....	53
Figure 4.4.6 The components in estimaed car-following model.....	54
Figure 4.4.7 The speed spacing relationship of observed data and estimation.....	55
Figure 4.5.1 Objective function and PI1 of dataset 1	56
Figure 4.5.2 PI2 and PI3 of dataset 1	57
Figure 4.5.3 Objective function and PI1 of dataset 2.....	58
Figure 4.5.4 PI2 and PI3 of dataset 2	58
Figure 4.6.1 Independent vehicle observed constantly decreases after entering sag section	59
Figure 4.6.2 Independent vehicle observed maintain the speed after realizing the sag effect...	60
Figure 4.7.1 Relationship between δ and τ	62
Figure 4.7.2 Cumulative frequency of δ	63
Figure 4.7.3 Estimated distribution of δ	64
Figure 4.7.4 Cumulative frequency of τ	65
Figure 4.7.5 Estimated distribution of τ	66
Figure 4.7.6 Joint cumulative frequency of δ and τ	67
Figure 4.7.7 1 st part of the joint distribution of δ and τ	67

Figure 4.7.8 Distribution estimation of the 1 st part of the joint distribution of δ and τ	68
Figure 4.7.9 2 nd part of the joint distribution of δ and τ	69
Figure 4.7.10 Cumulative frequency of δ and τ of 2 nd part of joint distribution.....	69
Figure 4.7.11 Estimated joint distribution of δ and τ of 2 nd part of joint distribution.....	70
Figure 4.7.12 Relationship between α_1 and Δt	70
Figure 4.7.13 Cumulative frequency of α_1	71
Figure 4.7.14 Distribution of α_1	72
Figure 4.7.15 Cumulative frequency of α_2	73
Figure 4.7.16 Distribution of α_2	74
Figure 4.7.17 Cumulative frequency of β	75
Figure 4.7.18 Distribution of β	76
Figure 4.7.19 Cumulative frequency of Δt	77
Figure 4.7.20 Distribution of Δt	78
Figure 5.2.1 Vertical layout of road segment in simulation	80
Figure 5.2.2 Feedback circle of simulation.....	81
Figure 5.2.3 Calculation of car-following behavior entering simulation.....	83
Figure 5.3.1 Trajectory of car No.28 with leading car behavior type 1	85
Figure 5.3.2 Time-speed diagram of car No.28 with leading car behavior type 1	86
Figure 5.3.3 Space-speed diagram of car No.28 with leading car behavior type 1	87
Figure 5.3.4 Trajectory of car No.28 with leading car behavior type 2	88
Figure 5.3.5 Time-speed diagram of car No.28 with leading car behavior type 2	89
Figure 5.3.6 Space-speed diagram of car No.28 with leading car behavior type 2.....	90
Figure 5.3.7 Trajectory of car No.28 with leading car behavior type 3	91
Figure 5.3.8 Time-speed diagram of car No.28 with leading car behavior type 3	92
Figure 5.3.9 Space-speed diagram of car No.28 with leading car behavior type 3.....	93
Figure 5.3.10 Example of negligent drivers.....	94
Figure 5.3.11 Number of aggressive cases, negligent cases and nimble cases under different leading car behavior.....	95
Figure 5.3.12 Joint cumulative frequency of δ and τ of aggressive drivers	96
Figure 5.3.13 Joint cumulative frequency of δ and τ of negligent drivers.....	97
Figure 5.3.14 Joint cumulative frequency of δ and τ of nimble drivers	98
Figure 5.3.15 Cumulative frequency of α_1 of aggressive drivers	99
Figure 5.3.16 Cumulative frequency of α_1 of negligent drivers	100
Figure 5.3.17 Cumulative frequency of α_1 of nimble drivers.....	101
Figure 5.3.18 Cumulative frequency of α_2 of aggressive drivers	102
Figure 5.3.19 Cumulative frequency of α_2 of negligent drivers	103
Figure 5.3.20 Cumulative frequency of α_2 of nimble drivers.....	104
Figure 5.3.21 Cumulative frequency of β of aggressive drivers.....	105
Figure 5.3.22 Cumulative frequency of β of negligent drivers.....	106
Figure 5.3.23 Cumulative frequency of β of nimble drivers	107
Figure 5.3.24 Cumulative frequency of Δt of aggressive drivers	108
Figure 5.3.25 Cumulative frequency of Δt of negligent drivers	109

Figure 5.3.26 Cumulative frequency of Δt of nimble drivers.....	110
Figure 5.4.1 choose car position based on randomly entering headway.....	111
Figure 5.4.2 Trajectories under traffic demand of 1,000 veh/h/lane	112
Figure 5.4.3 Trajectories under traffic demand of 2,200 veh/h/lane	113
Figure 5.4.4 Example of congestion free scenario with all the observed cars.....	114
Figure 5.4.5 Relationship of 5-min link flow rate and inner/outer lane flow rate (2 lanes in 1 link).....	115
Figure 5.4.6 Congestion occurrence observed on Japanese expressway bottleneck	115
Figure 5.4.7 Comparison of congestion occurrence with estimated car-following behavior and observation at another site	116
Figure 5.5.1 Congestion occurrence probability of estimated parameters values and distribution	117
Figure 6.1.1 Dynamic performance of ACC system	120
Figure 6.1.2 Dynamic performance of a human driver	121
Figure 6.1.3 Time space diagram of ACC platoon.....	122
Figure 6.1.4 Time speed diagram of ACC platoon	123
Figure 6.1.5 Space speed diagram of ACC platoon	124
Figure 6.2.1 Congestion occurrence probability with different ACC penetration rate (1).....	125
Figure 6.2.2 Congestion occurrence probability with different ACC penetration rate (2).....	126
Figure 6.2.3 Congestion occurrence probability of intentional introduction of ACC system (25%)	127
Figure 6.2.4 Congestion occurrence probability of intentional introduction of ACC system (50%)	127
Figure 6.2.5 Congestion occurrence probability of intentional introduction of ACC system (75%)	128
Figure 6.2.6 Congestion occurrence probability of intentional introduction of ACC system (100%)	128

List of Tables

Table 3.1.1 Detail of observation.....	28
Table 3.3.1 Summary of field observation data.....	33
Table 4.1.1 Number of estimation of desired spacing in dataset 1.....	38
Table 4.5.1 Summary of field observation data.....	58
Table 4.7.1 Descriptive statistics of car-following parameters.....	61
Table 4.7.2 Correlation of car-following model parameters	61

1 Introduction

1.1 Background and key issues

Traffic congestion is a big problem traffic managements face globally. It causes many monetary losses for drivers in developed countries. It is also a major source of air pollution.

Sag sections are the major basic segment bottlenecks on Japanese expressways. A sag section is a road segment on an expressway in which the vertical slope increases at a small but constant rate. Because the rate of slope increase is slight and constant, vehicle speeds are significantly reduced before drivers become aware of the change in slope. According to a research report by the Japanese National Institute for Land and Infrastructure Management, 60.5% of congestion incidents on Japanese expressways in 2011 occurred on uphill slope and sag sections and caused congestion amount of 105,649 km·h (National Institute for Land and Infrastructure Management).

Traffic managers find an urgent need to monitor and predict the occurrence of congestion, which requires systematic observation on the bottleneck phenomena at sag sections and analysis of its mechanism. The first systematic observation was made by Koshi et., al [越正毅, 1986]. Major features of traffic flow condition at sag section bottleneck were concluded. The bottleneck capacity would drop to around 2,200~2,700 veh/h/2lane, much lower than the theoretical capacity when the traffic demand reached to around 3,000 veh/h/2lane. Rapid speed reduction was observed at the start of bottleneck activation. On the other hand, as observed at many expressway bottlenecks, traffic capacity is a time-dependent feature and its definition remains not fully solved.(Banks, 1990) Congestion also occurs at a lower flow rate after a constant high flow passing the bottleneck. (Koshi, Kuwahara, & Akahane, 1992)(Patire & Cassidy, 2011) In other words, congestion occurs at same expressway bottlenecks under different flow rate.

It is therefore impossible to predict the exact bottleneck capacity of sag section as well as congestion occurrence from detector data consisting time-mean speed, volume, and occupancy, which is the major data source for road condition monitor. Researchers have focused on measures to infer the stages in congestion formation with real-time detector data since the recovery of probabilistic congestion occurrence. On the other hand, congestion formation is a dynamic process where the probability of congestion occurrence not only depends on traffic flow rate and speed but also on the change of flow composition such as the length of platoon. As Oguchi et, al.[大口敬、片倉正彦、鹿田成則, 2001] and Xing et.,al. (Xing, Tsuru, Ishida, & Muramatsu, 2010) pointed out, the length of platoon during congestion formation has a critical influence on congestion occurrence. 5-minute density, 3-minute density and 1 minute density were also proposed as a criterion for congestion occurrence based on the understanding of the dependency of congestion occurrence on

the size and density of platoon passing the sag section [大口敬、片倉正彦、鹿田成則, 2001]. But like the speed drop, platoon size is only collected by detector right at congestion occurrence, which makes prediction impossible.

After observing traffic flow condition at sag section for several years, researchers realize that the congestion is formed with an aggregation of individual car-following behavior. Xing and Koshi [Xing Jian、越正毅, 1996] studied the car-following behavior of drivers at the start of congestion with aerial image data. They modeled car-following behavior for every individual driver with trajectory data. They found that 75% of drivers in a platoon decelerate intensely while their spacing with the leading vehicle decreases slightly. This finding suggests certain kind of car-following behavior maybe a possible explanation for congestion occurrence at sag sections. It also suggests that variations in the behavior of drivers may be the main cause of the probabilistic occurrence of congestion and the lack of a certain observable bottleneck capacity.

A simple understanding of congestion formation because of car-following behavior at sag section is shown as in Fig. 1.1.1. Cars first decelerate because of the vertical grade. When drivers noted the speed drop, they try to restore the speed by acceleration. A series of small adjustment follow after the unnoticed deceleration and intended acceleration. Drivers naturally tend to keep a longer spacing with leading car in order to have enough spacing for speed adjustment. Bottleneck is activated after the accumulation of speed adjustment of following drivers in the platoon passing the sag section and causes congestion occurrence.

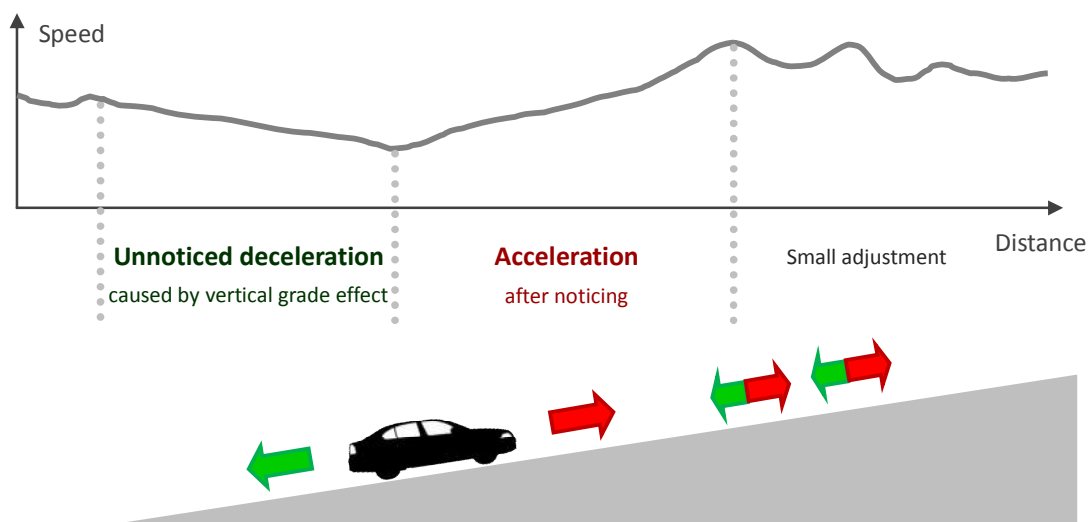


Figure 1.1.1 Driver's reaction to vertical grade effect

Behavior study tries to reveal the variations in individual car-following behavior at sag section. There are two kinds of variations in car-following behavior. One is intra-driver variations in car-following behavior. Intra-driver variations are the variations of car-following behavior of the same driver under different circumstances. For example, the car-following behavior of a same driver

at flat basic segment is different from that at sag section. The car-following behavior in free flow may also be different from the behavior in congested flow. The other is inter-driver variations in car-following behavior. Inter-driver variations are the difference of car-following behavior between different drivers. They not only reflect the variations of drivers' reaction to the driving condition change of leading vehicle, e.g. acceleration and deceleration, but also reflect the difference of drivers reaction to vertical slope change. Some drivers are not affected by the unnoticed deceleration caused by vertical slope change as much as other drivers. Both variations occur at sag section. Therefore, a car-following model to describe the behavior of drivers at sag section needs to describe both the intra-driver variations and the inter-driver variations.

Only after analyzing the variations of car-following behavior at sag section accurately, it is possible to simulate the car-following behavior of drivers in congestion formation in order to study the effect of both intra-driver and inter-driver variations to traffic flow condition.

As long as congestion occurs, it takes several hours to solve[越正毅, 1986][大口敬, 高速道路サグにおける渋滞の発生と道路線形との関係, 1995]. Therefore, prevention of congestion occurrence is the most essential task for traffic managers instead of alleviating congestion after occurrence. There are two things we want to do to prevent congestion occurrence right now. One is to control the input traffic demand when the probability of congestion occurrence is high. The other is to increase the bottleneck capacity by increase homogeneity in flow with advanced driving aid systems such as Adaptive Cruise Control (ACC) system (See Fig. 1.1.2).

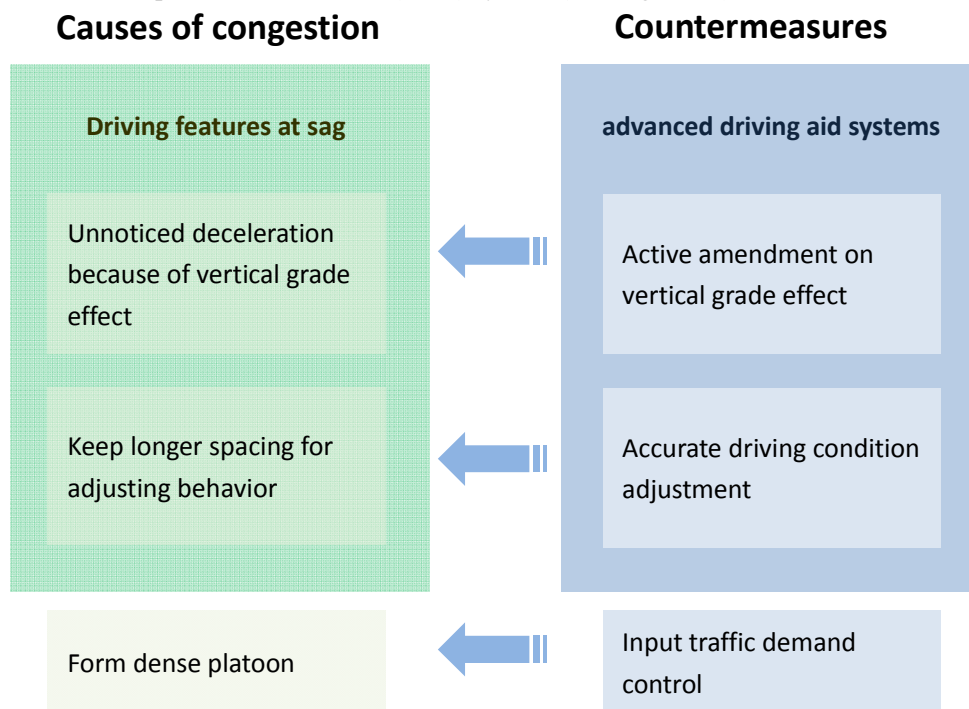


Figure 1.1.2 Countermeasures to prevent congestion occurrence

In order to achieve the first countermeasure, accurate prediction of congestion occurrence

probability with detector data is essential. While understanding the individual car-following behavior, comparing its difference to ACC system and measuring its reaction to ACC system is essential in order to achieve the latter countermeasure.

Previous studies have been made with small amount of observation [Xing Jian、越正毅, 1996] as well as experiment data (Oguchi & Konuma, 2009). They proposed several car-following behavior models for driving behavior at sag section. Their findings include drivers adapt to vertical slope change gradually at sag section(Oguchi & Konuma, 2009) [大口敬, 高速道路単路部渋滞発生解析-追従挙動モデルの整理と今後の展望, 2000] and they tend to decelerate intensely while their spacing with the leading vehicle only decreases slightly[Xing Jian、越正毅, 1996].

Detailed analysis on the cause of congestion occurrence was not made because of lack of observation data. The congestion at sag section always forms in a short time involving less than 100 vehicles and remains for a long time because of severe capacity drop. The observable congestion formation cases are very limited. Due to this, the research on quantifying the effect of individual behavior variations on bottleneck phenomena occurrence is insufficient.

1.2 Research aim and scope

This research focuses on analyze congestion formation mechanism at sag section with microscopic view of variations in individual car-following behavior. This study aims to provide a methodology to predict congestion occurrence probability with detector data. The prediction is based on simulation of individual car-following model. It not only contributes to the understanding of congestion formation mechanism at sag section but also serve as a criterion of traffic management in order to prevent congestion occurrence.

A total amount of 875 trajectories were observed during congestion formation at Yamato sag on Tomei Expressway in Japan. A car-following model considering the vertical slope effect is used. Parameters are obtained for every trajectory by regression, correlation analysis and cross-entropy method. Car-following behavior variations are thus studied with distribution of car-following parameters. A simulation platform is designed to reproduce the probabilistic nature of traffic congestion occurrence at a bottleneck of sag section including the effect of vertical slope increase. It is possible to quantify the probability of congestion occurrence by study the proportion of congested and uncongested cases under same 5 min traffic demand in the simulation. Countermeasures to prevent congestion occurrence such as input traffic flow control and advanced driving aid system are proposed based on these knowledge. Especially the effect of introducing ACC system is studied with simulation. Apart from the ACC penetration rate, two different ACC introduction schemes of 1) Random introduction and 2) Intentional introduction by replacing vehicles with certain features, e.g.

long desired spacing, is simulated and compared.

The main contribution of this research is:

1. Estimate individual car-following behavior variants modeled from voluminous field observation data at sag sections during congestion formation with regression, correlation analysis and Cross-Entropy method.
2. Present an estimation framework for car-following parameters from observation data which ensures the accuracy and comprehension of estimation.
3. Present a simulation system to reproduce congestion formation.
4. Quantify the influence in terms of the congestion occurrence probability under certain traffic demand with simulation.
5. Present a feedback circle of calibrating simulation result with variations in car-following parameters and congestion occurrence information.
6. Quantify the influence of penetration rate and different introduction schemes of ACC system on congestion occurrence at sag sections.

1.3 Structure of this research

This thesis is consisted with following parts:

In this chapter, the problem of traffic congestion at basic segment bottleneck on Japanese expressways is introduced. The objectives of this research are presented.

Previous researches concerning both traffic condition analysis and car-following behavior modeling at bottlenecks are reviewed in chapter 2.

In chapter 3, the observation data for car-following behavior modeling is presented. The assumption of analyses, boundary condition and the methods to choose the analysis range are explained. The analysis methodology and flow of work are also presented.

Car-following behavior modeling with actual data and calibration are presented in chapter 4. The car-following model parameter which represents the variations of car-following behavior at sag section during congestion formation is estimated.

The simulation of car-following parameters is presented in chapter 5, including the validation and reproduction of congestion occurrence.

Chapter 6 is consisted with a discussion and insights obtained from results. Further direction of measurements to assess congestion severity and countermeasures to alleviate congestion are also discussed.

The conclusions and future works are presented in Chapter 7.

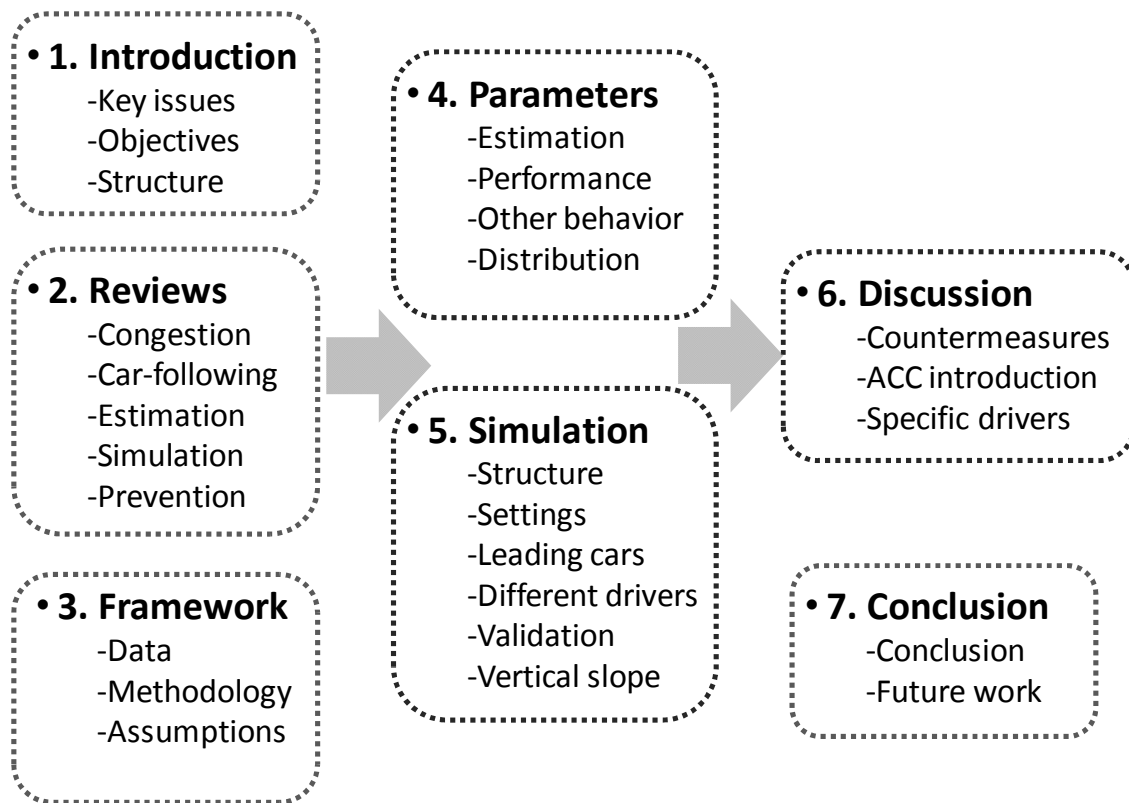


Figure 1.3.1 structure of this research

2 Literature review

Previous researches on the bottleneck phenomena at sag section as well as modeling driving behavior are reviewed in this chapter. 2.1 presents the research approaches on congestion and bottleneck capacity at sag section. The studies on modeling the driving behavior are reviewed in 2.2. In 2.3, the methods of driving behavior parameter estimation are reviewed. The simulation approaches of driving behavior and its components are presented in 2.4. Researches on using ACC system to prevent congestion are reviewed in 2.5.

2.1 Research approaches on congestion and bottleneck capacity at sag sections

The bottleneck phenomena at sag sections were first observed by Japanese road managers and researchers at 1980s. The traffic managers find an urgent need to monitor and predict the occurrence of congestion, which requires systematic observation on the bottleneck phenomena at sag sections and analysis of its mechanism. The first systematic observation was made by Koshi et., al(Koshi, Kuwahara, & Akahane, 1992). Major features of traffic flow condition in sag section bottleneck were concluded. The bottleneck capacity would drop to around 2,200~2,700 veh/h/2lane, much lower than the theoretical capacity when the traffic demand reached to around 3,000 veh/h/2lane. Rapid speed reduction was observed at the start of bottleneck activation. A further observation revealed that congestion occurs probabilistically under the same traffic demand at the same sag location.[越正毅、桑原雅夫、赤羽弘和, 1993] It is therefore impossible to predict the exact bottleneck capacity of sag section as well as congestion occurrence from detector data consists with time-mean speed, volume, and occupancy, which is the main data source for road condition monitor. Researches focus on measures to infer the stages in congestion formation with real-time detector data since the recovery of probabilistic congestion occurrence. On the other hand, congestion formation is a dynamic process where the probability of congestion occurrence is not only dependent on traffic flow rate and speed but also on the change of flow composition such as the length of platoon. Oguchi et., al [大口敬、片倉正彦、鹿田成則, 2001] studied the flow condition in congestion formation at basic segment bottlenecks. They defined the platoon as headway between adjacent vehicles smaller than 3s seconds. They also defined congestion as the speed of two adjacent vehicle smaller than 40km/h. By studying the flow condition at 1000m before congestion site, they found when the headway inside platoon was around 1.5s and the platoon size was big, congestion would easily occur. They proposed a determination of congestion using the 5-minute density difference based on these findings. As the probabilistic congestion occurrence at sag section was well observed, Xing et.,al(Xing, Tsuru, Ishida, & Muramatsu, 2010)[福島賢一、Xing Jian、瀬戸

稔和、佐藤久長, 2008] tried to estimate the probability of congestion occurrence by analyzing platoon size from detector data. They found the shockwave would occur when platoon flow rate was greater than 2,400 veh/h and it would further propagate when the flow rate afterward was greater than 30 veh/min or 80 veh/3min.

As Oguchi et, al.[大口敬、片倉正彦、鹿田成則, 2001] and Xing et.,al.(Xing, Tsuru, Ishida, & Muramatsu, 2010) pointed out, the length of platoon during congestion formation has a critical influence on congestion occurrence. 5-minute density, 3-minute density and 1 minute density were also proposed as a criterion for congestion occurrence based on the understanding of the dependency of congestion occurrence on the size and density of platoon passing the sag section. But like the speed drop, congestion occurs right after platoon size is collected by detector.

There are Macroscopic and microscopic aspects in observing and analyzing the phenomena. The macroscopic aspect deals with the overall flow condition, such as the flow rate, capacity, density. The microscopic aspect focuses on the aggregation of behavior characteristics of individual drivers as the cause of the phenomena. After observing traffic flow condition at sag section for several years, researchers realize that the most reliable way is through an aggregation of individual car-following behavior. Xing and Koshi [Xing Jian、越正毅, 1996] studied the car-following behavior of drivers at the start of congestion with aerial image data. They modeled car-following behavior for every individual driver with trajectory data. They found that 75% of drivers in a platoon decelerate intensely while their spacing with the leading vehicle decreases slightly. This finding suggests car-following behavior as a possible explanation for congestion occurrence at sag sections. It also suggests that variations in the behavior of drivers may be the main cause of the probabilistic occurrence of congestion and the lack of a certain observable bottleneck capacity. A further observation by Ozaki[尾崎晴男, 2003] also found that while the car right behind decelerating leading car reduces its spacing in deceleration, the latter cars in the platoon tend to have less reduction if not maintain the spacing in deceleration. This also cause capacity reduction at sag section.

A simple understanding of congestion occurrence or increasing heterogeneity at sag section is shown as in figure 1.1. Cars first decelerate because of the vertical grade. When drivers noted the speed drop, they try to restore the speed by acceleration. A series of small adjustment follow after the unnoticed deceleration and intended acceleration. Drivers naturally tend to keep a longer spacing with leading car in order to have enough spacing for speed adjustment. Bottleneck is activated after the accumulation of speed adjustment of drivers following drivers in the platoon passing the sag section and causes congestion occurrence.

Xing and Koshi [Xing Jian、越正毅, 1996] studied the car-following behavior of drivers at the start of congestion with aerial image data. They modeled car-following behavior for every individual

driver with trajectory data. They found that 75% of drivers in a platoon decelerate intensely while their spacing with the leading vehicle decreases slightly. This finding suggests car-following behavior as a possible explanation for congestion occurrence at sag sections. It also suggests that variations in the behavior of drivers may be the main cause of the probabilistic occurrence of congestion and the lack of a certain observable bottleneck capacity.

2.2 Car-following behavior modeling

Behavior study tries to reveal the driving behavior difference at sag section. There are two kinds of variations in car-following behavior. One is intra-driver variations in car-following behavior. Intra-driver variations are the difference of car-following behavior of the same driver. For example, the car-following behavior of a same driver at flat basic segment is different from the behavior at sag section. The car-following behavior in free flow might be different from the behavior in congested flow. The other is inter-driver variations in car-following behavior. Inter-driver variations are the difference of car-following behavior between different drivers. They not only reflect the difference of drivers reaction to the driving condition change of leading vehicle, e.g. acceleration and deceleration, but also reflect the difference of drivers reaction to vertical slope change. Some drivers are not affected by the unnoticed deceleration caused by vertical slope change as much as other drivers. A car-following model to describe the behavior of drivers at sag section needs to describe both the intra-driver variations and the inter-driver variations.

Only after analyzing the variations of car-following behavior at sag section accurately, it is possible to simulate the car-following behavior of drivers in congestion formation in order to study the effect of both intra-driver and inter-driver variations to traffic flow condition.

As long as congestion occurs, it takes several hours to solve [越正毅, 1986][大口敬, 高速道路サグにおける渋滞の発生と道路線形との関係, 1995]. Therefore, prevention of congestion occurrence is the most essential task for traffic managers instead of alleviating congestion after occurrence. There are two things we want to do to prevent congestion occurrence right now. One is to control the input traffic demand when the probability of congestion occurrence is high. The other is to increase the bottleneck capacity by increase homogeneity in flow with advanced driving aid systems such as Adaptive Cruise Control (ACC) system (See Fig. 1.1.2).

Car-following models are divided into continuous and discrete based on the characteristics of variables. In continuous model, all the variables are continuous. In discrete model, all the variables are discrete and divided into fixed length such as cellular automata. The interaction of vehicles or users is treated as instantaneous process. There exist many types of mathematical structure in these two model forms. 2 specific model structures for car-following model is studied in this review.

Coupled ordinary differential equations is a mathematical class where the continuous state variables of position, speed and acceleration of vehicle depend only on time t . The state variable position are coupled with the state variables of leading vehicle. A basic car-following model has this kind of structure. The relationship between position, speed and acceleration proposed by Pipes(Gipps, 1981) is:

$$a_i(t) = v_i'(t) = x_i''(t) \quad 1$$

where the acceleration of a vehicle at time t is the derivative of its speed while its speed is the derivative of its position. This is the most simple form of car-following model.

The other car-following model structure is the coupled iterated maps structure in which a discrete time step Δt was introduced. The set of state variables at time t are a function of these variables at $t-\Delta t$. The reaction time of drivers to a stimulus has long been observed on expressways. It has also been observed in car-following behavior. Therefore many car-following models are of this structure. A classic model proposed by Chandler, Herman and Montroll (Chandler, Herman, & Montroll, 1958) is an example:

$$a_1(t + \Delta t) = \alpha_1(v_0(t) - v_1(t)) \quad 2$$

where the acceleration of a following vehicle at a reaction time lag Δt after time t is a linear function of its speed difference with leading vehicle at time t .

The GM (General Motors) model proposed by Gazis, Herman and Rothery (Gazis, Herman, & Rothery, 1961) is a general model which consider the acceleration at $t+\Delta t$ as a function of the speed difference as well as spacing and the speed of following vehicle at time t . There are several researches working on estimating the variables especially m and l in this model(Brackstone & McDonald, Car-following: a historical review, 1999).

$$a_1(t + \Delta t) = \alpha_1 \frac{\{v_1(t)\}^m}{\{x_0(t) - x_1(t)\}^l} (v_0(t) - v_1(t)) \quad 3$$

There are also more complicated models considering the optimal velocity of following vehicle (Bando, Hasebe, Nakanishi, Nakayama, Shibata, & Sugiyama, 1995), the acceleration of leading vehicle (Kometani & Sasaki, 1961), the highest possible speed under the spacing (Gipps, 1981) and the tradeoff between achieving desired speed and maintaining desired minimum gap (Kesting, Treiber, & Helbing, Enhanced intelligent driver model to access the impact of driving strategies on traffic capacity, 2010).

There are two models especially designed to reflect the car-following behavior at basic segment bottlenecks.

Koshi, Kuwahara, and Akahane [越正毅、桑原雅夫、赤羽弘和, 1993] proposed a car-following model consisted with two phases for driving behavior during congestion formation at sag section. In free flow, the car-following model is:

$$v'(t) = \delta_1 \frac{\varepsilon S'(t-T_3)}{S(t-T_3)^n} + \delta_2 \frac{\zeta \{S(t-T_4) - g[v(t-T_4)]\}}{S(t-T_4)^p} - \eta \sin \theta + \lambda [V_D - v(t-T_5)] \quad 4$$

In congested flow, the model is:

$$v'(t) = \frac{\alpha S'(t-T_1)}{S(t-T_1)^n} + \frac{\beta \{S(t-T_2) - f[v(t-T_2)]\}}{S(t-T_2)^m} - \gamma \sin \theta \quad 5$$

where

v = Speed of the follower;

t = Time;

S = Spacing between the follower and the leading vehicle,

T_1, T_2, T_3, T_4 = Time lags;

θ = Gradient difference at a sag;

V_D = Desired speed of the follower;

f = Desired spacing as a function of speed;

g = Normal following spacing as a function of speed;

$\delta_1 = 0$ when $v(t-T_3) \geq V_D$ and $S(t-T_3) \geq 0$

= 1 otherwise;

$\delta_2 = 0$ when $v(t-T_4) \geq V_D$ and $S(t-T_4) \geq g[v(t-T_4)]$

= 1 otherwise ;

$\alpha, \beta, \gamma, l, m, \varepsilon, \zeta, \eta, \lambda, n, p$ = constants.

In this model, vehicles try to maintain desired speed and normal following spacing while decelerating because of the vertical slope in free flow condition. In congested flow, vehicles follow the leading vehicle with a desired spacing while decelerating because of the vertical slope. The reaction time for speed, desired speed and following spacing are independent parameters while the effect of vertical slope is constant.

Xing and Koshi [Xing Jian、越正毅, 1996] built a simulation with the Koshi model and parameters obtained from 39 trajectories during congestion formation. The estimated parameters showed good simulation accuracy compare to the initial trajectory. But further knowledge was not obtained because of the limitation of observation data.

Helly designed a model to describe drivers' behavior particularly in studying the cause of traffic bottlenecks (Helly, 1959). The model was a reaction time-lagged system where the acceleration of vehicle is a linear function of its speed difference and spacing difference from its desired spacing .

The function is:

$$a_1(t + \Delta t) = \alpha_1(v_0(t) - v_1(t)) + \alpha_2(x_0(t) - x_1(t) - s_1^*)$$

$$s_1^* = \alpha x_1(t) + \beta v_1(t) + \gamma a_1(t) \quad 6$$

where

Δt = Driver's reaction time;

$a_i(t)$ = Acceleration of following vehicle;

$v_i(t)$ = Speed; $i = 0$ for leading vehicle; $i = 1$ for following vehicle;

$x_i(t)$ = Position; $i = 0$ for leading vehicle; $i = 1$ for following vehicle;

s_i^* = Desired spacing between leading and following vehicle;

α, β, γ = constants.

Helly's model was especially studied and utilized in behavior modeling in this research because it was exactly designed to describe the driving behavior close to congestion formation where vehicles following their preceding vehicles closely without attempting to over pass where localized small variations in driver intent or vehicle capability would cause bottlenecks. It was proved to reproduce the traffic condition of bottleneck consisted with isolated platoons where the average bottleneck time headway within the platoon was independent of the vehicles' position.

The initial model treated drivers' error of sense by adding suitably distributed random numbers with mean zero. The driving behavior

Oguchi, Konuma (Oguchi & Konuma, 2009) and Shibuya, Oguchi [渋谷公佑、大口敬、洪性俊, 2013] used the Helly's model among other classic car-following models to analyze the car-following behavior at sag sections in Japan with experiment data. Helly's model showed good fitness in these researches.

表 4.2: $OF_{headway}$ の最小値が小さい上位 3 つの追従挙動モデル

実験 1					実験 2				
車両	車間	1 位	2 位	3 位	車両	車間	1 位	2 位	3 位
A	L	Model 9	Model 12	Model 10	A	L	NoData	NoData	NoData
A	M	N/A	N/A	N/A	A	M	NoData	NoData	NoData
A	S	Model 9	Model 7	Model 6	A	S	NoData	NoData	NoData
B	L	Model 9	Model 12	Model 10	B	L	Model 9	Model 7	Model 6
B	M	Model 9	Model 11	Model 12	B	M	Model 6	Model 9	Model 7
B	S	Model 9	Model 7	Model 12	B	S	Model 7	Model 9	Model 6
C	L	Model 12	Model 10	Model 11	C	L	Model 7	Model 9	Model 6
C	M	Model 12	Model 9	Model 7	C	M	Model 9	Model 7	Model 6
C	S	Model 12	Model 11	Model 9	C	S	Model 7	Model 9	Model 12
D	L	Model 9	Model 12	Model 10	D	L	Model 6	Model 3	Model 1
D	M	Model 9	Model 12	Model 10	D	M	Model 6	Model 3	Model 7
D	S	Model 12	Model 7	Model 9	D	S	Model 6	Model 3	Model 1
E	L	Model 9	Model 12	Model 10	E	L	Model 6	Model 7	Model 1
E	M	Model 9	Model 12	Model 10	E	M	Model 9	Model 3	Model 7
E	S	Model 9	Model 7	Model 8	E	S	Model 9	Model 3	Model 6
F	L	Model 12	Model 10	Model 11	F	L	Model 9	Model 7	Model 6
F	M	Model 9	Model 12	Model 10	F	M	Model 9	Model 3	Model 7
F	S	Model 7	Model 12	Model 9	F	S	Model 7	Model 9	Model 6
G	L	Model 12	Model 9	Model 11	G	L	Model 7	Model 3	Model 4
G	M	Model 9	Model 12	Model 7	G	M	Model 7	Model 9	Model 6
G	S	Model 9	Model 7	Model 6	G	S	Model 6	Model 4	Model 3
H	L	Model 9	Model 2	Model 4	H	L	Model 9	Model 6	Model 3
H	M	Model 6	Model 7	Model 3	H	M	Model 9	Model 6	Model 3
H	S	Model 7	Model 9	Model 6	H	S	Model 9	Model 7	Model 3
					I	L	Model 9	Model 7	Model 3
					I	M	Model 9	Model 7	Model 3
					I	S	Model 9	Model 7	Model 3
					J	L	Model 9	Model 7	Model 6
					J	M	Model 9	Model 7	Model 3
					J	S	NoData	NoData	NoData

Figure 2.2.1 Calibration result of car-following models in Shibuya's research

From the results of Shibuya's research, model 9 and model 7 performed best in car-following parameter estimation. Model 7 stands for Helly's model and model 9 stands for IDM (Intelligent Driver Model)(Kesting, Treiber, & Helbing, Enhanced intelligent driver model to access the impact

of driving strategies on traffic capacity, 2010). Despite being a simple linear model, Helly's model out performed some much more complicated and sophisticated car-following models.

Yoshizawa et.al.(Yoshizawa, Shiomi, Uno, Iida, & Yamaguchi, 2012) modeled car-following behavior at sag section with Helly's model with driving simulation experiments of 37 participants.. The parameters were then utilized to estimate the behavior difference of same driver at different vertical gradient sections. The parameters of driver showed significant difference at different vertical gradient sections.

2.3 Parameter estimation methods

An objective function is an equation to be optimized in optimization. It is divided into loss function which should be minimized so that the loss in optimization is minimal and utility function which should be maximized so that the optimization generates maximum profit or reward. In car-following behavior modeling, an objective function indicates how modeled car-following behavior can reflect the actual behavior. Errors in spacing were widely used as objective function of car-following behavior because the spacing is the most dynamically stable and unbiased variable (Ossen & Hoogendoorn, 2005)(Treiber & Kesting, 2012). Oguchi, Konuma (Oguchi & Konuma, 2009) used root mean square error of spacing objective function in car-following behavior modeling with driving simulator experiment of 33 participants. This method is good for estimating car-following behavior with experiment data because the number of participants is quite limited that the variations between participants do not affect the performance of objective function.

One problem of using root mean square error is that the length of original spacing may generate some biases for the estimation. Kesting et., al. (Kesting & Treiber, Calibrating Car-Following Models using Trajectory Data: Methodological Study, 2008) pointed out that when the original spacing is long, the root mean squared error tends to be longer than those with short original spacing. This makes it difficult to set up a global standard for objective function. Ossen and Hoogendoorn (Ossen & Hoogendoorn, 2005)(Hoogendoorn S. , 2008) (Hoogendoorn & Ossen, 2006)verified and calibrated car-following model estimation with both clean data and real trajectory data. The influence of structure objective, objective function, choice of model and errors in data were studied for Gipps car-following model. It was found that when a random noise was added to clean data, some parameters were the same with different objective functions such as Mean Absolute Error, Mean squared error, Mean Relative Absolute Error, Mean Root Square Error, while others were better estimated in some cases when relative performance measures were used.

Cross-Entropy method is an optimization method to find the optimal solution of combinatorial and

continuous nonconvex problems. It is based on Kullback-Leiber cross-entropy, importance sampling, Markov chain and Boltzmann distribution. The core concept in this method is to adaptively adjust the occurrence of the events more likely in the vicinity of a global extremum by using important sampling. A unimodal importance sampling distribution is used as an estimate of the optimal solution for continuous optimization. Markov chains were used for combinatorial optimization. It was proved and well accepted to be an efficient global random search procedure.

2.4 Simulating of driver's behavior

Traffic simulation is a methodology to reproduce traffic conditions by building computational models. Simulations are widely used in traffic and transportation system analysis, especially for its dynamic evolution. Microscopic simulation is a kind of traffic simulation that simulates the traffic condition on single road section with detailed driving behavior data containing acceleration data calculated for every time step. It can reproduce the real-time microscopic traffic phenomena such as stop-and-go waves and other observed instabilities of traffic flow on a road section.

Drivers' dynamic behavior need to be well modeled and carefully calibrated in order to carry out a microscopic simulation. Treiber and Kesting (Treiber & Kesting, 2012) concluded the calibration process and simulation of car-following model, especially for car-following behavior at expressway bottlenecks. They also pointed out that instabilities of traffic flow resulting in stop-and-go waves are caused by the delays in adapting the speed to the actual traffic conditions. If traffic density in the platoon is sufficiently high, this delay leads to an increase on density and speed perturbations along the platoon. The intuitive reason behind these instabilities is that in order to adapt to the deceleration wave considering the time delays, every following vehicle try to keep safety spacing with leading vehicle by decelerate harder. If the platoon is consisted with mostly stable drivers, the instability may not happen. In this case, the cars have already adapted their speed to the new situation at the time where a new car comes within interaction distance, so the stop-and-go mechanism is not effective. So if there is no the time delay in the car-following models, they cannot reproduce stop-and-go mechanism. Accidents such as collision and sudden stop in simulation if the instability threshold is extremely exceeded. However, in some models representing "short-sighted" drivers, accidents may happen even for parameters corresponding to perfectly stable traffic.

Perturbation propagation in traffic flow is also an important composition of congestion mechanism analysis. There are two kinds of perturbation propagation especially of interest in traffic flow research. One is local instability which only relates to the car-following dynamics of a single vehicle following a leader with a predetermined trajectory (typically introducing a perturbation by a temporary speed drop while driving at constant speed for the rest of the time). If the gap and speed

fluctuations of the follower do not decay with time, the system is unstable.

The other kind is platoon stability which describes the propagation of perturbation in a platoon. This stability concept is only applicable for microscopic models. It is also relevant when developing the feedback controllers of ACC systems.

Traffic flow is platoon stable if local perturbations decay everywhere even in arbitrarily long vehicle platoons. Platoon stability is a much more restrictive concept compared to local stability: Traffic flow may be platoon unstable even if speed fluctuations within a platoon of finite size decay quickly, or even if there are no local oscillations at all. This has immediate practical implications for developers of ACC controllers: Even if the ACC is optimized to be perfectly free of oscillations when following a leading vehicle with a prescribed speed profile, traffic flow consisting of such ACC vehicles may be absolutely platoon unstable. In the presence of local instabilities or platoon instabilities, even following a single vehicle leads to sustained oscillations.

2.5 Prevent congestion with driving assistant system

Congestion continues for a long time after occurrence. In a previous research, congestion was observed to continue for more than 4 hours, as shown in Figure 2.5.1 [大口敬, 高速道路サグにおける渋滞の発生と道路線形との関係, 1995]. Therefore, prevention of congestion occurrence is the most essential task for traffic managers instead of alleviating congestion after occurrence.

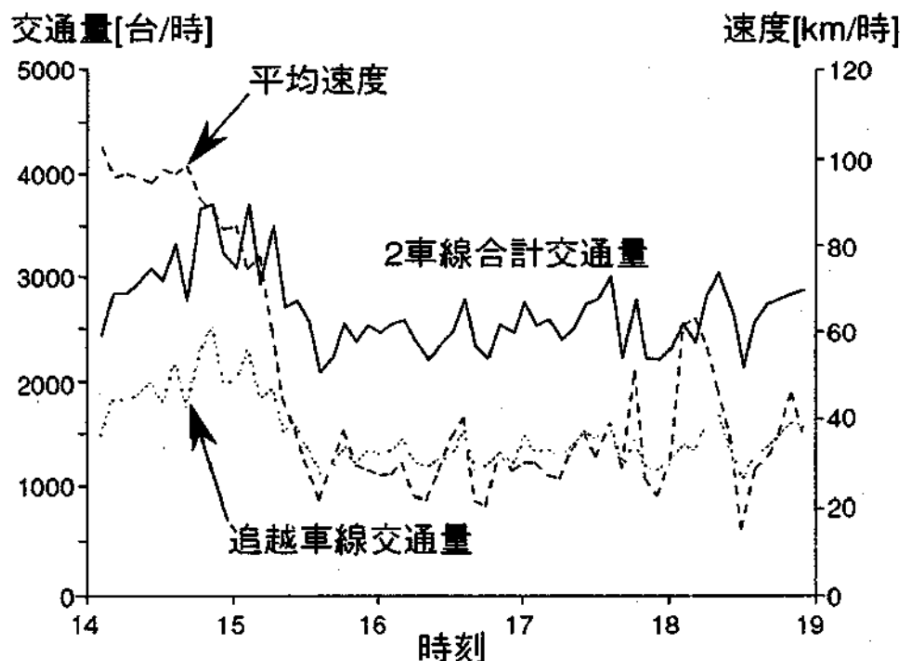


Figure 2.5.1 Congestion duration observed on Japanese expressway bottleneck

There are two things we want to do to prevent congestion occurrence right now. One is to control the

input traffic demand when the probability of congestion occurrence is high. The other is to increase the bottleneck capacity by increase homogeneity in flow with advanced driving aid systems such as Adaptive Cruise Control (ACC) system (See Fig. 2.5.2).

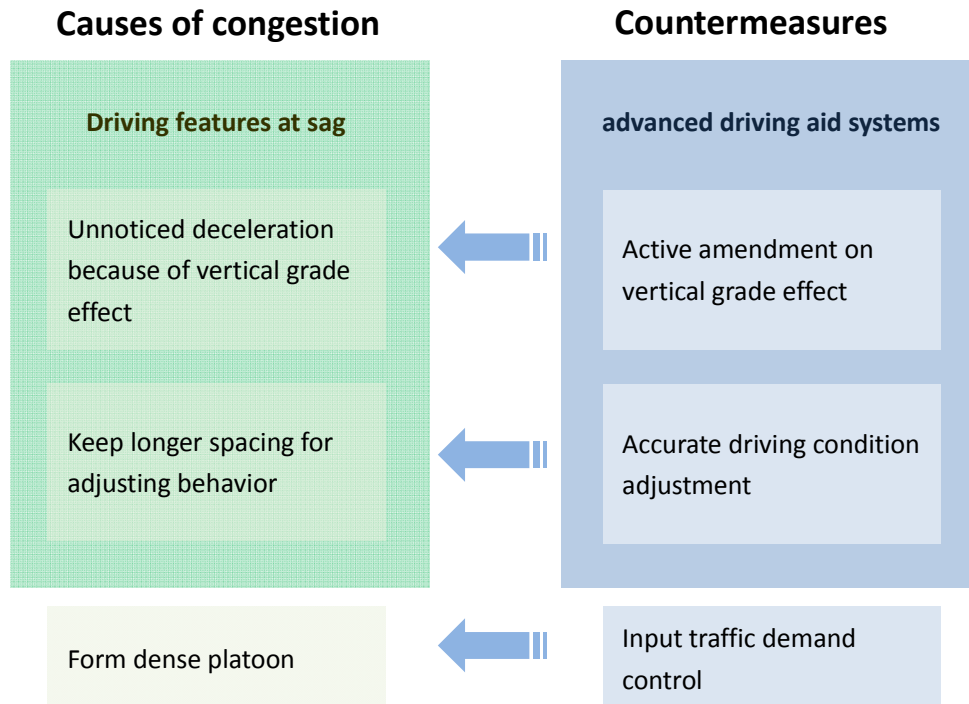


Figure 2.5.2 Countermeasures to prevent congestion occurrence

In order to achieve the first one, accurate prediction of congestion occurrence probability with detector data is essential. While understanding the individual car-following behavior, comparing it difference to ACC system and measuring the reaction to ACC system is essential in order to achieve the latter countermeasure.

Adaptive Cruise Control (ACC) system can detect the exact driving condition of current vehicle as well as the spacing with leading vehicle. It is able to maintain a specified spacing or time headway with leading vehicle based on the accurate detection. It is well established that ACC systems can reduce accidents caused by human errors (Vahidi & Eskandarian, 2003). It has also been suggested that traffic efficiency can be improved with advanced ACC systems because of its ability to measure actual distances and speed differences and thus maintain a selected time gap and desired speed in a stable manner[Goñi Ros, Knoop, van Arem, Hoogendoorn, 2012]. Unlike human drivers, whose performance varies from one to another, the performance of ACC is always consistent and stable. Therefore, it is possible for ACC vehicles to reduce traffic congestion and prevent breakdown by reducing variations in follow-the-leader behavior in traffic flow. Kesting, Treiber, Schonhof, and Helbing proposed that traffic breakdown could be completely prevented if 30% of the vehicles in the traffic stream had ACC (Kesting, Treiber, Schönhof, & Helbing, 2008). Yoshida, Koshi, and Yasui suggested that it is possible to use ACC systems to prevent congestion at sag sections because ACC

systems can maintain closer spacings between vehicles than most human drivers can at speeds below 50 km/h (Yoshida, Koshi, & Yasui, 1997). Several researchers have proposed their own ACC algorithms rather than use a currently available commercial system because of the restrictions posed by trade secrets and the rapid development of technological innovations in this area.

3 Field observation

This research consists of two parts. One is car-following behavior modeling with field survey data. The other is simulation with individual car-following behavior parameters. The detail of field observation is introduced in this chapter.

3.1 Data

The Tomei Expressway connects Tokyo and Nagoya, which are the two major metropolitan areas in Japan. Connecting with Meishin Expressway, it is on the most important artery with the heaviest traffic volume in Japan.

Two datasets were obtained for the study of variations in car-following behavior at sag sections. Dataset 1 and dataset 2.

Table 3.1.1 Detail of observation

Observation date	Time period	Congestion duration	Number of cars observed
Dataset 1			
Jul.15, 2006	4:30–7:30	6:15–18:50	104
Jul.22, 2006	4:30–7:30	6:45–11:10	92
Jul.29, 2006	4:30–7:30	5:55–13:40	78
Aug.4, 2006	6:00–9:00	7:25–12:55	119
Total			393
Dataset 2			
Nov. 2010~ Aug. 2011	-	-	482

Dataset 1 is a trajectory dataset obtained by Muto and Akahane (Muto & Akahane) from a 1.2-km section of roadway, including a sag section, on the Tomei Expressway during congestion formation. The observation were carried on at the outer lane on a two lane basic segment. Details of the dataset are given in Table 3.1.1. With recognition of videos taken from 11 recording points along the observation area, the trajectory, speed, acceleration, space headway, and speed difference were obtained for all vehicles within the observation area, as illustrated in Fig. 3.1.1, every 1/30s.

The trajectories were processed through several fixed-site videos along the observation area using video recognition technology. Position, speed, and acceleration data were obtained from the trajectories and were properly smoothed for analysis. The observation was carried out during the formation of congestion. The total of 393 trajectories were observed.

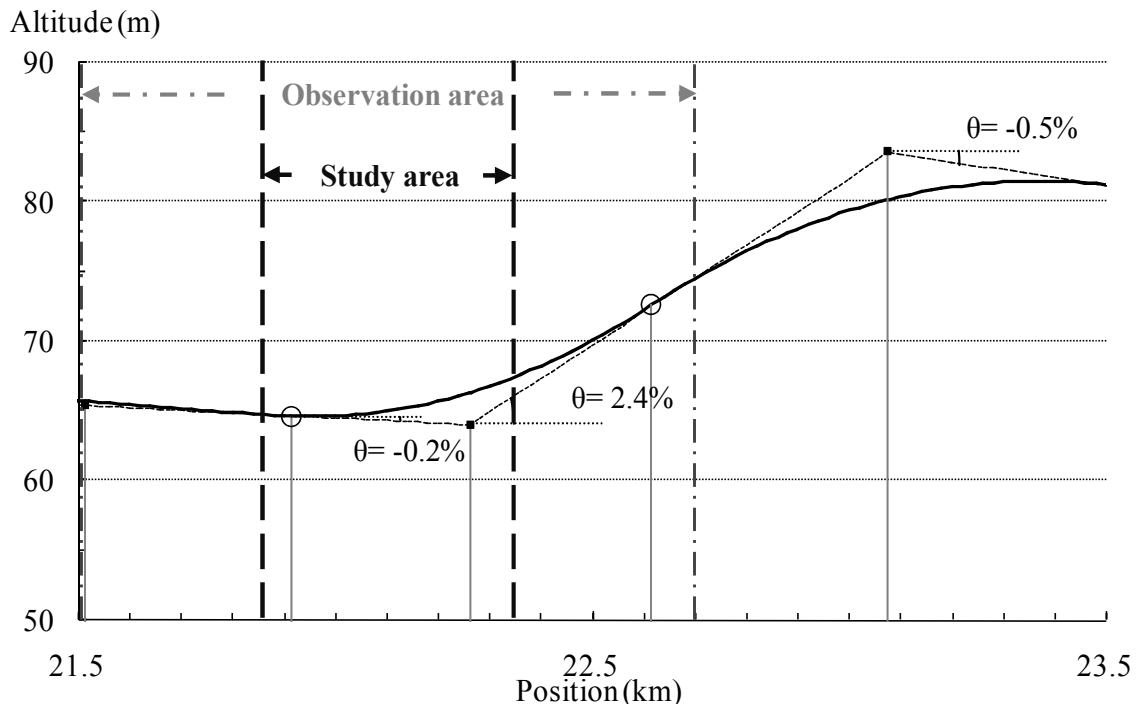


Figure 3.1.1 Vertical layout of observation location of dataset1

System errors occur in the video recognition, capture, and data smoothing processes. In addition, human driving behavior exhibits randomness. This is especially noticeable when there is no specific stimulus to drivers to change their driving status. Therefore, the study area was extracted from every vehicle trajectory to focus on in car-following behavior modeling and the specific study interest of reaction time.

A study area for follow-the-leader behavior modeling was further extracted from the overall trajectory to focus on car-following behavior at a sag section as well as minimizing the errors that occurred in the video recognition, capture, and data smoothing processes. The study area in the dataset is 500~650m area from 21.85 km to 22.35~22.5 km. The starting point is chosen to avoid errors occurring in video recognition and smoothing process. The end point is chosen to avoid lane-changing and other behaviors that may affect the analysis.

Dataset 2 is a calibration dataset of 482 trajectories during congestion formation at the same location obtained by NILIM. The observation was carried out on weekends during Nov. 2010 to Aug. 2011. The data consisted of distance for every 0.1s and speed and acceleration for every 1s. The speed was filled with linear interpolation for every 0.1s. The average study area length is 1 km. Number of observed cases at the observation location is shown in Fig. 3.1.2.

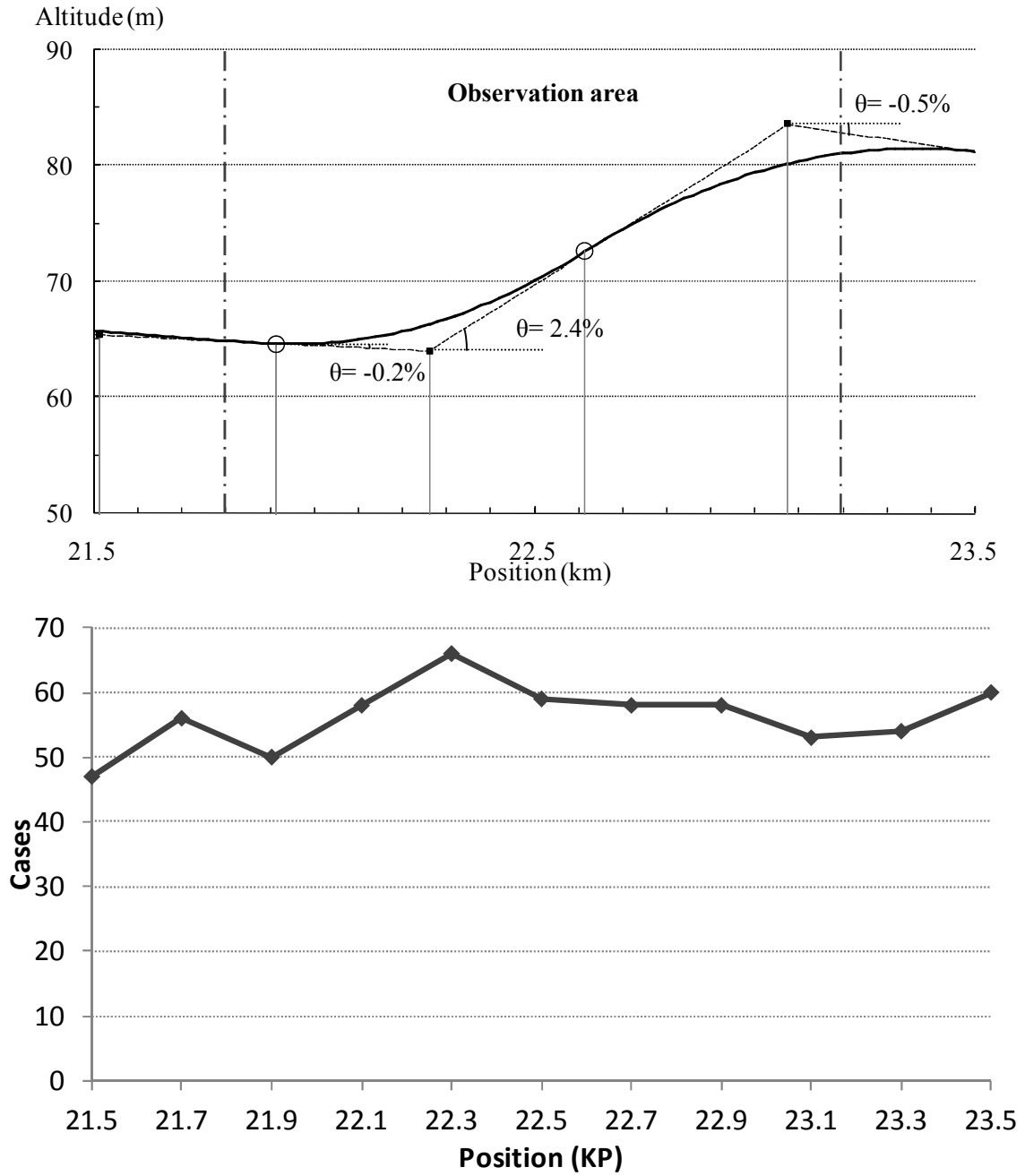


Figure 3.1.2 Observation location of dataset 2

3.2 Methodology

In this research, A model first proposed by Oguchi and Konuma (Oguchi & Konuma, 2009) that has a vertical force effect component added to Helly's model as shown in function 7 is used.

$$a_1(t + \Delta t) = \begin{cases} \alpha_1(v_0(t) - v_1(t)) + \alpha_2(x_0(t) - x_1(t) - s_1^*) & t < t_0 \\ \alpha_1(v_0(t) - v_1(t)) + \alpha_2(x_0(t) - x_1(t) - s_1^*) - \beta g[\sin \theta(t) - \sin \theta_u] & t > t_0 \end{cases}$$

$$s_1^* = \delta + \tau v_1(t)$$

7

where,

- Δt – Driver's reaction time;
- $a_1(t)$ – Acceleration of following vehicle;
- $v_0(t)$ – Speed of leading vehicle;
- $v_1(t)$ – Speed of following vehicle;
- $x_0(t)$ – Position of leading vehicle;
- $x_1(t)$ – Position of following vehicle;
- s_1^* – Desired spacing of following vehicle;
- g – Gravity acceleration;
- $\theta(t)$ – Vertical slope;
- θ_u – Initial vertical slope before sag section;
- $\alpha_1, \alpha_2, \beta$ – Coefficients;
- δ – Standstill spacing;
- τ – Spacing change with speed change;
- t_0 – Time of entering the sag section;

There are two reasons for using Helly's model as the basic model. One is that the physical relationships of acceleration, speed difference and spacing represent the actual experience in observation well. As Helly pointed out, in a platoon with comparatively high density, vehicles only try to keep up with the leading vehicles. Therefore, they mainly react to the difference in the state with its leading vehicle. In driving experiments at sag sections, Helly's model appeared to fit to the car-following behavior well [渋谷公佑、大口敬、洪性俊, 2013] (Oguchi & Konuma, 2009) Helly's model can also reproduce the overreaction of drivers in speed reduction observed by Yoshida (Yoshida, Koshi, & Yasui, 1997), while some models with more complex structure like Intelligent Driver Model appear to produce impassive reactions. The other reason is that a simple linear model with limited numbers of variables will make estimation and analysis of variables easier as well as manifest clear physical relationships in parameters distribution and simulation.

The parameters of driver showed significant difference at different vertical gradient sections. Oguchi and Konuma (Oguchi & Konuma, 2009) used the Helly's model among other classic car-following models to analyze the car-following behavior at sag sections in Japan with experiment data. Helly's model showed good fitness in these researches.

The intra-driver variations are described with sag effect parameter β to reflect the unnoticed deceleration caused by the vertical change. The inter-driver variations are described by the different values of parameters of different drivers. Note that the best sag effect parameter β obtained in their

research was a linear equation of $\beta(t)$ which also considered another two parameters of adaption time of drivers. We tested it and found that the $\beta(t)$ didn't make significant difference to estimation accuracy with the objective equation of relative spacing. Therefore, β is simplified to a constant parameter to reduce the parameters in simulation.

Desired spacing can be described with more complex structures, such as a linear function of spacing, speed and acceleration(Helly, 1959) as well as curves with different bending direction for free flow and congested flow[Xing Jian、越正毅, 1996]. In this research, desired spacing is assumed to be a linear function of speed because the objective is to model the formation of congestion where the speed of vehicle is between 40km/h to 100km/h, which is at the flat part of speed and spacing curve in speed-spacing curve. Acceleration only has a minor effect(Helly, 1959) on desired spacing and thus ignored.

3.3 Assumptions and analysis boundaries

The observation was carried out at a two lane basic segment, where there were a few vehicles changing lane to overpass the preceding vehicle. These lane-changing behaviors are excluded from analysis. The spacing of vehicle decreases severely while speed increases when vehicle change lane to overpass the preceding vehicle. The lane-changing behaviors are thus recognized from dataset and are excluded from analysis as error data.

Two kinds of vehicles which were not in car-following state are also excluded from analysis. One is vehicles under independent driving state. Vehicles under independent driving state are far enough from their preceding vehicles that their driving behavior is not affected by the behavior of preceding vehicles. They are independent in driving state instead of under car-following state. The other is vehicles already involved in congestion. Vehicles already involved in congestion are forced to maintain a low speed equal to it preceding vehicle and a close spacing. Their behavior is highly restricted within the dense low speed flow so that it is not a normal car-following behavior.

Time headway and spacing are common criterion for estimating whether vehicle is under car-following state or not. Highway Capacity Manual suggests that vehicles travelling with a headway smaller than 3s is considered as following vehicles(TRB, 2000). Pasanen and Salmivaara (Pasanen & Salmivaara, 1993) also suggested 3s be the threshold for following vehicles and non following vehicles. Vogel (Vogel, 2002) found that the time headway for urban roads is around 6s and the spacing is 50-70m. Both criterion are used in this study. Vehicles having spacing bigger than 80m or time headway bigger than 3s with preceding vehicle are regarded as vehicles driving independently regardless of preceding vehicles' driving state and eliminated from car-following behavior analysis.

After congestion formed, the speed inside platoon is small and the density of traffic flow is high. The traffic flow inside platoon is condensed that the speed of leading and following vehicle will be forced to decrease to the speed inside the congestion. Therefore, instead of following the leading vehicle and pursuing desired spacing, the following vehicle is simply force to maintain the same congestion speed as the leading vehicle in the congestion. Considering the research objective is the car-following behavior of vehicles during free flow to the formation of congestion, this kind of vehicles involved in congestion is eliminated from analysis. Congestion formation at sag section is a dynamic process. There are many definitions of congestion occurrence (大口敬、片倉正彦、鹿田成則, 2001)(Xing Jian、越正毅, 1996; Xing, Tsuru, Ishida, & Muramatsu, 2010). A simple and practical definition of congestion occurrence at sag section is two adjacent vehicles speed smaller than 40km/h at the same time. This threshold is used in this research. As long as there are two adjacent vehicles' speed smaller than 40km/h, the later vehicles are regarded as involved in the congestion and eliminated from car-following behavior analysis.

The effective samples are shown in Table 3.3.1.

Table 3.3.1 Summary of field observation data

	all	error	independent	congested	Not well estimated	effective samples
Dataset 1	393	64	7	40	65	217
Dataset 2	482	27	63	0	86	326

3.4 3.4 Analysis Framework

The analysis of driving behavior variations is carried out with 3 steps.

- 1) The desired speed s_1^* is estimated with regression of vehicle's speed spacing relationships under steady driving state ($a < 0.01g$).
- 2) The range of reaction time Δt is estimated with correlation analysis within 0~5 seconds.
- 3) The other parameters are estimated with cross-entropy method, where objective function is the relative percentage error of spacing and 3 performance indicators are also studied.

4 Driving behavior parameter estimation

The estimation method of driving behavior parameters reflecting the variations in driving behavior were presented in this chapter. According to the analysis framework in Chapter 3, the desired spacing is firstly estimated with regression. The range of reaction time is then estimated with correlation analysis. Finally, the other parameters are estimate with a heuristic search method called cross-entropy method.

Trajectories in Dataset 1 are smoothed for every 1/30s while those in dataset 2 are smoothed for every 0.1s. So dataset 1 is used in the search for best parameter estimation methods and dataset 2 are used to calibrate the parameters distribution obtained from the estimation method.

The desired spacing and reaction time range can be directly obtained from observed data. On the other hand, α_1 , α_2 , β and the exact value of Δt is unobservable and therefore obtained with cross-entropy method. The ranges of the parameter values were set as follows: $\Delta t \in [0,5]$ s, $\alpha_1 \in [0,1]$, $\alpha_2 \in [0,0.3]$, $\beta \in [0,1]$, $\delta \in [0,100]$, and $\tau \in [0,5]$.

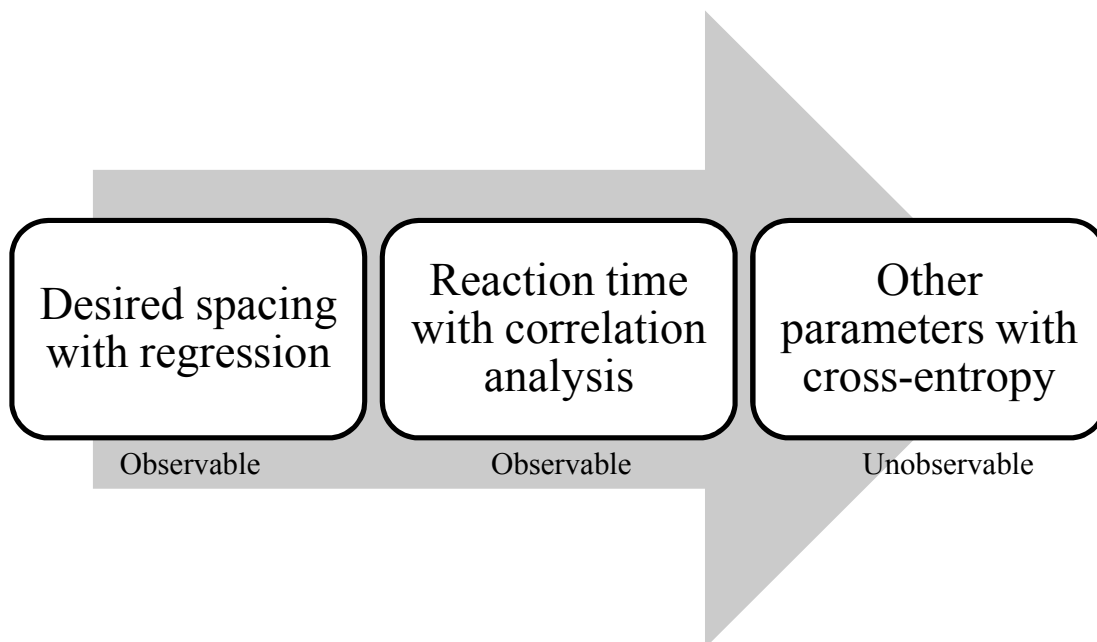


Figure 3.4.1 Estimation approach

4.1 Estimate desired spacing

Vehicles always adjust the spacing and speed difference with preceding vehicles. This dynamic adjustment is shown as accelerate and decelerate in driving states.

$$a_1(t + \Delta t) = \begin{cases} \alpha_1(v_0(t) - v_1(t)) + \alpha_2(x_0(t) - x_1(t) - s_1^*) & t < t_0 \\ \alpha_1(v_0(t) - v_1(t)) + \alpha_2(x_0(t) - x_1(t) - s_1^*) \\ \quad - \beta g[\sin \theta(t) - \sin \theta_u] & t > t_0 \end{cases}$$

$$s_1^* = \delta + \tau v_1(t)$$

7

Vehicles adjust the spacing with preceding vehicle according to its speed. When the speed of vehicle is bigger, it tends to keep bigger spacing with preceding vehicle. When the speed of vehicle is smaller, it keeps smaller spacing with preceding vehicle. There exists a desired spacing for every vehicle to maintain with its preceding vehicle under certain speed. When vehicle achieves its desired spacing, it will maintain a certain speed if there is no further change of traffic condition. Steady driving state is the state when vehicles maintain a very small acceleration or deceleration. At steady driving state, vehicles don't accelerate or decelerate to adjust to the driving state of preceding vehicle. Therefore, the steady driving state reflects a state of vehicles under some ideal speed and spacing relationship. Steady driving state is defined as acceleration smaller than 0.01g according to previous research experiences (Oguchi & Konuma, 2009)[渋谷公佑、大口敬、洪性俊, 2013]. A simple way of reflecting this relationship between desired spacing and speed is linear relationship(Newell & Frank, 2002).

For the steady driving states of all the trajectories the value of $\delta_0 = 5$ and $\tau_0 = 1.2078$ are estimated with linear regression ($r^2 = 0.2176$) as shown in Fig.4.1.1. The free independent driving state of headway bigger than 3s is excluded from estimation.

Therefore, the desired spacing of all the vehicles are as shown in function (8).

$$s_i^* = 5 + 1.2078 \cdot v_i(t)$$

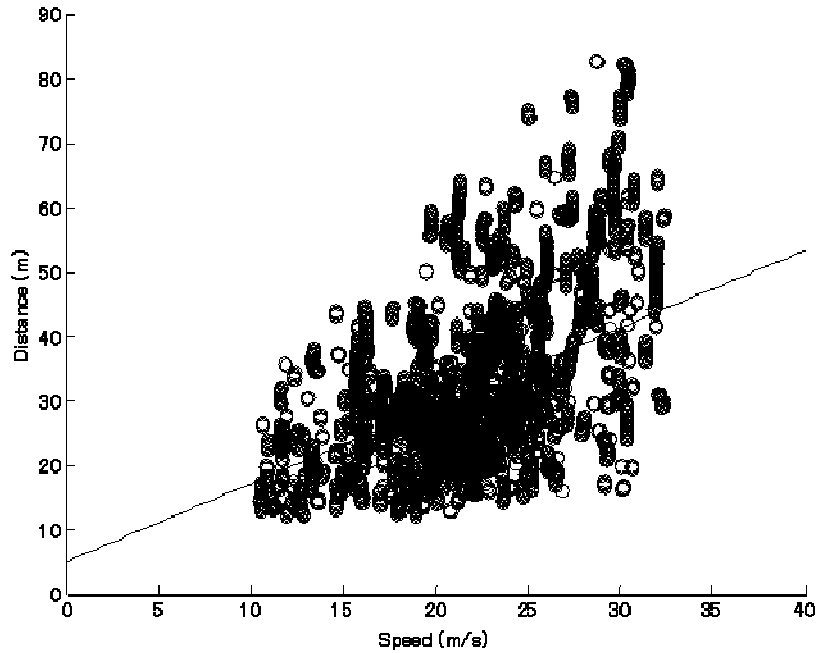


Figure 4.1.1 Desired spacing estimation with all vehicle trajectories

It can be observed from Fig. 4.1.1 that the desired spacing of drivers under high speed (>25 m/s) is more dispersed than that of low speed.

The speed-desired spacing relationship is also estimated for every separate vehicle. There are two kinds of condition in observed speed and desired spacing relationship.

One is that several steady driving states exist in a trajectory, δ and τ are estimated from the steady driving states. The data is a time-series data, thus the errors also have a time-series structure which may be accumulated to cause bias in regression. To avoid the bias caused by errors, Tobit model is used instead of linear regression. The Tobit model supposes that the dependent variable is latent, which is linearly dependent on independent variable and consists an additional normally distributed error term (See function (9)).

$$y_i^* = \beta \cdot x_i + u_i$$

$$u_i \sim N(0, \sigma^2)$$

9

The value of τ is set to $\tau \in [0, 5]$. The desired spacing should not be smaller than a minimum distance when speed is low. According to a research of the U.K. Department of Transport (Department for Transport and Driver and Vehicle Standards Agency, 2007), it is generally established that the stopping distance of vehicles at 20mph (32km/h) is 12m. The spacing is 16m considering the 4m length of vehicle. Therefore, the estimated desired spacing should not be smaller than 16m when the speed is at 32km/h. The lower bound of dependent variable is 16m. δ and τ are estimated with maximum likelihood in Tobit model.

The result is shown as Fig. 4.1.2. δ is the intercept and τ is the slope of the estimated line.

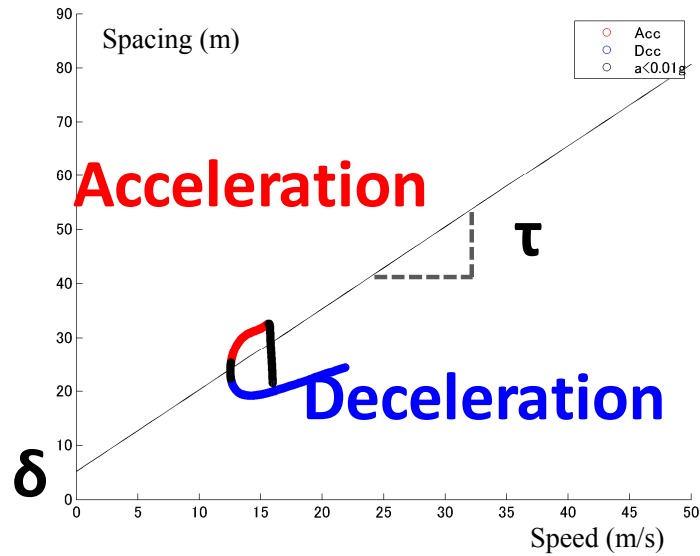


Figure 4.1.2 Desired spacing estimation with individual trajectory (several stable states)

The red dots represent the acceleration phase of vehicle and the blue dots represent the deceleration phase of vehicle. Vehicle accelerates when the spacing is bigger than its desired spacing and decelerates when the spacing is smaller. These two different phases are well separated by the estimated desired spacing line in Fig. 4.1.2.

In the other condition, there is only one steady driving state in a trajectory, where the speed difference of steady driving state is smaller than 5% (See Fig.4.1.3). This condition occurs especially when obvious propagation of deceleration is observed. Vehicle has less time to adjust to their desired spacing than to decelerate like the leading vehicle. Under this condition, the desired spacing is assumed to be a constant where $\tau=0$, and δ is the mean speed of the steady state in the desired spacing function.

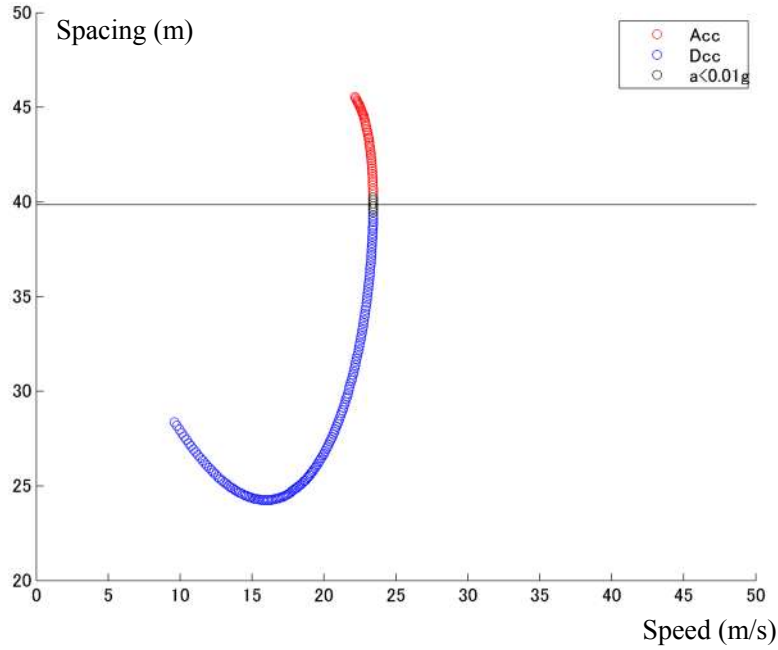


Figure 4.1.3 Desired spacing estimation with individual trajectory (single stable state)

There are 118 trajectories having only one stable state, 9 trajectories having no stable state and 155 trajectories having several stable states. The $\delta_0 = 5$ and $\tau_0 = 1.2078$ are used for the nine trajectories with no stable state.

To conclude, the approaches taken in desired spacing estimation are:

1. One desired spacing function parameters for all the trajectories: $s_1^* = 5 + 1.2078 \cdot v_1(t)$
2. Desired spacing function parameters estimated for every single trajectory.
 - (1) Several steady states exist, desired spacing function parameters are estimated by Tobit model with maximum likelihood estimator. $\tau \in [0, 5]$ and $s_1^* | v_1(t) = 40 \text{ km/h} > 16 \text{ m}$.
 - (2) Only one steady state exists, $\tau = 0$, and δ is the mean speed of the steady state.
 - (3) No steady state, use the desired spacing parameters in 1: $s_1^* = 5 + 1.2078 \cdot v_1(t)$

The number of different types of desired speed estimated with approach 1 and 2 is shown in Table 4.1.1.

Table 4.1.1 Number of estimation of desired spacing in dataset 1

	Total number	Multiple steady states	Single steady state
Approach 1	282	-	-
Approach 2	282	155	118

The estimated desired spacing by approach 1 and 2 are shown in Fig. 4.1.4. The desired spacing estimated by approach 1 is $s_1^* = 5 + 1.2078 \cdot v_1(t)$ and presented in blue circle, while the desired spacing estimated by approach 2 is presented in dark grey rhombus. 118 cases with only single steady state and $\tau = 0$, the other cases have an obvious negative relationship of δ and τ .

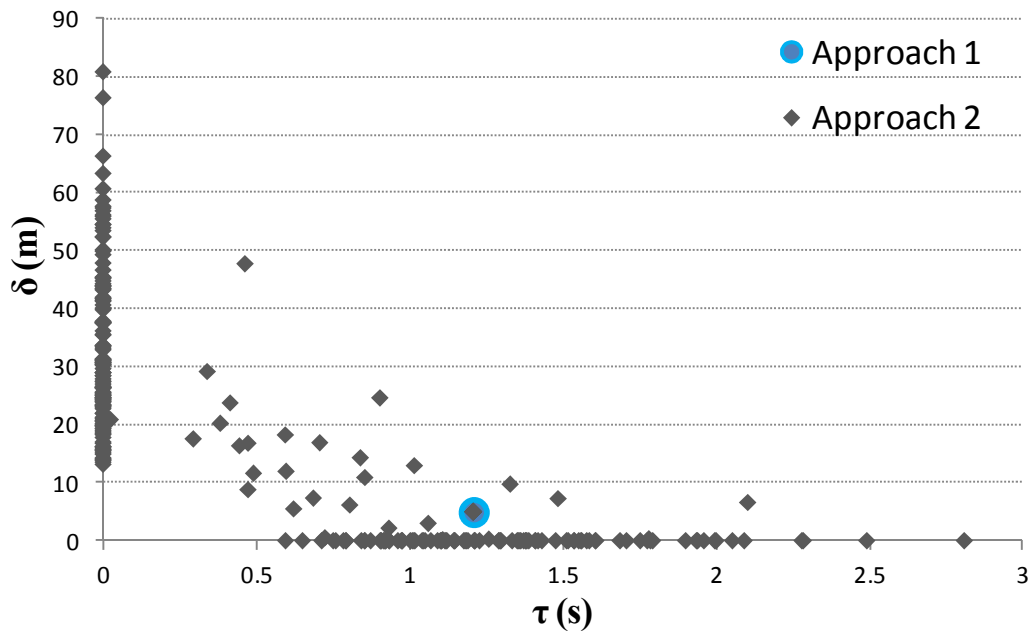


Figure 4.1.4 Estimated result of desired spacing

4.2 Estimate reaction time

The parameter Δt reflects the reaction time of a driver to the relative speed and spacing difference from the desired spacing with the leading vehicle, as expressed by function (7). The most suitable value of Δt should generate the best correlation of the driver's acceleration with either the relative speed or the spacing difference from the desired spacing with the leading vehicle. Therefore, Δt was estimated from the results of a correlation analysis within the range of [0,5] s. The analysis area was extracted to capture the dynamics of speed change (See Fig. 4.2.1).

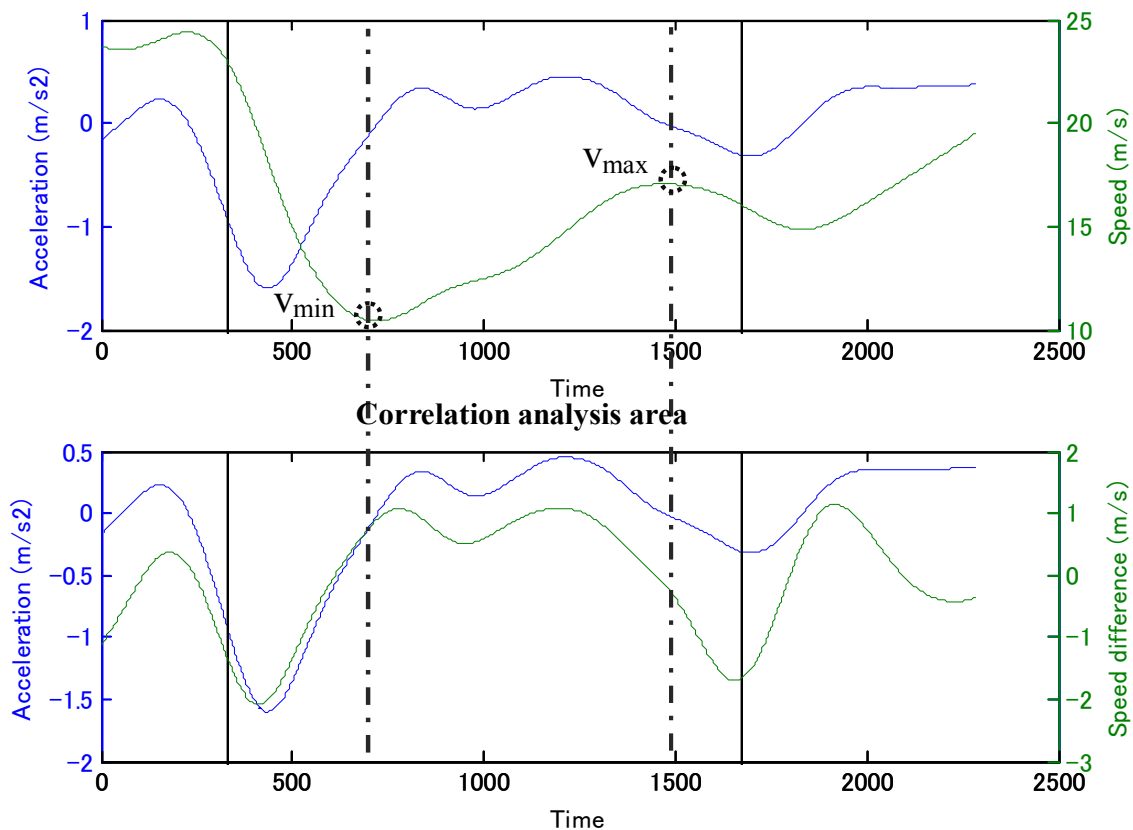


Figure 4.2.1 Correlation analysis area of Δt

The correlation analysis of reaction time is carried out on trajectories with enough change in driving state in terms of difference of maximum speed and minimum speed bigger than 10% as shown in function. When speed change is small, the acceleration and deceleration are more due to other random adjustment instead of car-following incentive to adjust to the driving state of preceding vehicle.

$v_{\max} - v_{\min} > 10\% \cdot v_{\max}$ At least 10 seconds range including v_{\max} and v_{\min} is chosen for correlation analysis of reaction time. The time length of twice the reaction time upper limit 10 seconds is chosen to provide enough range for correlation and limit the error caused by random acceleration/deceleration.

Fig. 4.2.2 shows 3 different cases of correlation analysis range based on the time between v_{\max} and v_{\min} .

1. When the time between v_{\max} and v_{\min} is bigger than 10s, the whole time range between v_{\max} and v_{\min} is the analysis range. (See case a)
2. When the time between v_{\max} and v_{\min} is smaller than 10s, the time range is expand on both sides to 10s including v_{\max} and v_{\min} . (See case b)
3. When the time between v_{\max} and v_{\min} is smaller than 10s and the time range reaches the analysis

range boundary, the time range is expanded on one side to 10s including v_{\max} and v_{\min} . (See case c for expanding to the lower boundary and d for expanding to the upper boundary).

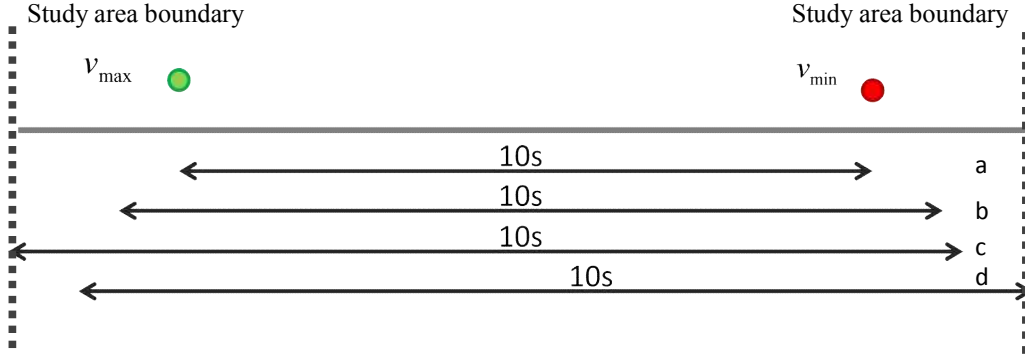


Figure 4.2.2 Analysis range for reaction time

Detailed algorithm of reaction time analysis range is shown in function 10.

if $t | v_{\max} > t | v_{\min}$

$$\left\{ \begin{array}{l} \frac{t | v_{\min} \rightarrow t | v_{\max}}{2} - (5 \text{ min} - \frac{t | v_{\max} - t | v_{\min}}{2}) \rightarrow \frac{t | v_{\max} - t | v_{\min}}{2} + (5 \text{ min} - \frac{t | v_{\max} - t | v_{\min}}{2}) \\ 0 \rightarrow 10 \text{ min} \\ t_{\text{end}} \rightarrow (t_{\text{end}} - 10 \text{ min}) \end{array} \right. \begin{array}{l} \frac{t | v_{\max} - t | v_{\min}}{2} + (5 \text{ min} - \frac{t | v_{\max} - t | v_{\min}}{2}) \geq 10 \text{ min} \\ \frac{t | v_{\max} - t | v_{\min}}{2} - (5 \text{ min} - \frac{t | v_{\max} - t | v_{\min}}{2}) < 0 \\ \frac{t | v_{\max} - t | v_{\min}}{2} + (5 \text{ min} - \frac{t | v_{\max} - t | v_{\min}}{2}) > 0 \end{array}$$

10

if $t | v_{\min} > t | v_{\max}$

$$\left\{ \begin{array}{l} \frac{t | v_{\max} \rightarrow t | v_{\min}}{2} - (5 \text{ min} - \frac{t | v_{\min} - t | v_{\max}}{2}) \rightarrow \frac{t | v_{\min} - t | v_{\max}}{2} + (5 \text{ min} - \frac{t | v_{\min} - t | v_{\max}}{2}) \\ 0 \rightarrow 10 \text{ min} \\ t_{\text{end}} \rightarrow (t_{\text{end}} - 10 \text{ min}) \end{array} \right. \begin{array}{l} \frac{t | v_{\min} - t | v_{\max}}{2} + (5 \text{ min} - \frac{t | v_{\min} - t | v_{\max}}{2}) \geq 10 \text{ min} \\ \frac{t | v_{\min} - t | v_{\max}}{2} - (5 \text{ min} - \frac{t | v_{\min} - t | v_{\max}}{2}) < 0 \\ \frac{t | v_{\min} - t | v_{\max}}{2} + (5 \text{ min} - \frac{t | v_{\min} - t | v_{\max}}{2}) > 0 \end{array}$$

After the correlation analysis range is defined, the Pearson's r of acceleration with relative speed and with spacing difference is calculated for every 1/30s of $\Delta t \in [0,5]$ seconds as the indicator of the degree of correlation.

R of acceleration and relative speed $a_1(t + \Delta t) \leftrightarrow (v_0(t) - v_1(t))$

R of acceleration and spacing difference from desired spacing $a_1(t + \Delta t) \leftrightarrow (x_0(t) - x_1(t) - s_1^*)$

Correlation distribution of acceleration with relative speed and spacing difference with desired spacing with reaction time of 0~5 seconds are studied and the reaction time range of Pearson's correlation $r > 0.8$ were extracted (See Fig. 4.2.3, where the correlation of acceleration and relative

speed is shown in blue line according to the left axis and the correlation of acceleration and spacing difference is shown in green line according to the right axis. The extracted range of reaction time is within the dotted lines). Of the best correlations between acceleration and relative speed more than 50% are greater than 0.8, which indicates a strong correlation between acceleration and relative speed.

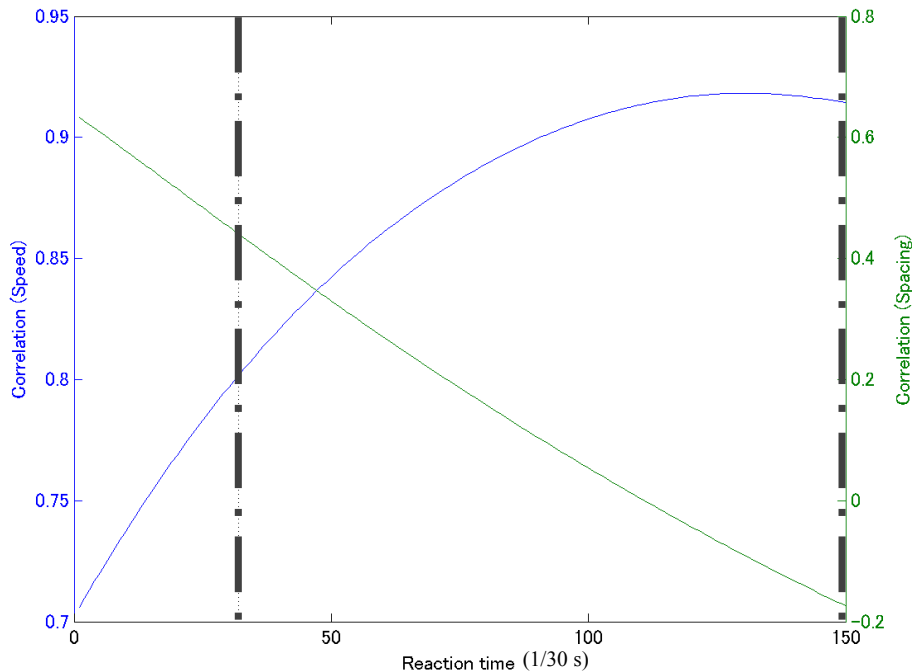


Figure 4.2.3 Reaction time range with correlation analysis

It can be observed that the correlation of acceleration and relative speed as well as the spacing difference changes gradually with reaction time. Therefore, there exists a wide range of high correlation of acceleration and relative speed /spacing difference. Meanwhile, the changing direction of correlation with relative speed is different from the correlation with spacing difference in the figure. The correlation with relative speed increases when reaction time is bigger, while the correlation with spacing difference decreases when reaction time is bigger. Considering of the structure of car-following model where acceleration is affected by both the relative speed and the spacing difference, both should be considered in the calculation of reaction time. Helly suggested that relative speed had a major influence on acceleration within the modeling structure. So the correlation of acceleration and relative speed is given priority in searching reaction time. The reaction time is thus searched within the range of correlation of acceleration with relative speed bigger than 0.8 so that both relative speed and spacing difference is considered.

If both of the best correlations were less than 0.4, which would indicate no significant correlation in the observed trajectories, Δt is to be searched with cross-entropy method within $\Delta t \in [0,5]$ s. For the trajectories with best correlation r of reaction time between 0.4~0.8, the reaction time of best

correlation is used as the reaction time.

To conclude, the conditions and approaches in reaction time are:

1. If the maximum correlation of acceleration with relative speed >0.8 , the range of reaction time with correlation of acceleration with relative speed >0.8 is taken as the range of Δt .
2. If the maximum correlation of acceleration with relative speed <0.8 , and the maximum correlation of acceleration with spacing difference >0.8 , the range of reaction time with correlation of acceleration with spacing difference >0.8 is taken as the range of Δt .
3. If both the maximum correlation of acceleration with relative speed and spacing difference <0.8 , the reaction time is to be searched by cross-entropy method within $\Delta t \in [0,5]$ s.

4.3 Cross-Entropy method

It is difficult to obtain values for α_1 , α_2 , and β directly from observations, while it is easy to obtain reasonable values for δ , and τ from analysis of the trajectory data as shown in 4.1. For Δt , it is easy to estimate the range of value from observation data as shown in 4.2. But because Δt affected on both relative speed and spacing difference, so the exact value of Δt is hard to be estimated directly from observation. Therefore, four out of six parameters in car-following model need to be searched at the same time.

A heuristic search method called cross-entropy method is used to search for the best combination of α_1 , α_2 , Δt , and β fitted to the trajectory. It is based on Kullback-Leiber cross-entropy, importance sampling, Markov chain and Boltzmann distribution. The core concept in this method is to adaptively adjust the occurrence of the events more likely in the vicinity of a global extremum by using important sampling.

Mixed error measure of the relative error and the absolute error is used as objective function to balance the weight of distance in error.

The objective function is defined as function 9, which was proposed by Kesting et.al.(Kesting & Treiber, Calibrating Car-Following Models using Trajectory Data: Methodological Study, 2008).

$$\sqrt{\frac{1}{E(|s_{obs}(t)|)} \cdot E\left(\frac{(s_{obs}(t) - s_{sim}(t))^2}{|s_{obs}(t)|}\right)} \quad 11$$

where,

$s_{obs}(t)$ – Observed distance;

$s_{sim}(t)$ – Simulated distance;

The root mean square error (RMSE) of the spacing, speed, and acceleration were used as performance indicators (PI) to reflect whether or not the actual driving conditions were properly described by the estimated parameter values(see function 12). The vehicle behavior entering sag

section are time series with a natural temporal order. So the dynamic change of car-following behavior is also very important for congestion formation. This dynamic in driving behavior is reflected by PI2 and PI3.

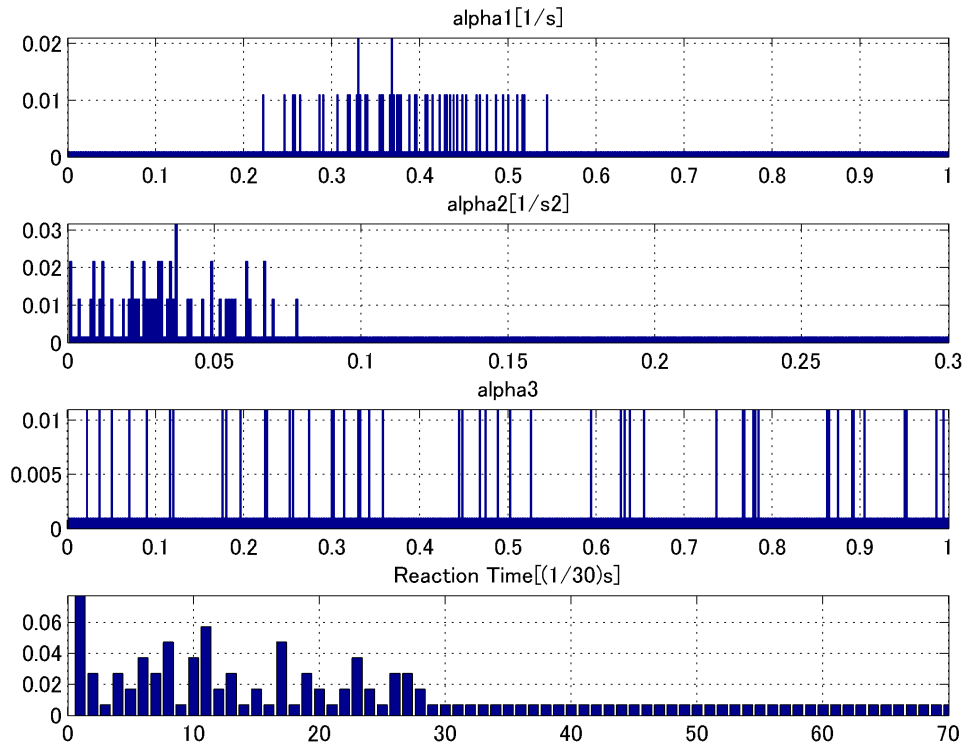
$$PI1 = \sqrt{\frac{1}{n} \sum (s - s_{sim})^2}$$

$$PI2 = \sqrt{\frac{1}{n} \sum (v - v_{sim})^2}$$

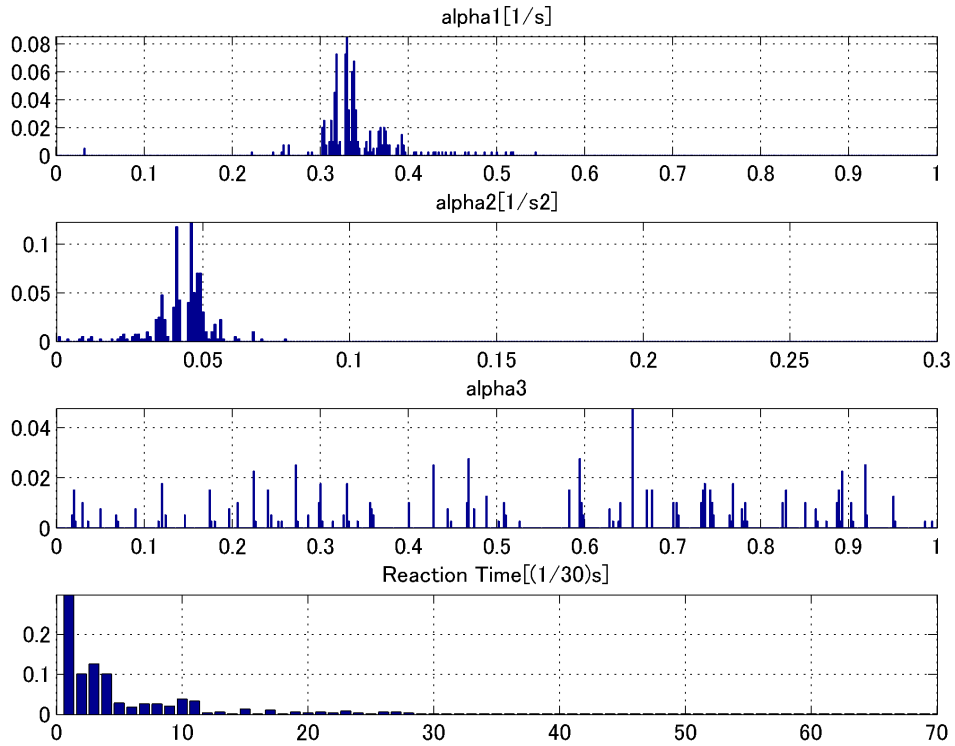
$$PI3 = \sqrt{\frac{1}{n} \sum (a - a_{sim})^2}$$

12

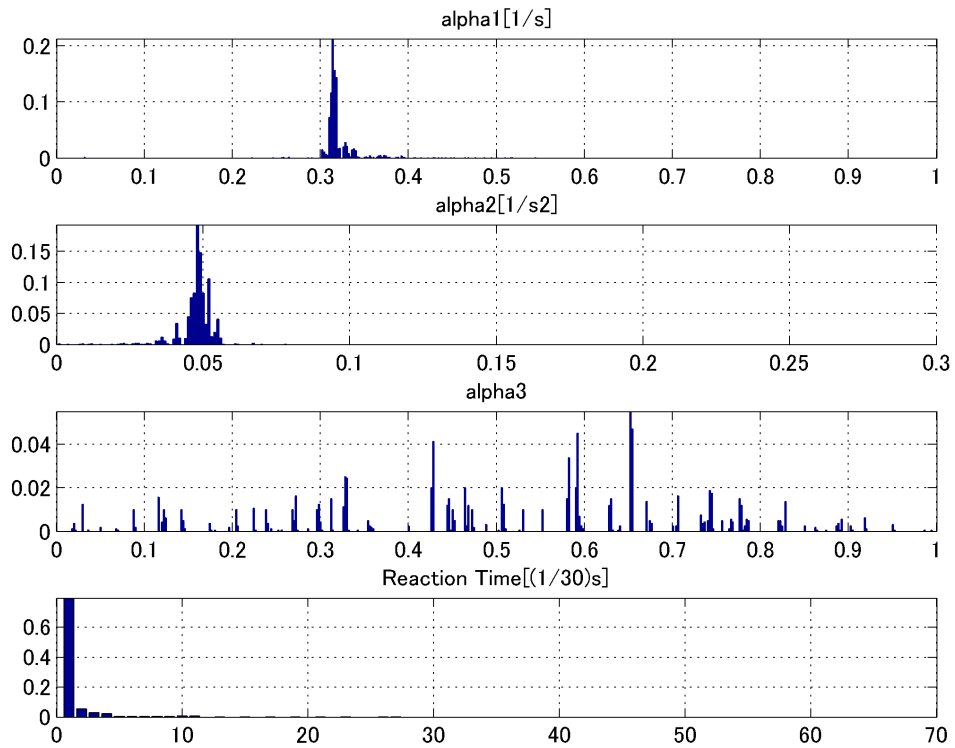
Cross-Entropy method was used to estimate parameters in this research. The core concept is to adaptively adjust the occurrence of the events more likely in the vicinity of a global extremum by using important sampling. Fig. 4.3.1 showed an example on how parameter values merge to a global extremum (Rubinstein, 1999). Fig. 4.3.1a showed the initial value of parameters values generated from Δt with correlation of acceleration and relative speed >0.8 , $\alpha_1 \in [0,1]$, $\alpha_2 \in [0,0.3]$, $\beta \in [0,1]$. The weight of parameter values is equal. 5000 combinations of parameter values are generated at every round. The objective function is then calculated for every parameter value combinations. The parameter values are re-distributed within the range of the best 10% objective function values. The iteration continues until the best fitted values of parameters are finally estimated when the best objective function converge to a best objective function value (See Fig. 4.3.1f).



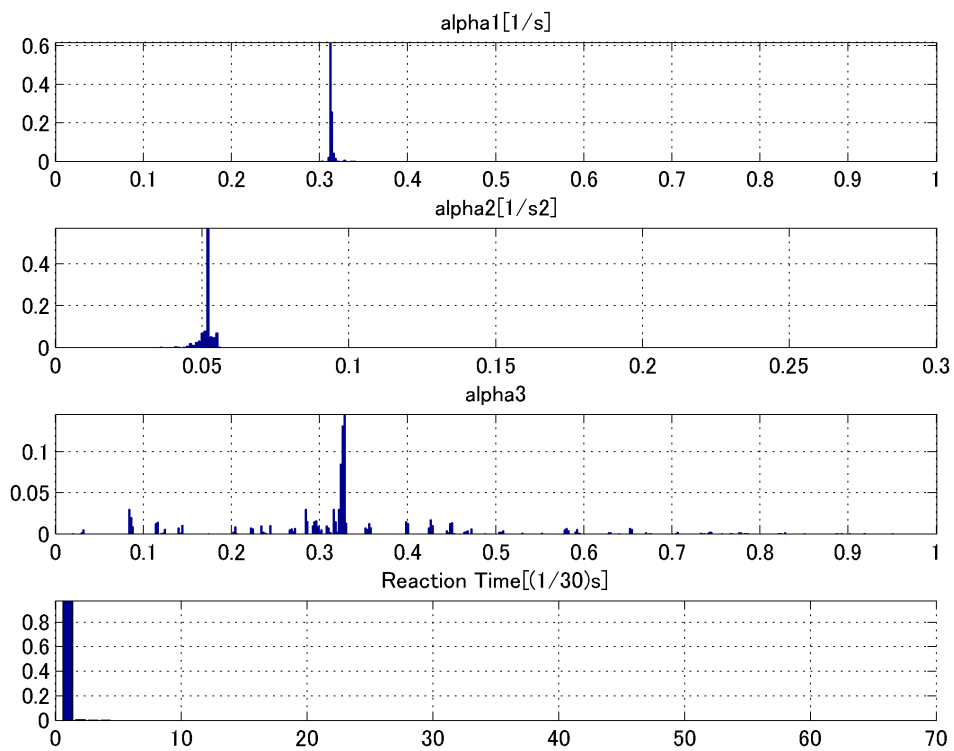
a. Initial distribution of parameters



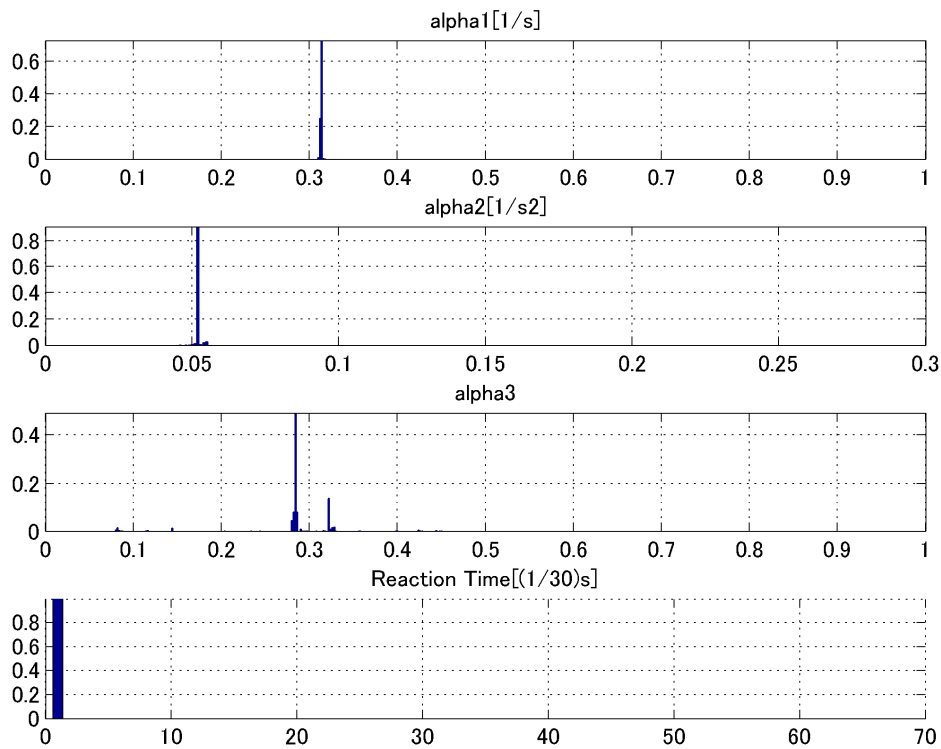
b. Iteration towards best parameters



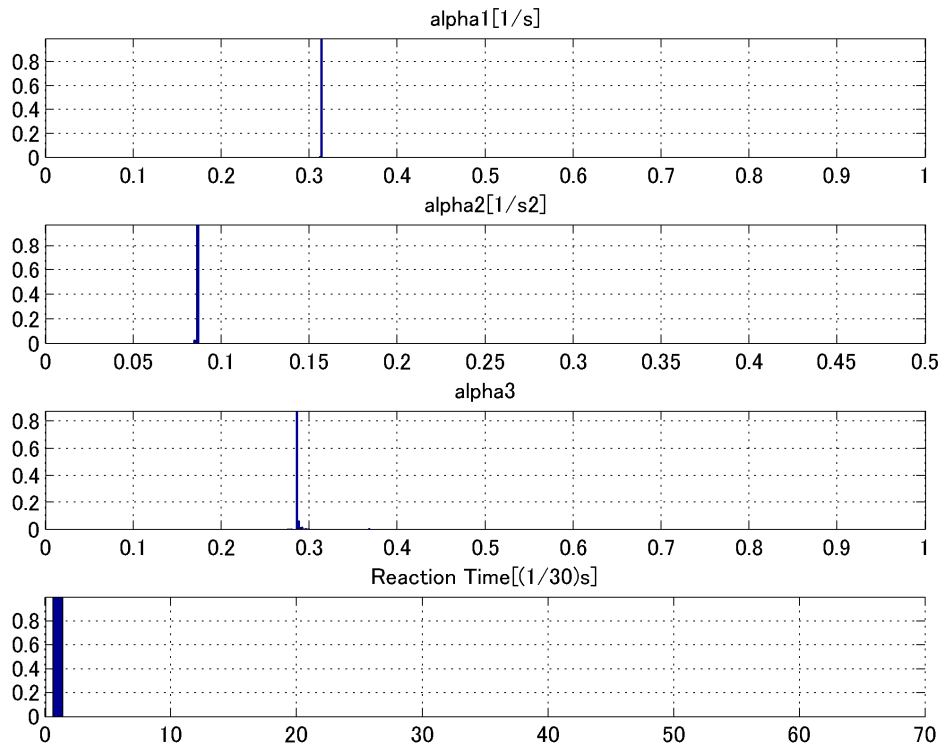
c. Iteration towards best parameters



d. Iteration towards best parameters



e. Iteration towards best parameters

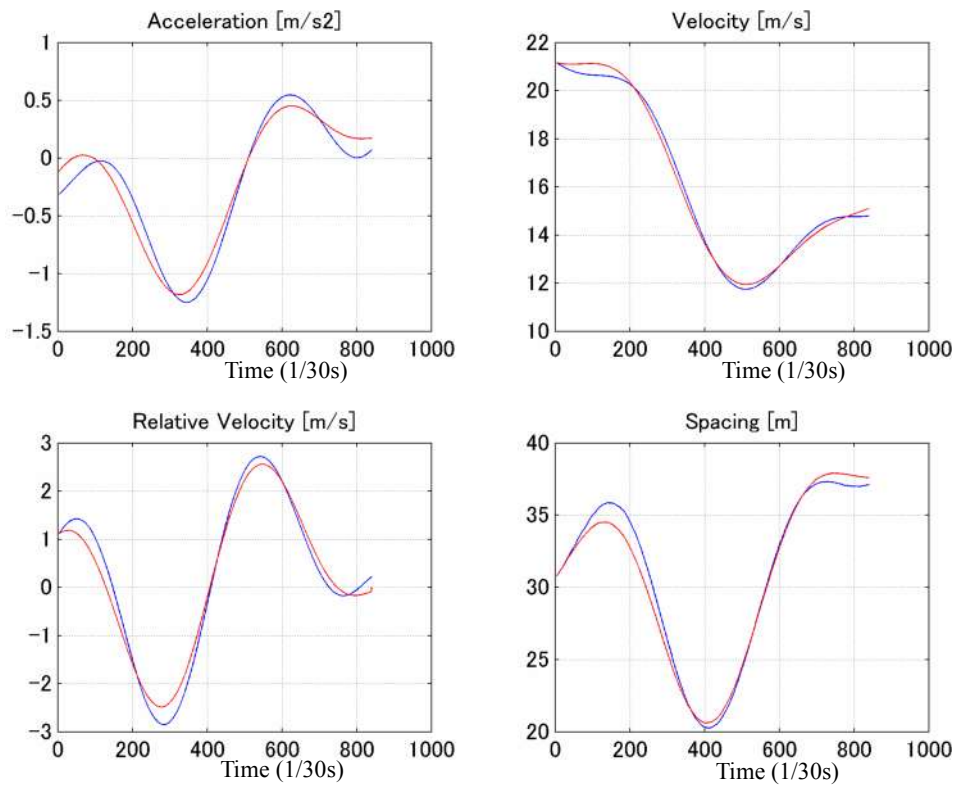


f. The best fitted parameter values

Figure 4.3.1 Cross-entropy method for searching best combination of parameters

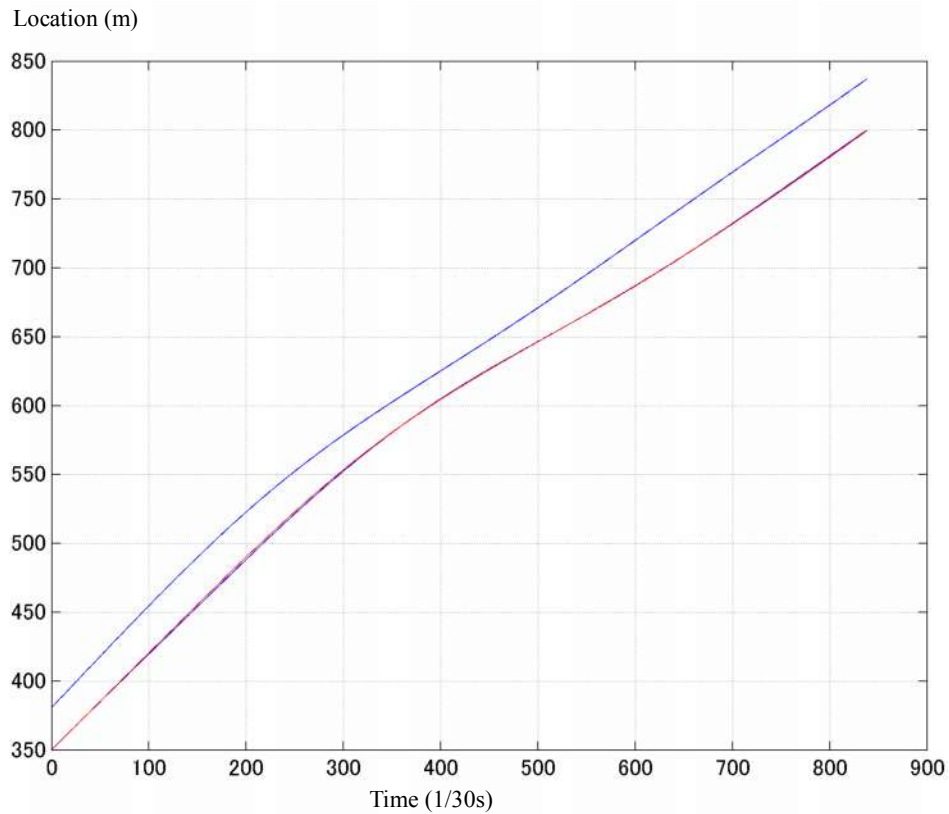
The search range of α_1 , α_2 is estimated with several times of heuristic search. Initially a wide range of α_1 and α_2 are set: $\alpha_1 \in [0, 1.5]$, $\alpha_2 \in [0, 1]$, most estimated α_1 and α_2 are found to be within in the range of $\alpha_1 \in [0, 1]$, $\alpha_2 \in [0, 0.3]$ while a few cases are at both boundary. The cases with either α_1 or α_2 value at the boundary is a failure of the heuristic search because no extremum value is reached inside the range. In order to eliminate the failure of heuristic search and obtain reasonable parameter estimation values, the range of α_1 and α_2 for heuristic search are finally shorten to $\alpha_1 \in [0, 1]$, $\alpha_2 \in [0, 0.3]$.

The fitted behavior of vehicle is shown in Fig. 4.3.2 and The fitted trajectory is shown in Fig. 4.3.3. The behavior of vehicle consists with acceleration, speed, relative speed and spacing with leading vehicle where the blue line stands for the actual behavior from observation and the red line stands for the fitted behavior with car-following model. We can see good fitness from both figures. The objective function and PI values are collected for further analysis.



Blue line: Actual data; Red line: Estimated

Figure 4.3.2 The fitted behavior of vehicle with car-following model



Blue line: Actual data; Red line: Estimated

Figure 4.3.3 The trajectory with car-following model

4.4 Estimation results

Following the estimation steps in this chapter, an example of the estimation of car-following parameters with field observation trajectory data is presented here.

1. Study area extraction

The study area is chosen as introduced in 3.1. The area within the dotted lines in Fig. 4.4.1 is the study area.

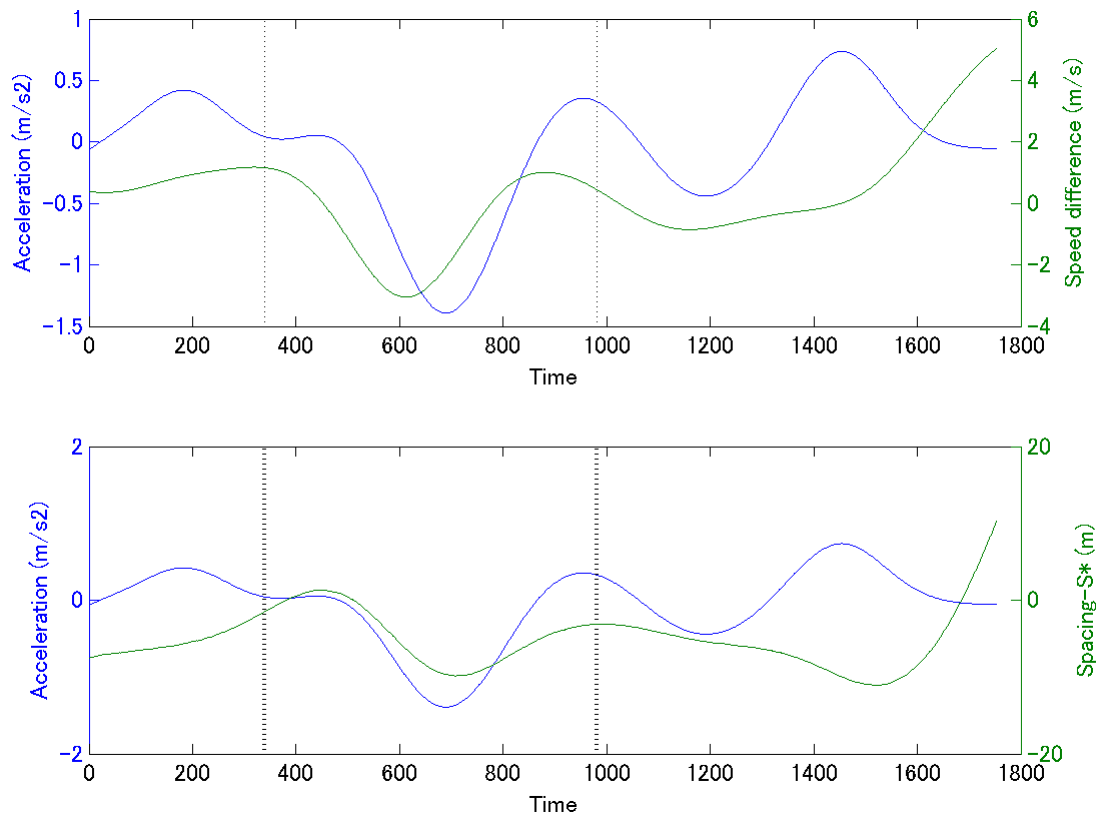


Figure 4.4.1 The extraction of study area

2. The parameters of desired spacing function is estimated with linear regression. There are several steady states in this trajectory, so the δ and τ are estimated with linear regression with constrains that $\tau \in [0,5]$ and $s_1^* > 16\text{m}$ when $v_1(t) = 32\text{km/h}$. The result of estimated desired spacing function for this trajectory is: $s_1^* = 5.7784 + 1.1538 \cdot v_1(t)$

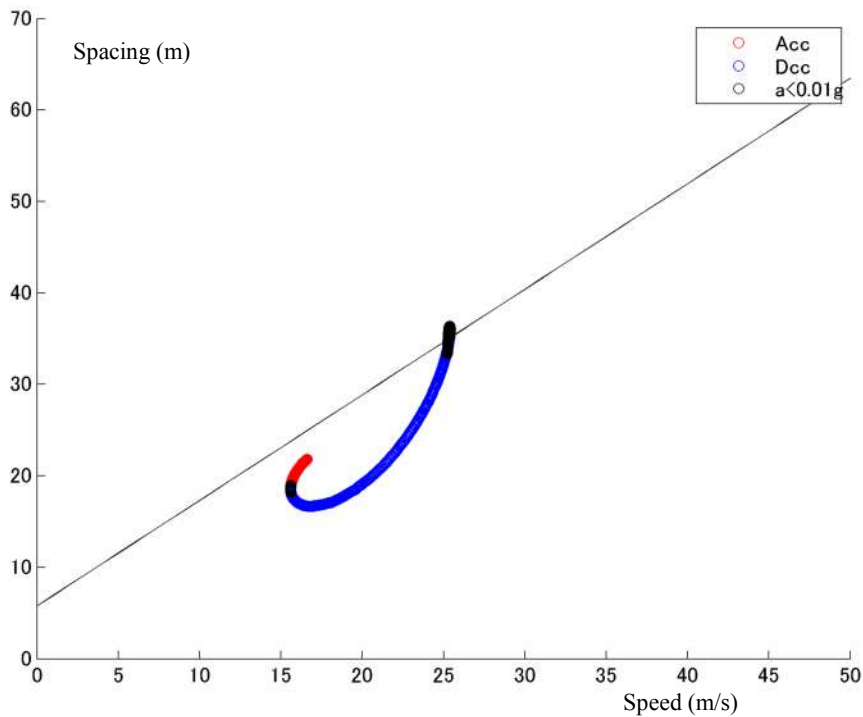


Figure 4.4.2 The desired spacing function estimated with linear regression

3. The range of reaction time is estimated with correlation of acceleration with relative speed and spacing difference. The correlation of acceleration and relative speed in this trajectory ranges from 0.89 to 0.99. The correlation for the whole range of reaction time is higher than 0.8, therefore the range of reaction time is 0-5 seconds.

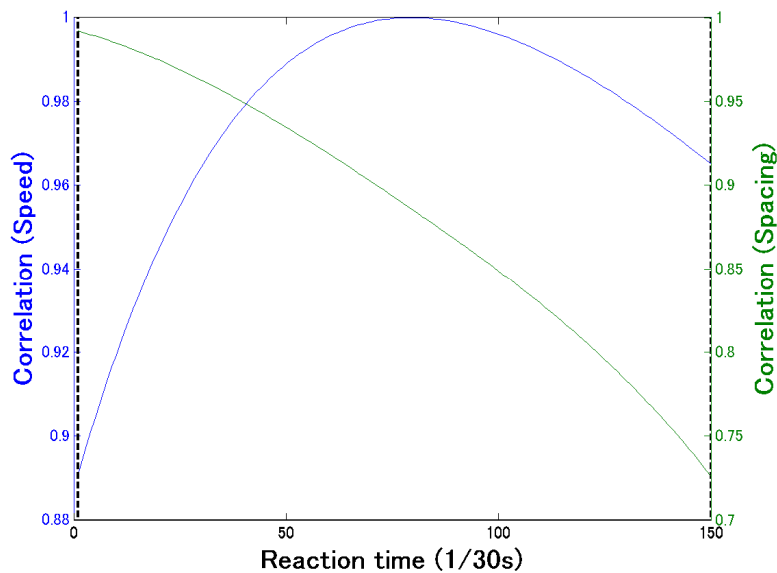
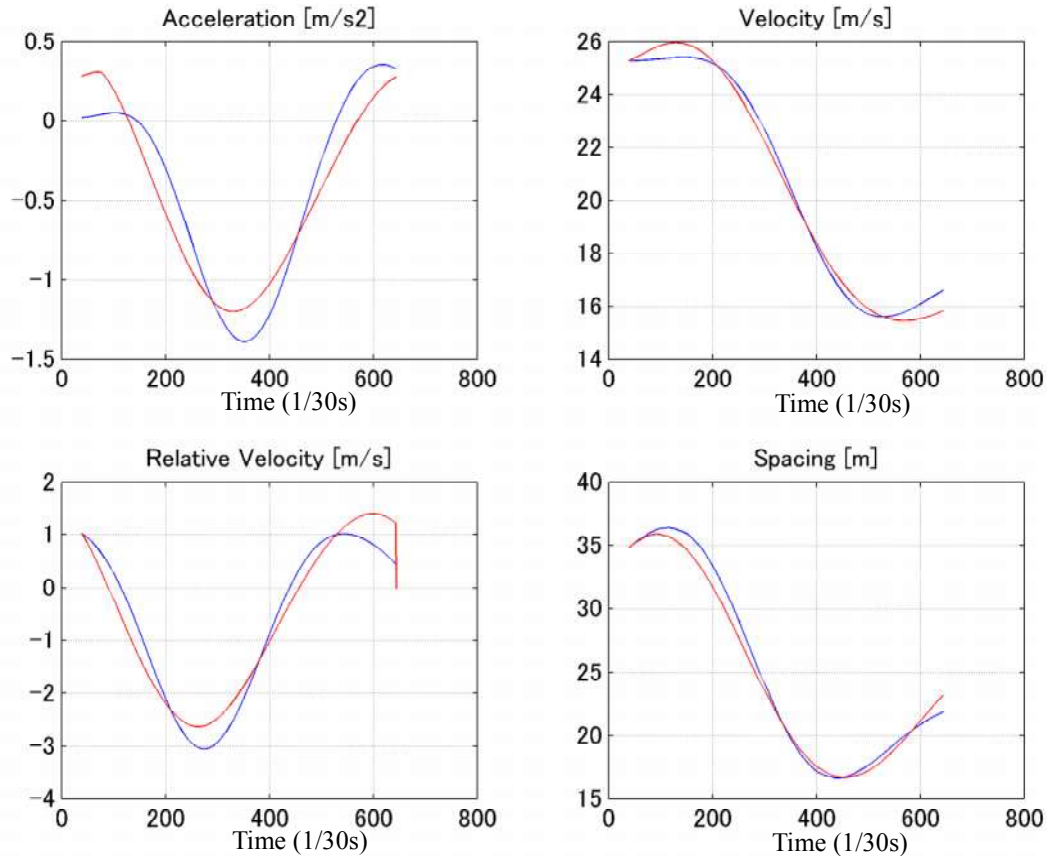


Figure 4.4.3 Correlation of acceleration with relative speed and spacing difference within reaction time range

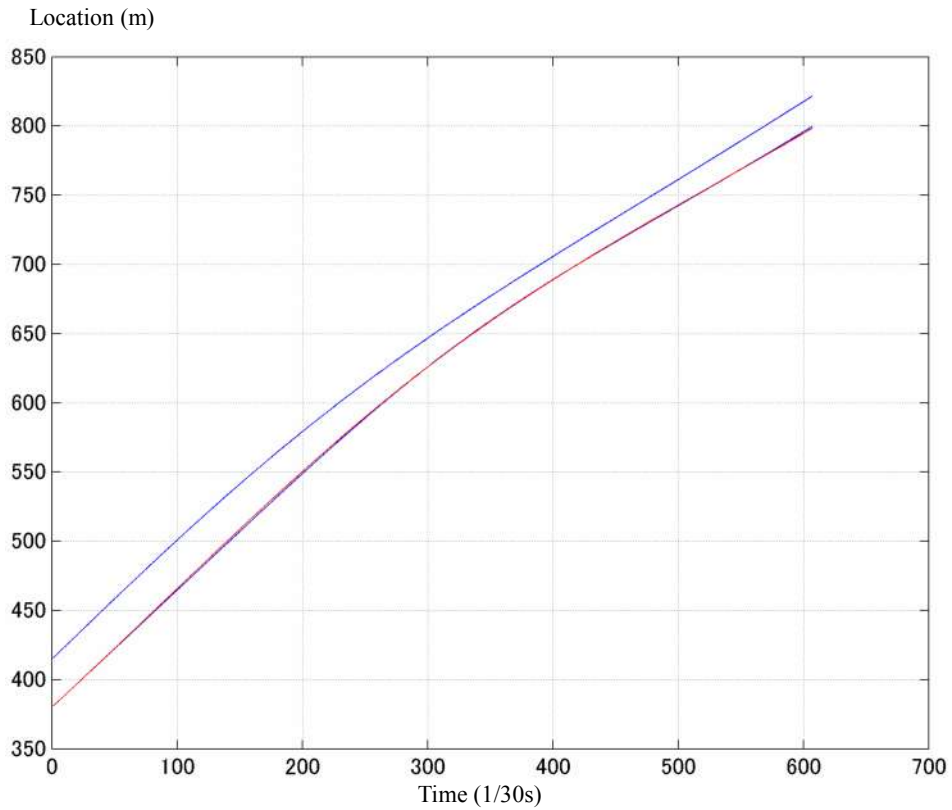
4. α_1 , α_2 , β , and Δt are estimated with cross-entropy method. The objective function of balanced

relative percentage error of spacing is 0.0054, the RMSE of spacing is 0.8018, the RMSE of speed is 0.3675 and the RMSE of acceleration is 0.1898. The behavior of vehicle including acceleration, speed, relative speed and spacing is shown in Fig. 4.4.4 and the trajectory is shown in Fig. 4.4.5. It can be observed from both figures that the car-following model is well fitted to reflect actual driving behavior. The objective function and PIs are also small enough to show good fitness. The detail of comparison in objective function and PIs will be shown in section 4.5.



Blue line: Actual data; Red line: Estimated

Figure 4.4.4 Behavior of vehicle estimated with car-following model



Blue line: Actual data; Red line: Estimated

Figure 4.4.5 Trajectory of vehicle estimated with car-following model

The car-following model function of acceleration is consisted with influence of relative speed, spacing difference from desired spacing and the effect of vertical slope. These components in the car-following model is plotted in Fig. 4.4.6. In this example, both relative speed and spacing difference have obvious influence on acceleration while the effect of vertical slope is very small.

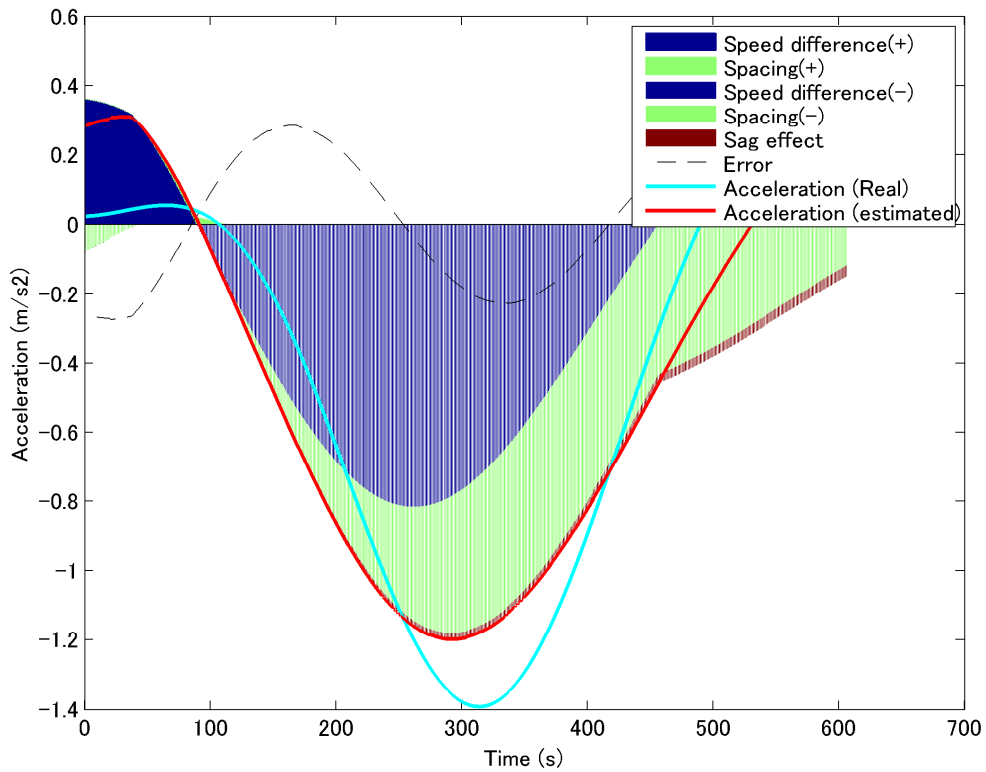


Figure 4.4.6 The components in estimated car-following model.

The figure of speed spacing relationship change is consisted with a line connecting the starting condition of speed and spacing before entering the sag section to the origin. It features the development of speed spacing relationship of vehicle travelling in sag section. It helps us to examine the driving style as shown in Fig.4.4.7 is keeping a close spacing with leading vehicle when speed is reduced. The development of speed and spacing relationship on the lower plain from the line connecting the starting condition to the origin shows the vehicle keeps a smaller spacing than the linear relationship when speed is reduced. The contrary condition is when the relationship develops on the upper plain from the line connecting the starting condition to the origin, which shows that the vehicle keeps a big spacing with leading vehicle when its speed is reduced. This condition is found to be appearing in 75% of vehicles at sag section when congestion formed in Xing et. al.'s research(Xing Jian、越正毅, 1996).

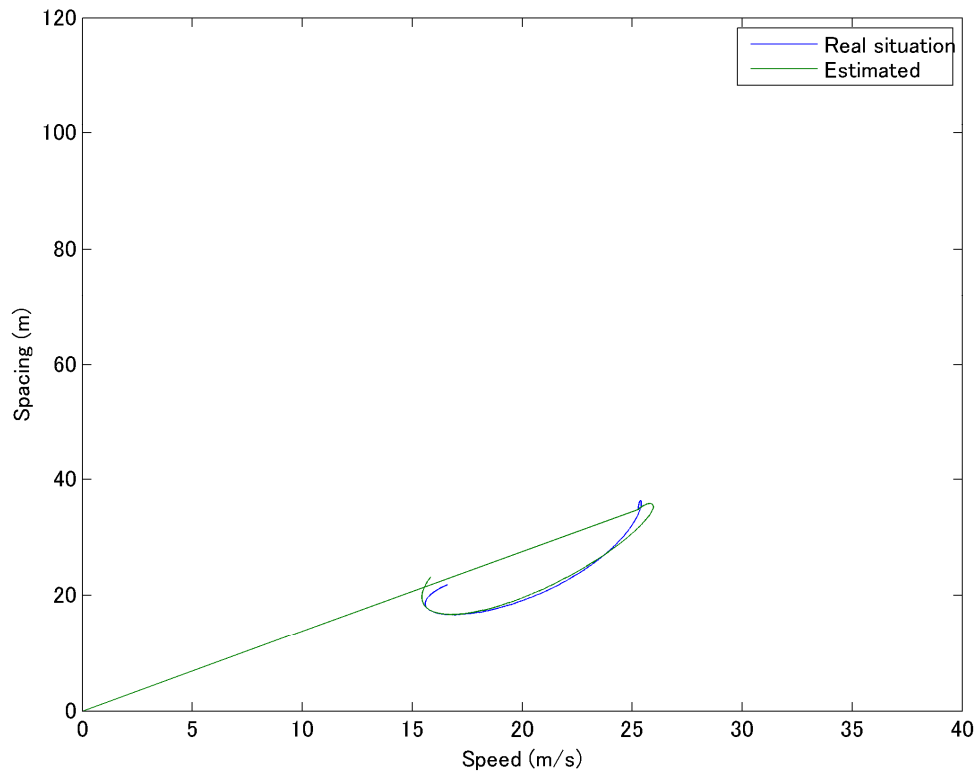


Figure 4.4.7 The speed spacing relationship of observed data and estimation

4.5 Performance analysis of car-following parameters estimation

The performance of objective function and PIs of both datasets are studied in this section. This performance indicates how well the car-following model and its parameters can reflect the actual condition.

The performance of car-following model in dataset 1 is firstly studied. Fig. 4.5.1 shows the PI1 (RMSE of spacing) in ascending order and the corresponding objective function values. With the same percentage of change in spacing, PI1 is bigger when the initial spacing is bigger. It can be observed that PI1 grows drastically when it's bigger than 4 and the corresponding objective functions are obviously big for small spacing cases. The physical meaning of PI1 is the average absolute difference of spacing in every estimation time step. The cases with $PI1=4$ means that at every time step, the average absolute difference of spacing is around 4m, which is about 10% of the average actual spacing. Therefore, $PI1 < 4$ is acceptable as the threshold for goodness of fit. The cases with $PI1 > 4$ and objective function > 0.02 are obviously less well fitted than other trajectories. Based on this observation, the cases with $PI1 > 4$ and objective function > 0.02 are excluded from analysis.

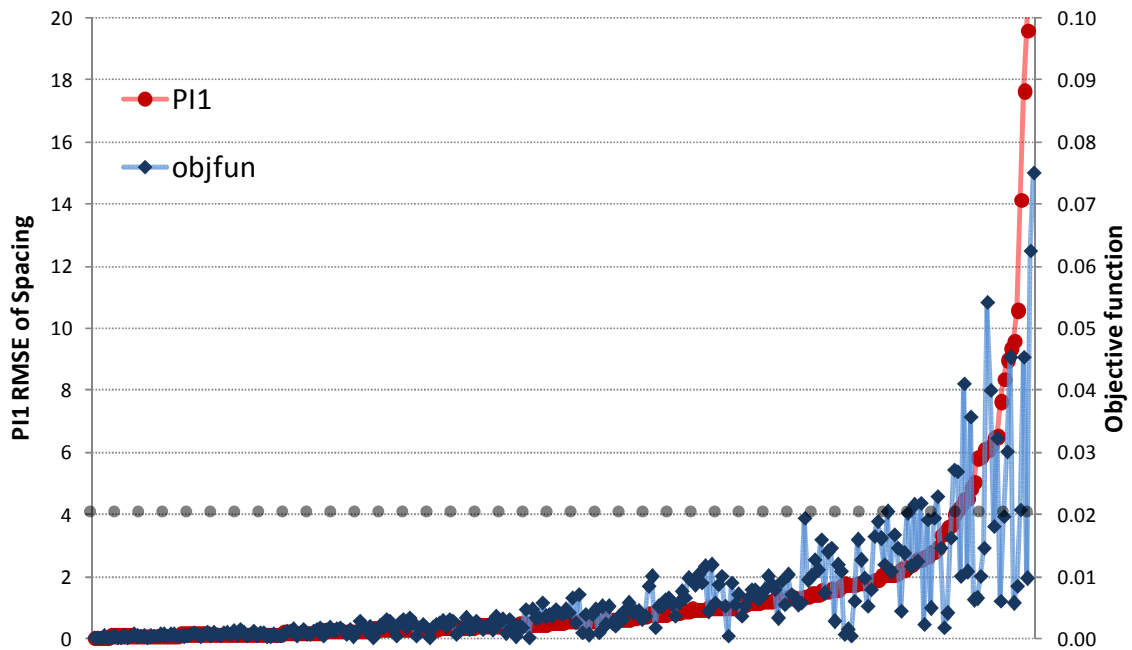


Figure 4.5.1 Objective function and PI1 of dataset 1

The behavior of vehicles are further studied with PI2 (RMSE of speed) and PI3 (RMSE of acceleration) as shown in Fig. 4.5.2 in the same ascendant order of PI1. PI2 and PI3 The same drastic growth of PI2 and PI3 can be observed for cases with $PI2 > 1$ or $PI3 > 0.5$. A big PI2 or PI3 indicates that the dynamic behavior of driving behavior in term of speed and acceleration is not well fitted with car-following model. The trajectories cannot well reflect the dynamic behavior should be excluded from analysis since the car-following behavior of vehicle entering sag-section is a time series data. Therefore, the trajectories with $PI2 > 1$ or $PI3 > 0.5$ are excluded from analysis.

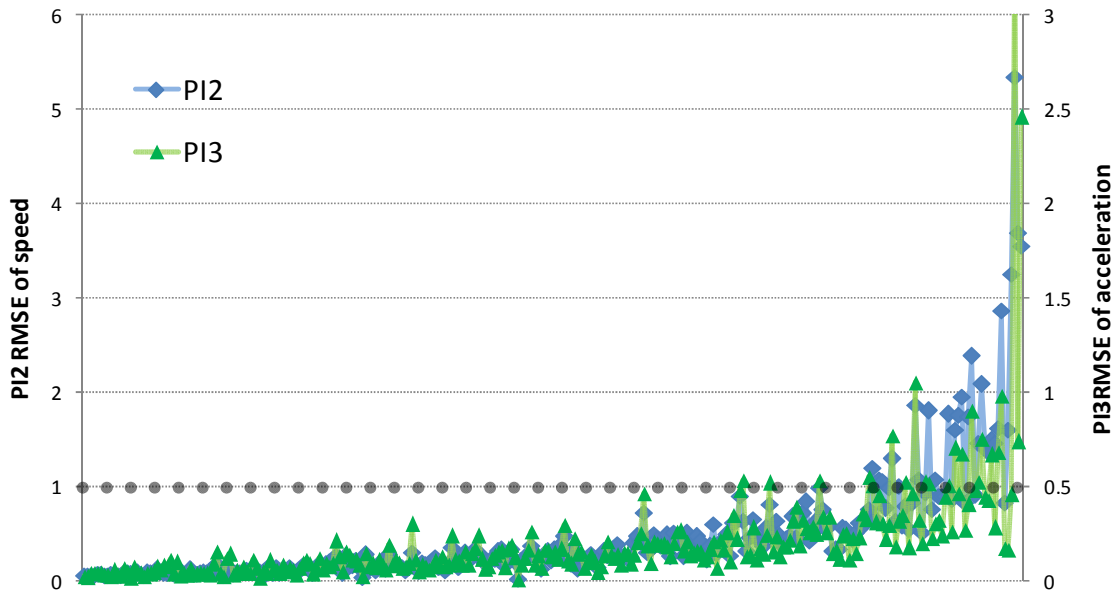


Figure 4.5.2 PI2 and PI3 of dataset 1

The same analysis is also carried out for dataset 2. The spacing is obtained for every 0.1s in dataset 2 and the observation area length is around 1 km, which is about two times the length of observation in dataset 1. The objective function and PI1 are plotted in ascending order of PI1 in Fig. 4.5.3 and PI2 and PI3 are plotted in Fig. 4.5.4. The same tendency of value change in objective function and PIs can be observed in both figures. Therefore, the threshold of goodness of fit is set as twice the threshold in dataset 1 considering the study area length of dataset 2. The cases with $PI1 > 8$ and objective function > 0.08 or $PI2 > 2$ or $PI3 > 1$ are excluded from analysis.

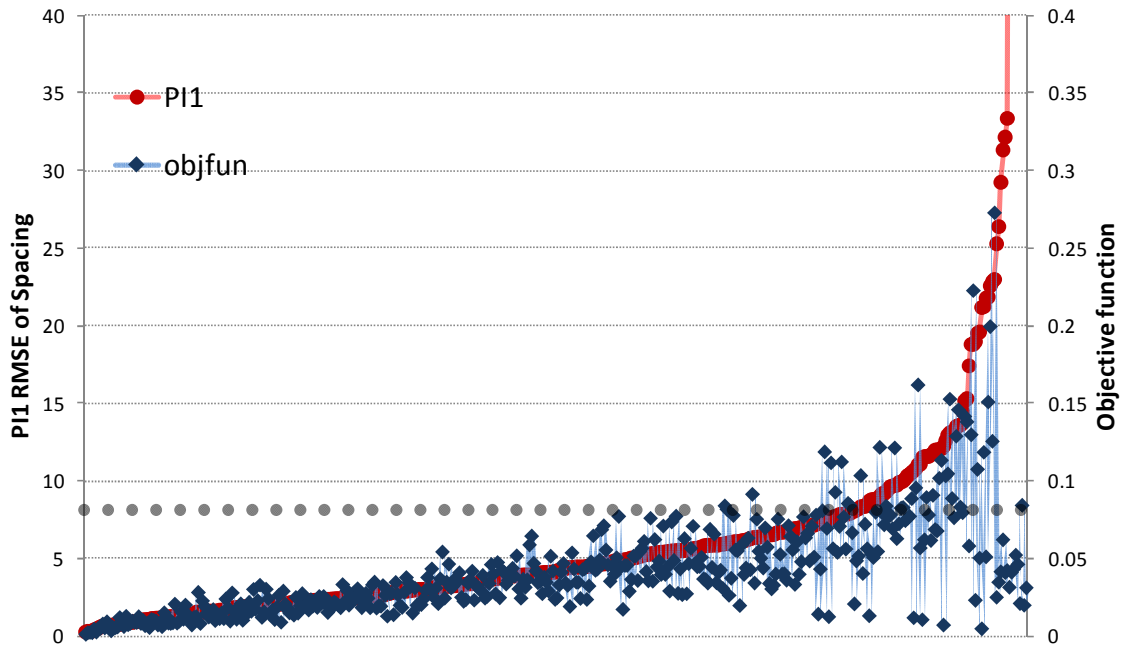


Figure 4.5.3 Objective function and PI1 of dataset 2

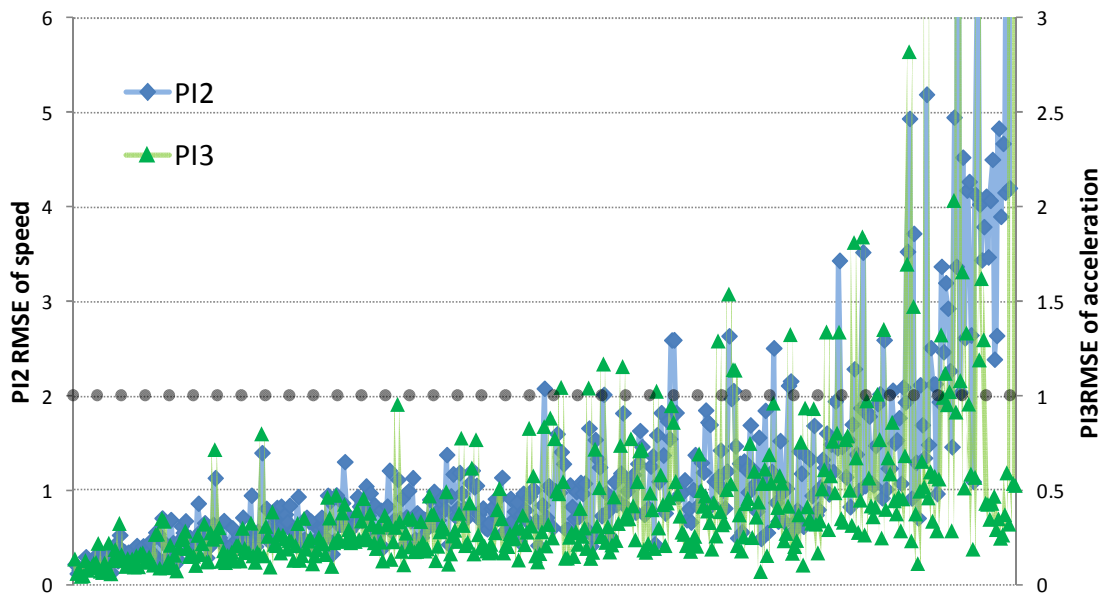


Figure 4.5.4 PI2 and PI3 of dataset 2

The final result of effective samples in field observation data is shown in Table 4.5.1.

Table 4.5.1 Summary of field observation data

	all	error	independent	congested	Not well estimated	effective samples
Dataset 1	393	64	7	40	65	217

4.6 Independent vehicle behavior

The independent vehicles are the vehicles with a headway bigger than 3 seconds or a spacing bigger than 80m as defined in 3.3. There are seven independent vehicles observed during congestion formation in field observation. The number of independent vehicles is limited because the traffic flow during congestion formation is dense. Two kinds of independent vehicle behaviors are assumed for simulation based on the analysis of the seven observed independent vehicles.

1. Constant decrease after entering sag section

One kind of drivers decrease after entering sag section and suffer from the speed lost constantly in the sag section as shown in Fig. 4.6.1. The speed reduction can be obviously observed after the vehicle entering the sag section. The attempt for restore the speed before entering is small that doesn't make much difference in the change of speed.

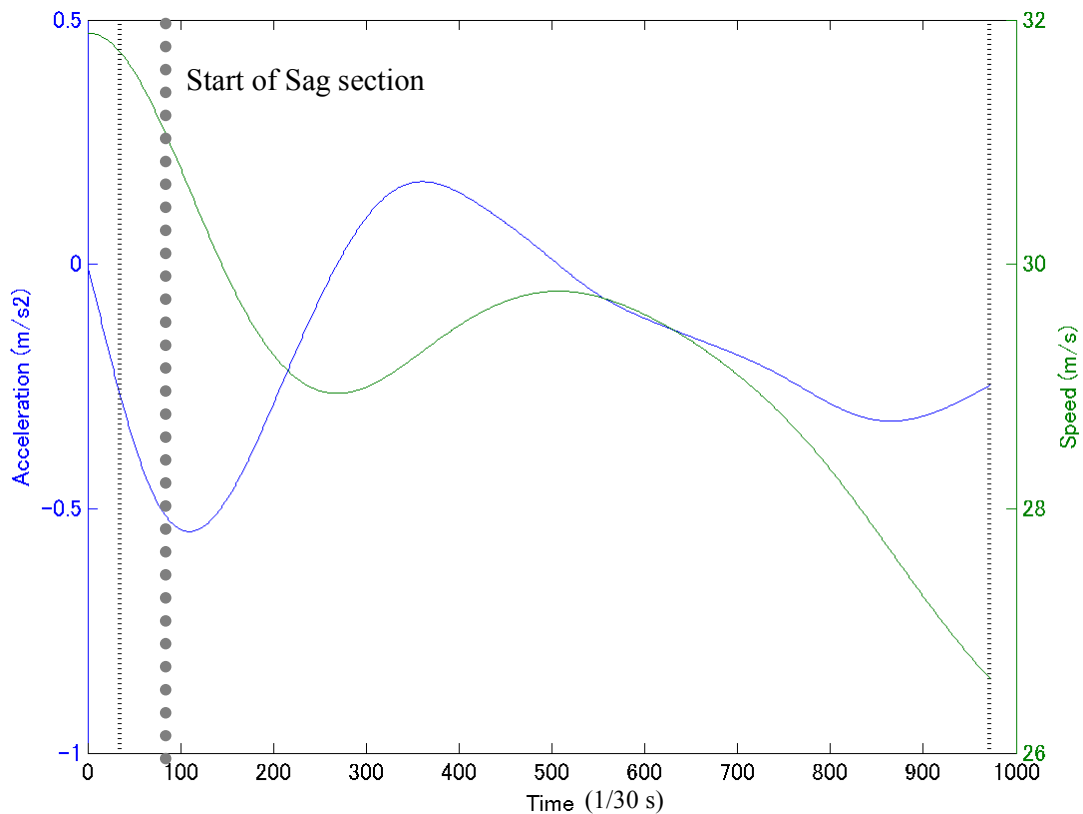


Figure 4.6.1 Independent vehicle observed constantly decreases after entering sag section

The mathematical description is:

$$a_1(t + \Delta t) = \begin{cases} 0 & t < t_s \\ -\beta g[\sin \theta(t) - \sin \theta_u] & t \geq t_s \end{cases} \quad 13$$

2. Decrease before realizing the sag effect and maintain the speed afterwards

Another type of drivers decrease after entering sag section and try to stop deceleration and restore speed after realizing the sag effect. The example showed in Fig. 4.6.2 restores its speed after realizing the sag effect to a smaller speed.

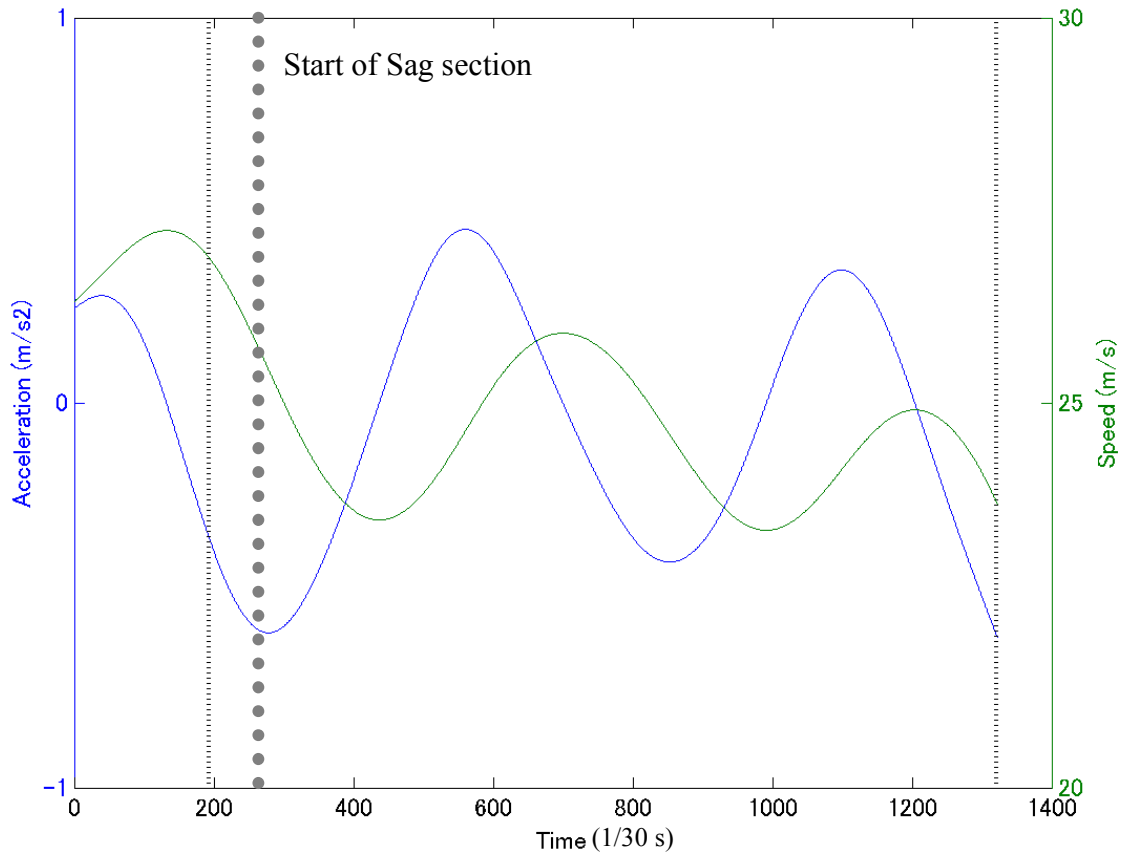


Figure 4.6.2 Independent vehicle observed maintain the speed after realizing the sag effect

4.7 Parameter distribution

The desired spacing in approach 2 as well as all the other parameters are estimated separately for every single driver, which may be affected by the accumulation of systematic error. In data smoothing process, Kalman filter is used to limit the systematic error. But it is impossible to eliminate the systematic error. Therefore, distribution of parameters is used in simulation instead of the exact value.

Table 4.7.1 Descriptive statistics of car-following parameters

	α_1	α_2	β	Δt	τ	δ
Mean	0.3960	0.0384	0.6190	1.9690	0.8817	16.5220
Median	0.2960	0.0110	0.7520	1.4000	0.7450	11.3803
Std. Deviation	0.3050	0.0667	0.3871	1.5079	0.9140	16.9268

The distribution of car-following model parameters is estimated in this section. The distribution is estimated separately for dataset 1 and dataset 2 so that it is possible to compare the distribution in two independent datasets. The distribution of dataset 1 is firstly estimated.

The correlation of parameters are firstly checked with Pearson's r to reveal the inner connection of car-following model parameters. The result is shown in Table 4.7.1

Table 4.7.2 Correlation of car-following model parameters

	α_1	α_2	β	Δt	τ	δ
α_1	-					
α_2	0.2786**	-				
β	-0.0231	-0.0448	-			
Δt	-0.4354**	-0.1939**	-0.0101	-		
τ	-0.2477**	-0.1382**	-0.1795**	-0.0192	-	
δ	-0.0118	0.0720	0.0862*	0.1720**	-0.7380**	-

** $p < 0.01$

* $p < 0.05$

Pearson's r of δ and τ is -0.7380 and significant. This indicates the desired spacing parameters δ and τ have high negative linear correlation. It can also be observed in the δ and τ figure shown in Fig. 4.7.1.

(Brackstone & Waterson, Determinants of following headway in congested traffic, 2009)

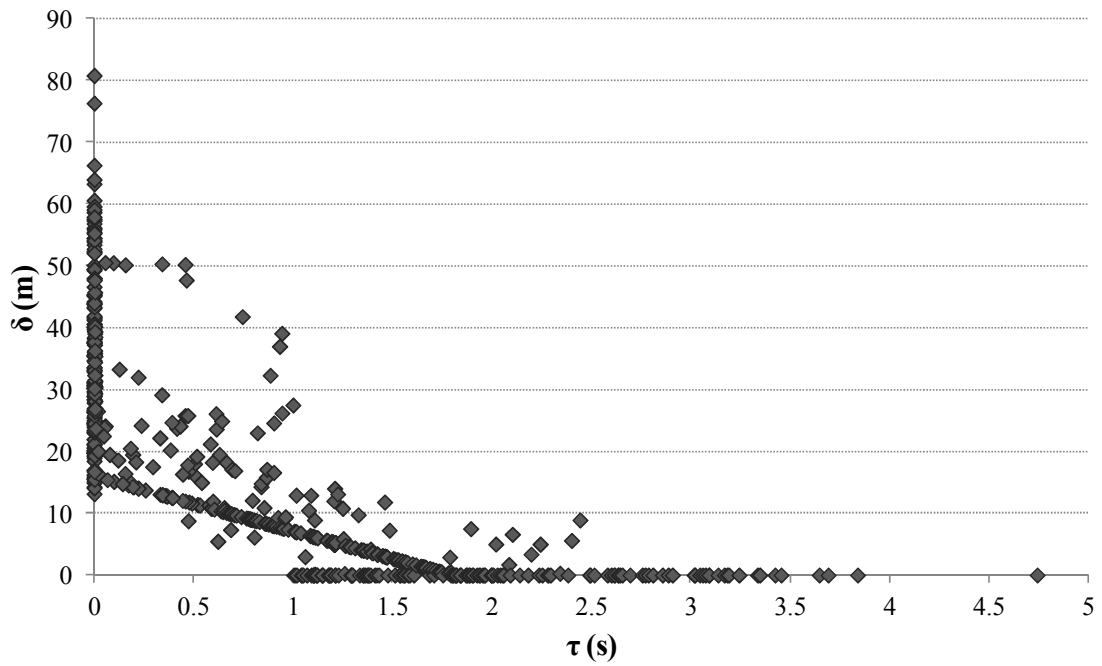


Figure 4.7.1 Relationship between δ and τ

The distribution of δ and τ are firstly estimated separately. The cumulative frequency of δ and τ are shown in Fig. 4.7.2 and Fig 4.7.4, the estimated distribution of δ and τ are shown in Fig. 4.7.3 and Fig. 4.7.5. The estimated distribution of δ is negative exponential distribution of $\exp(0.0605)$ and the estimated distribution of τ is negative exponential distribution of $\exp(1.1341)$.

δ all

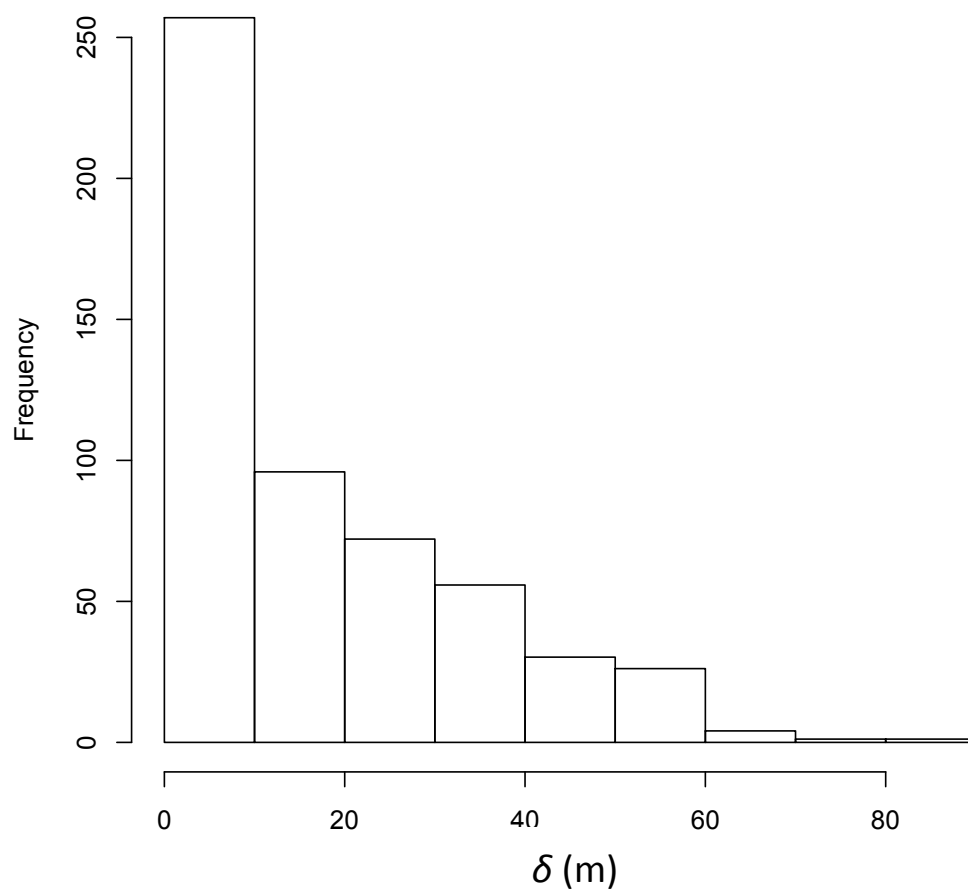


Figure 4.7.2 Cumulative frequency of δ

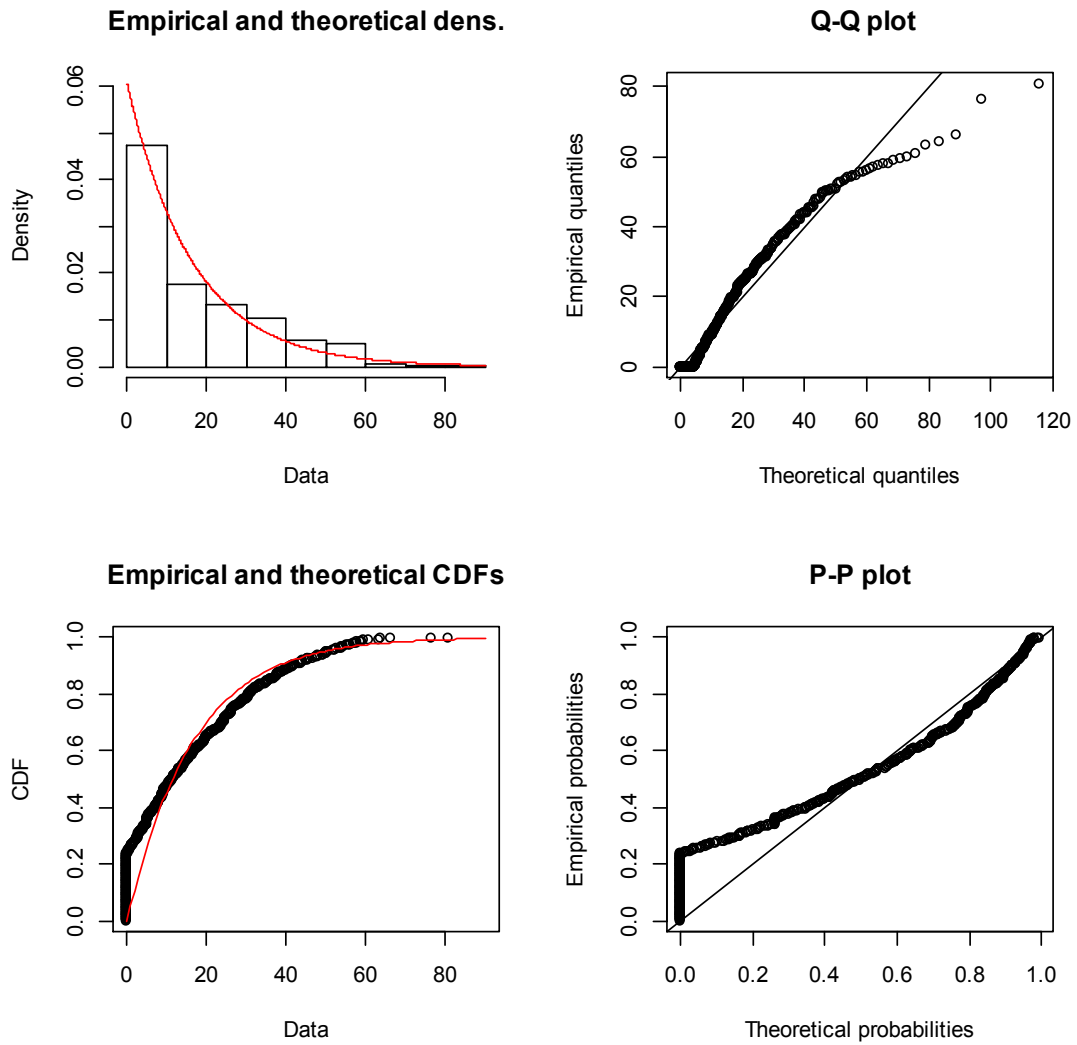


Figure 4.7.3 Estimated distribution of δ

τ all

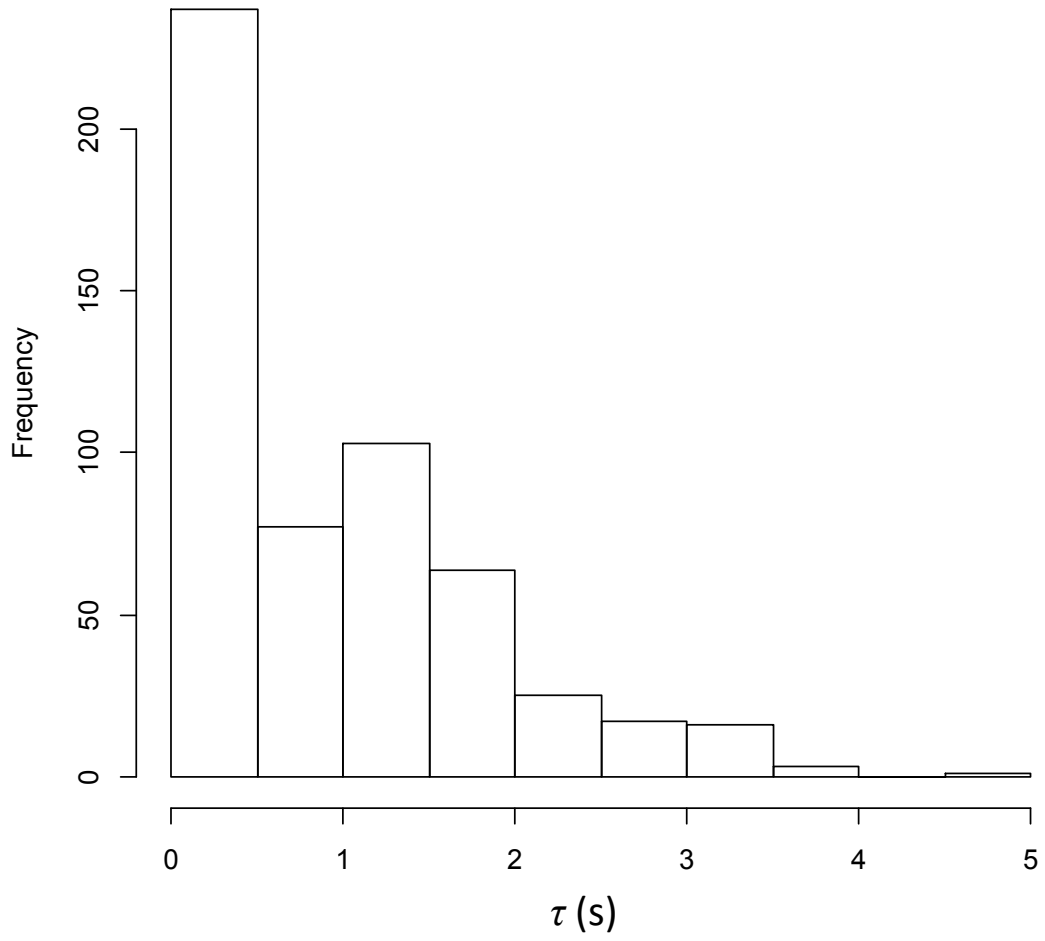


Figure 4.7.4 Cumulative frequency of τ

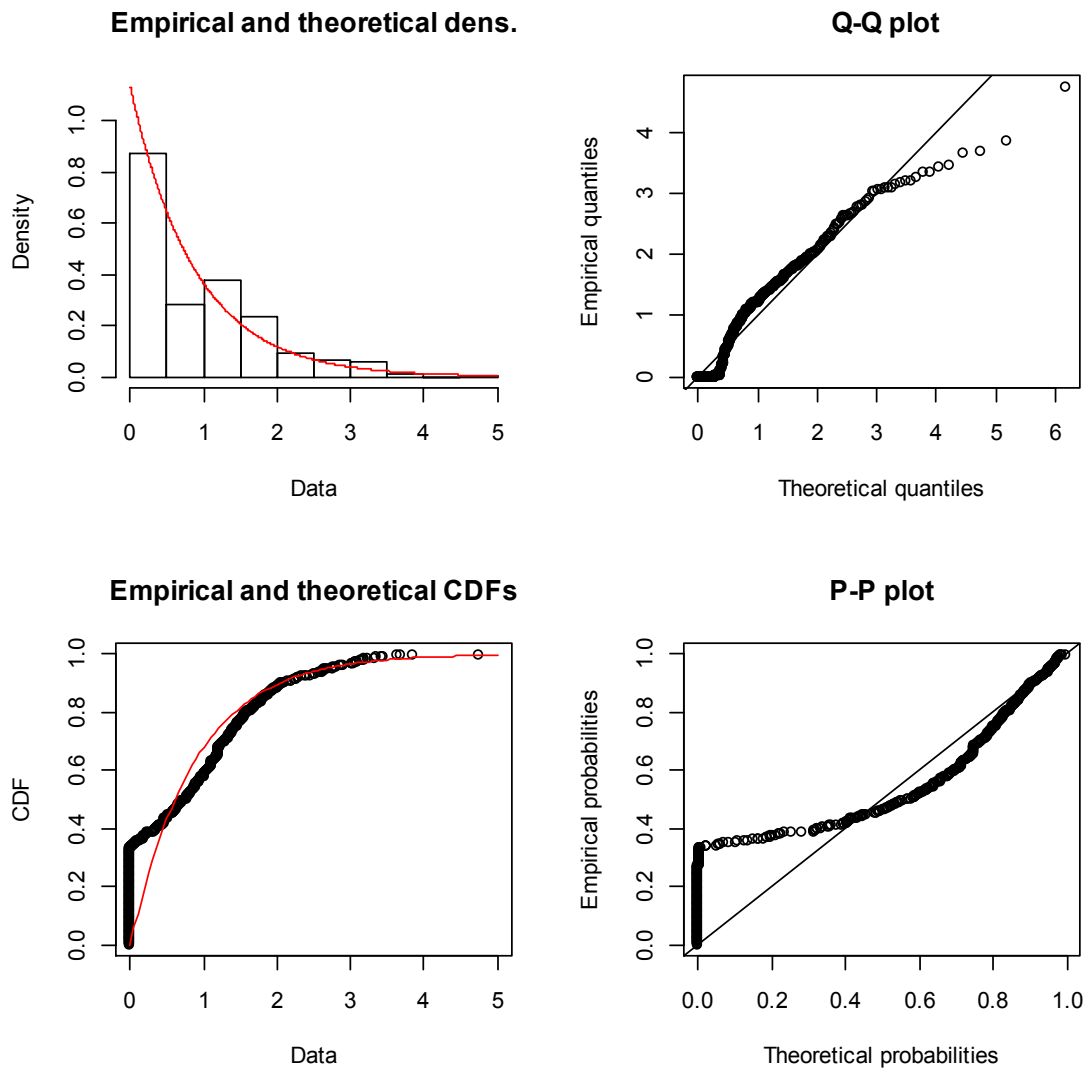


Figure 4.7.5 Estimated distribution of τ

Both δ and τ are of negative exponential distribution. According to this separately estimated distribution of δ and τ , the majority of δ and τ combination is concentrated on the small value range, where the desired spacing is smaller than safety spacing. This doesn't reflect the reality nor other theoretical findings. On the other hand, the high correlation between δ and τ indicates a linear connection between the two parameters. Therefore, they need to be estimated simultaneously in a joint distribution.

The joint cumulative frequency of δ and τ is shown in Fig. 4.7.6. It is consisted with a distribution of δ along the $\tau < 0.2$ range and a distribution of δ and τ at other value ranges. The former composition is a single distribution of δ and the latter composition is a joint distribution of δ and τ . The two parts are shown in Fig. 4.7.7 and Fig. 4.7.8.

δ, τ all parameters

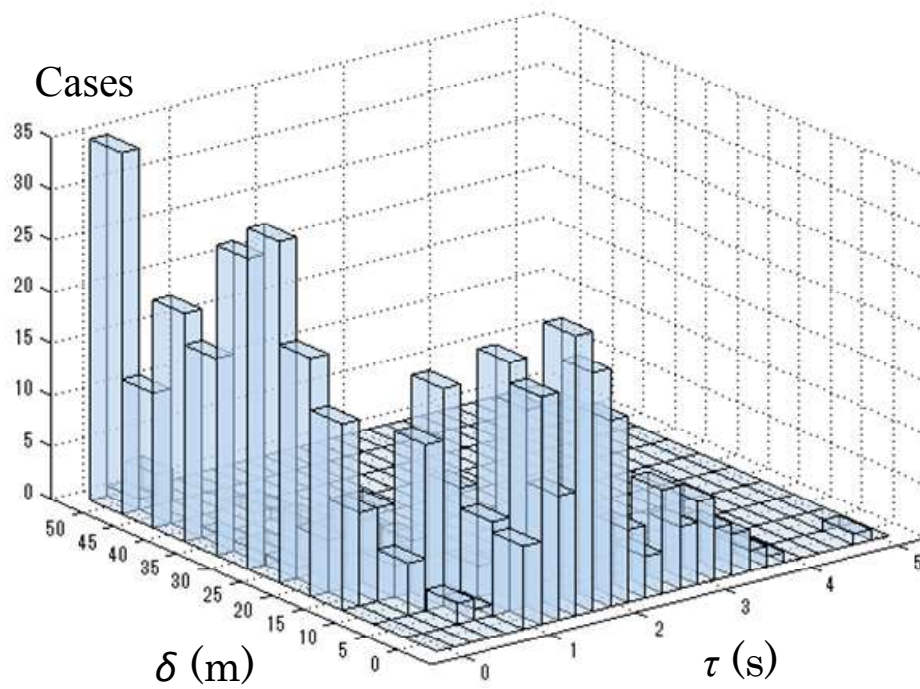


Figure 4.7.6 Joint cumulative frequency of δ and τ

$\delta, \tau (\tau < 0.05)$

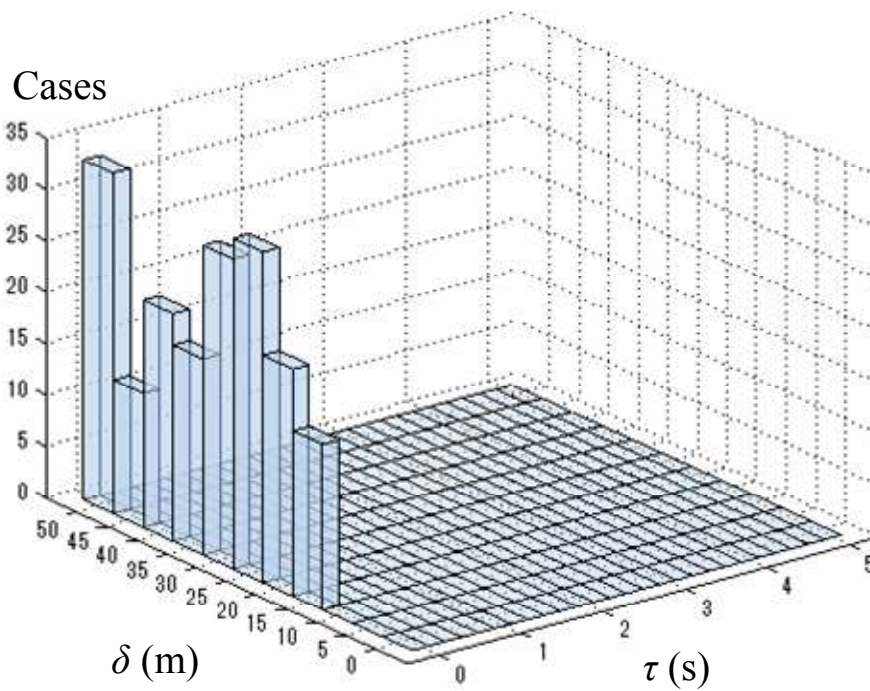


Figure 4.7.7 1st part of the joint distribution of δ and τ

There are 187 cases in the first part of the joint distribution of δ and τ , which consists 34.3% of all

the cases. The distribution of these cases is a shifted gamma distribution $\text{Gamma}(1.8478, 0.1019)$ with an intercept of 16m, which is the minimum spacing of vehicles in congestion. The estimated result is shown in Fig. 4.7.8.

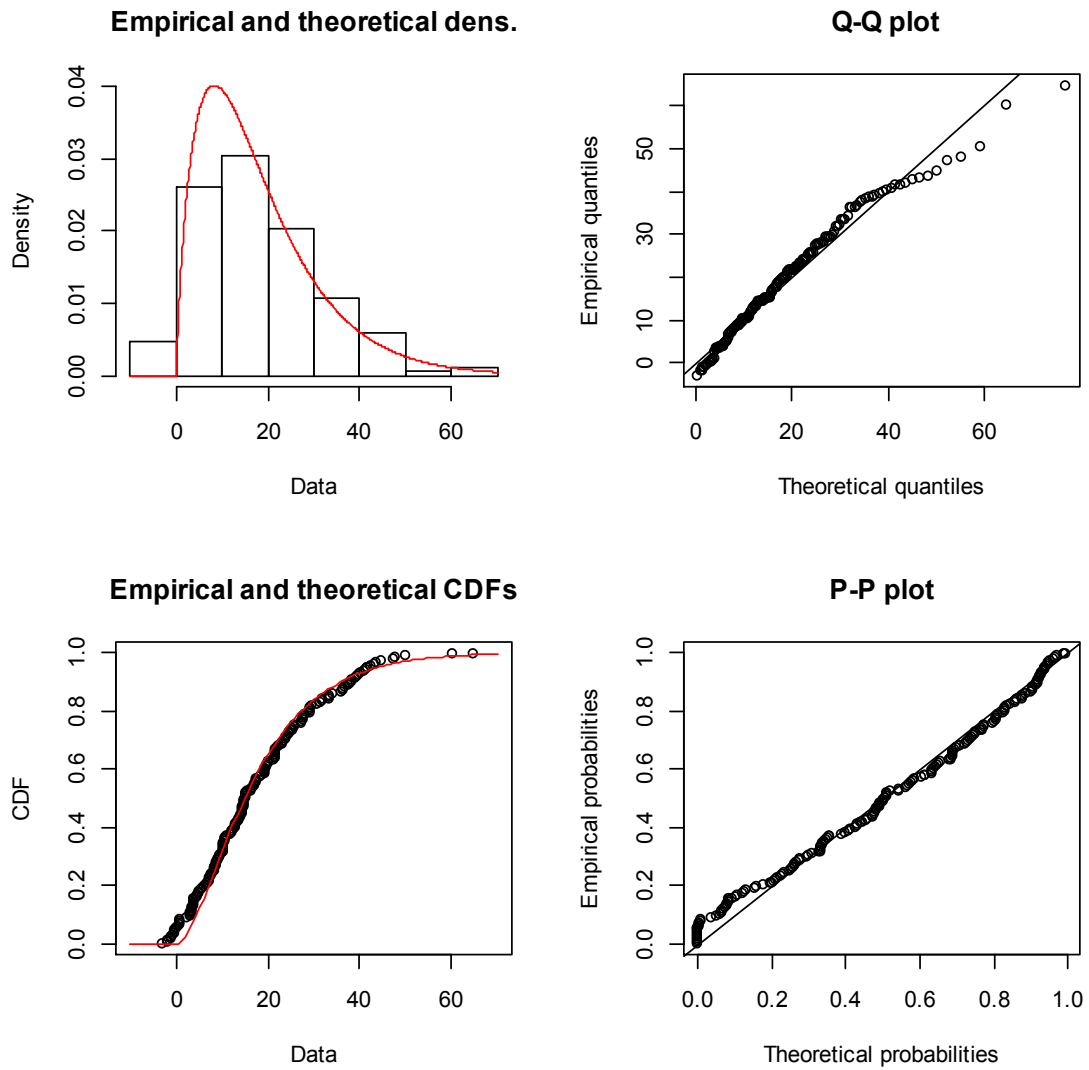


Figure 4.7.8 Distribution estimation of the 1st part of the joint distribution of δ and τ . The rest 356 cases are in the second part of the joint distribution which is a bivariate gamma distribution.

$\delta, \tau (\tau > 0.05)$

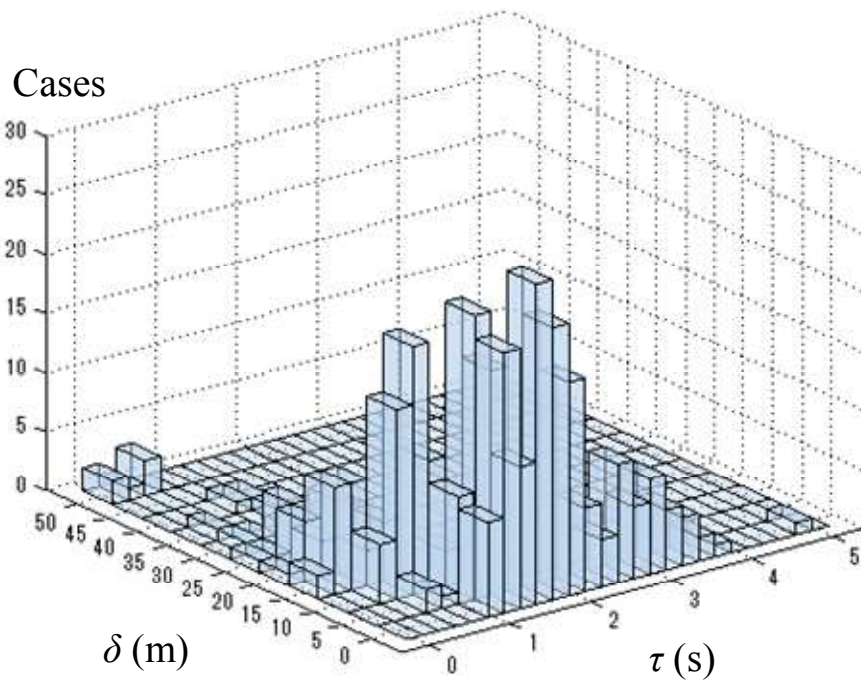


Figure 4.7.9 2nd part of the joint distribution of δ and τ

τ 2nd part of joint distribution

δ 2nd part of joint distribution

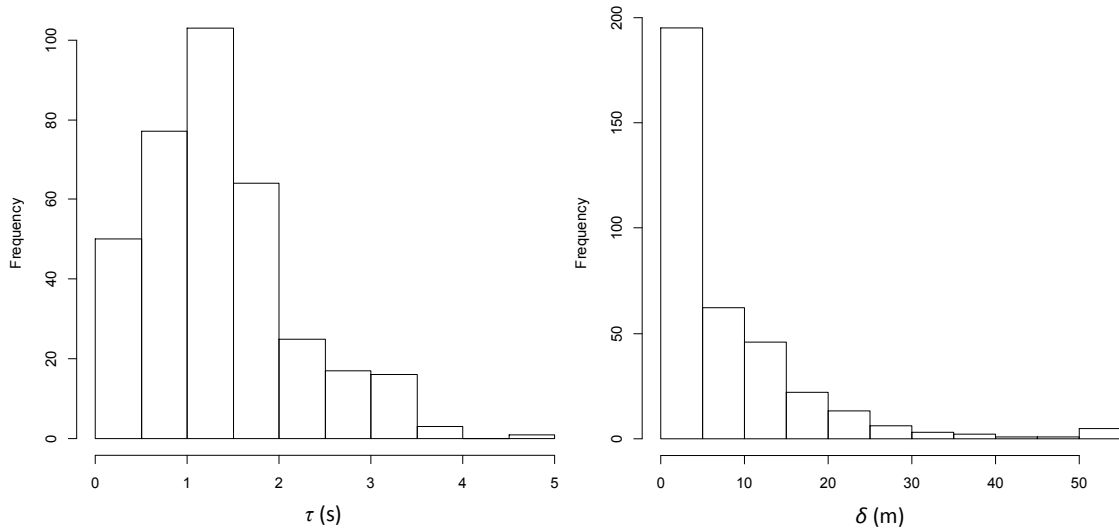


Figure 4.7.10 Cumulative frequency of δ and τ of 2nd part of joint distribution

$(5 - \tau)/5$ and δ obeys a bivariate Mckay's gamma distribution of $p=0.4954, q=4.4171, a= 0.1476$.

Probability function

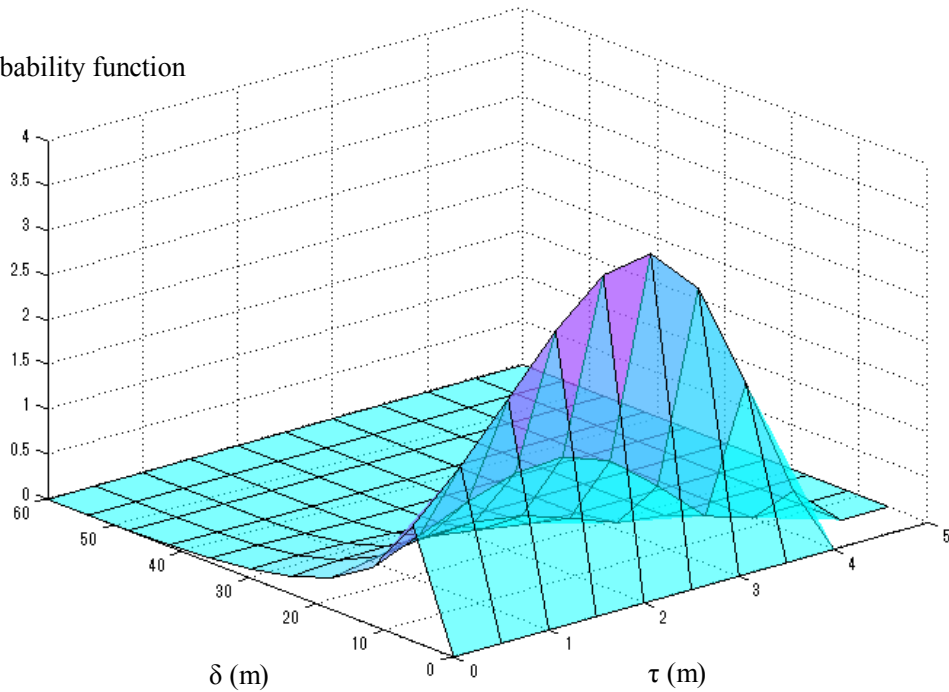


Figure 4.7.11 Estimated joint distribution of δ and τ of 2nd part of joint distribution

Pearson's r of α_1 and Δt is -0.4354 and significant. It's not a very strong linear correlation. But Helly (Helly, 1959) suggested that negative correlation existed in α_1 and Δt . Therefore, they are further studied. Other correlations are small enough to be neglected. Fig. 4.7.2 shows the relationship between all α_1 and Δt . When $\Delta t > 1.1s$, most α_1 is smaller than 0.5 . on the other hand, when $\Delta t \leq 1.1s$, α_1 is more evenly distributed within the value range.

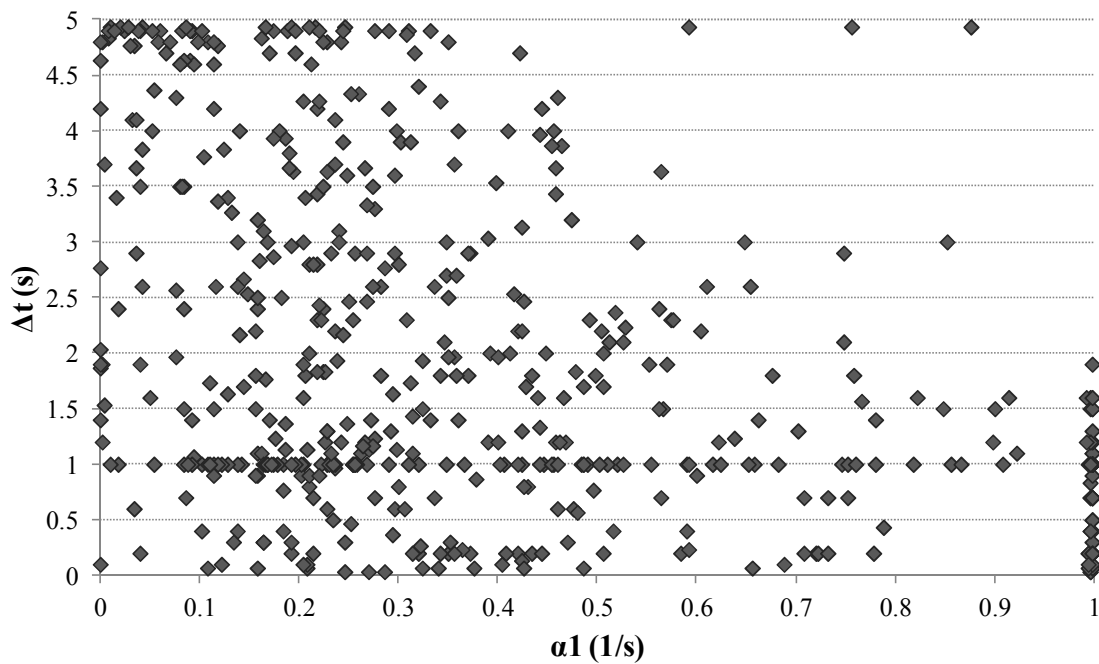


Figure 4.7.12 Relationship between α_1 and Δt

The distribution of other parameters is separately estimated. As shown in Fig. 4.7.12 and 4.7.13, α_1 is of a Gamma distribution: Gamma(1.689480,4.266007).

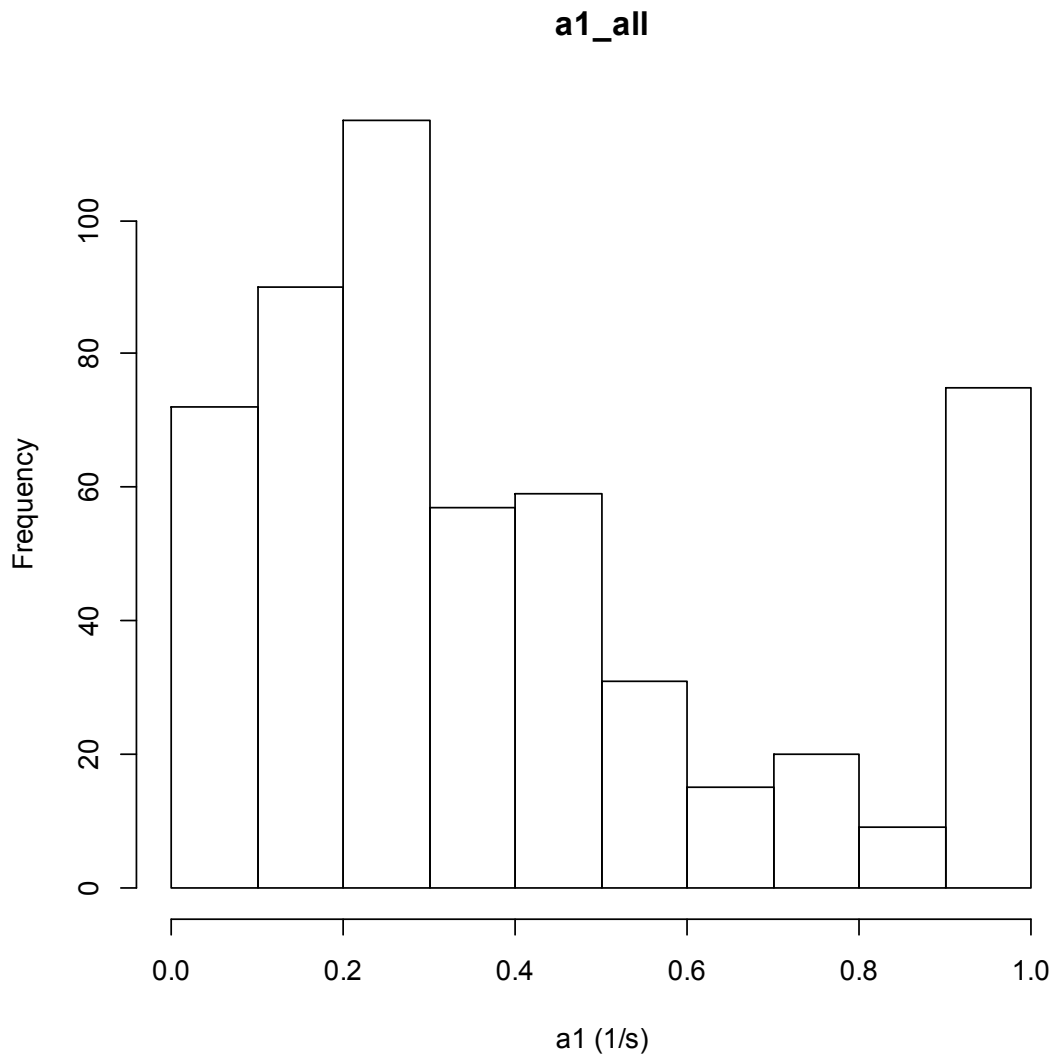


Figure 4.7.13 Cumulative frequency of α_1

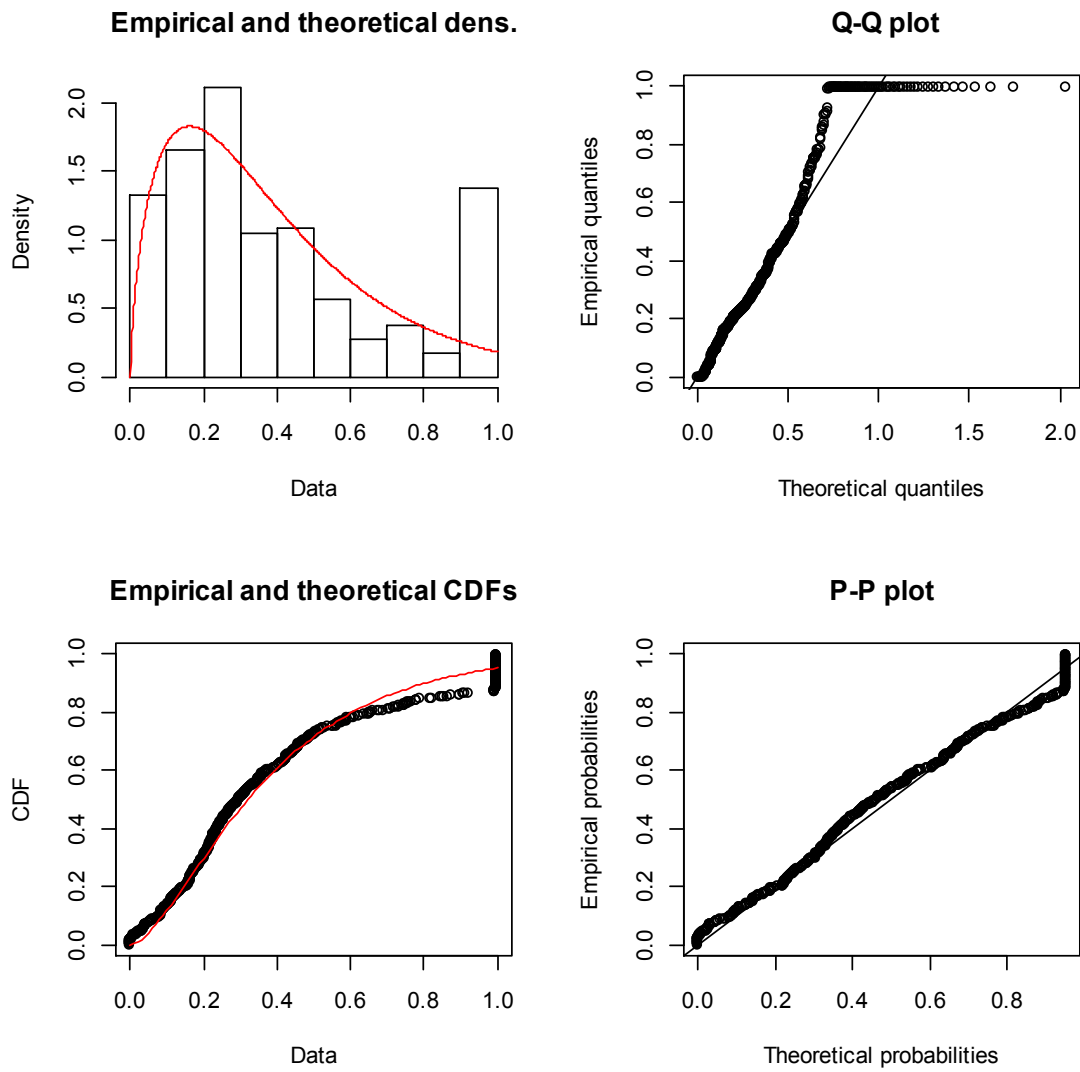


Figure 4.7.14 Distribution of α_1
 As shown in Fig. 4.7.14 and 4.7.15, α_2 is of a negative exponential distribution: $\text{Exp}(26.05566)$.

a2_all

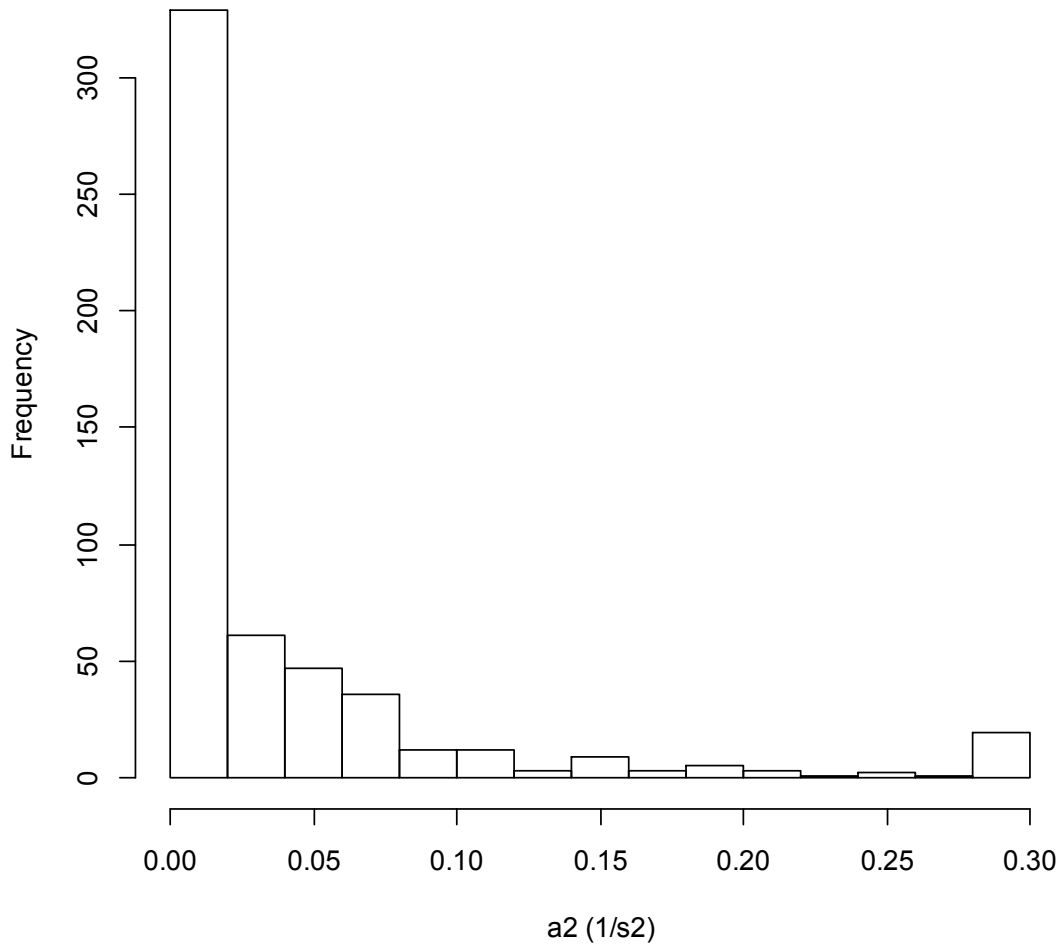


Figure 4.7.15 Cumulative frequency of a_2

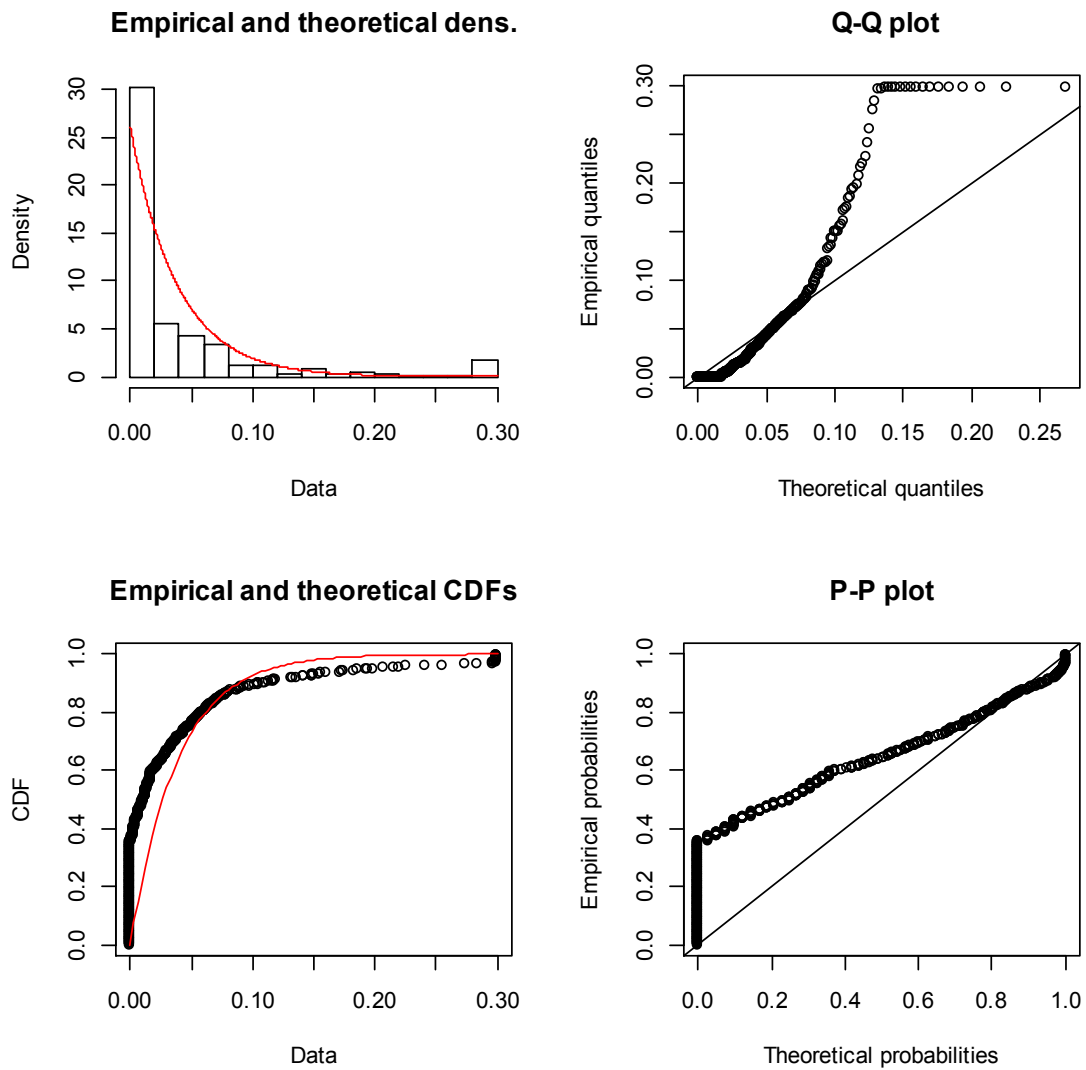


Figure 4.7.16 Distribution of α_2

As shown in Fig. 4.7.16 and 4.7.17, β is of a beta exponential distribution: Beta (0.3568652, 0.2196074).

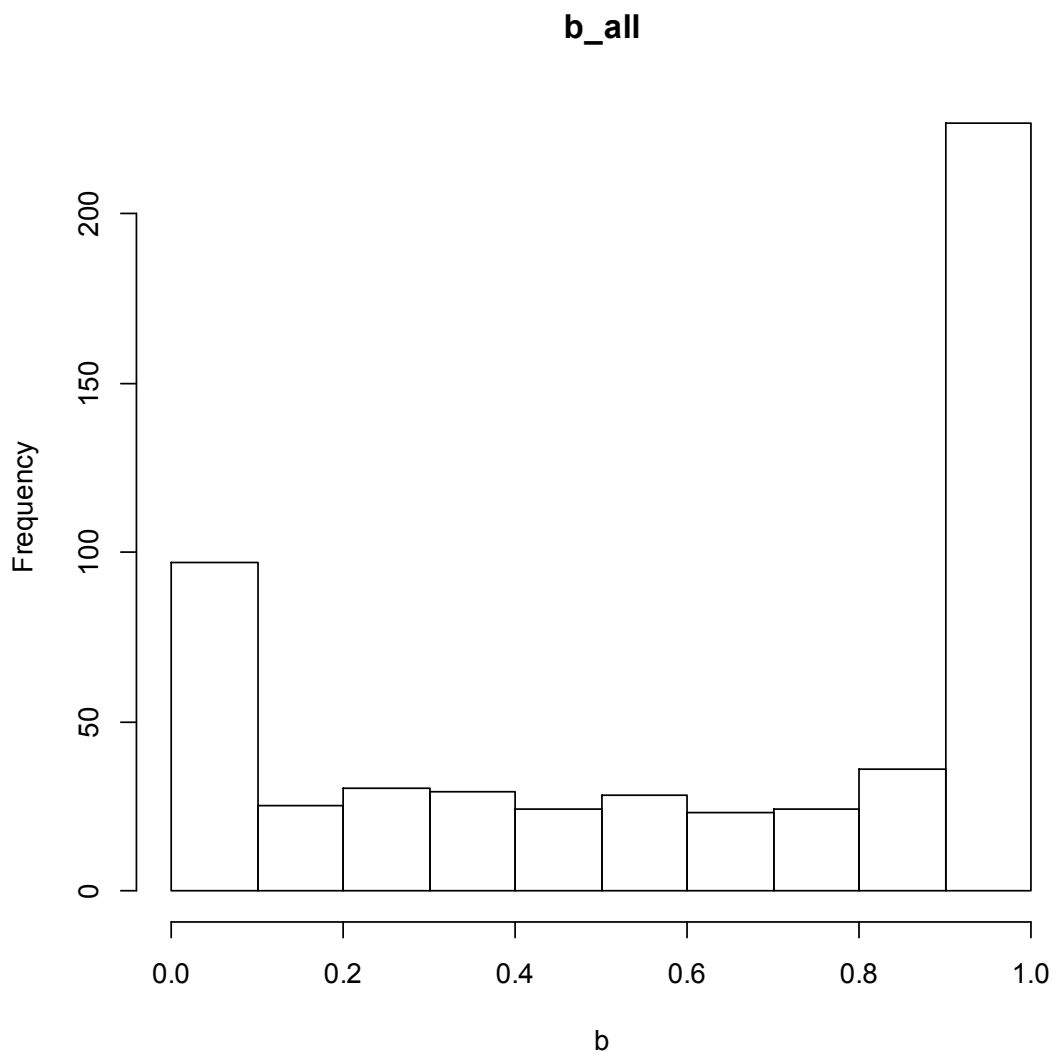


Figure 4.7.17 Cumulative frequency of β

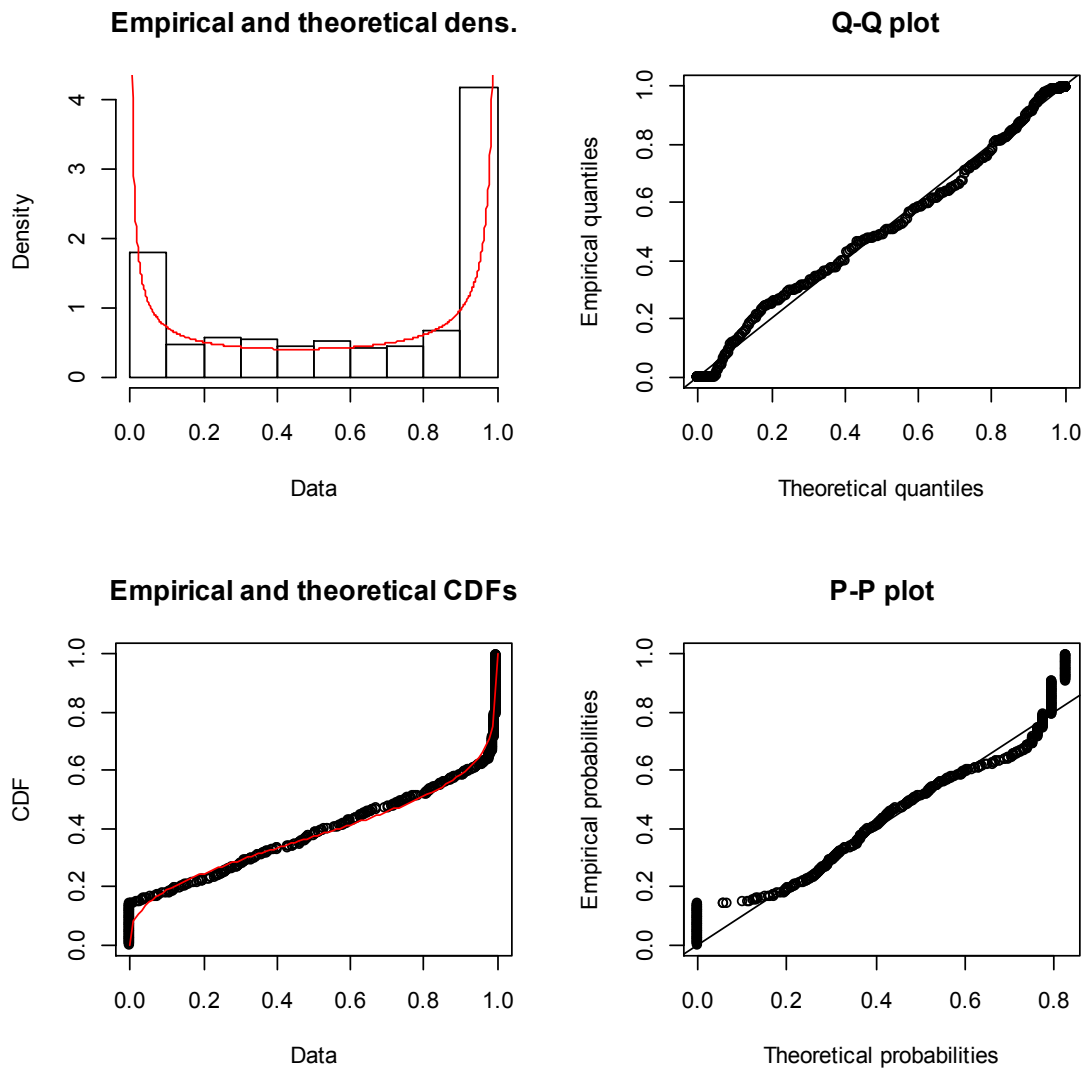


Figure 4.7.18 Distribution of β

As shown in Fig. 4.7.18 and 4.7.19, Δt is of a Gamma exponential distribution: Gamma(1.7081664, 0.8675302).

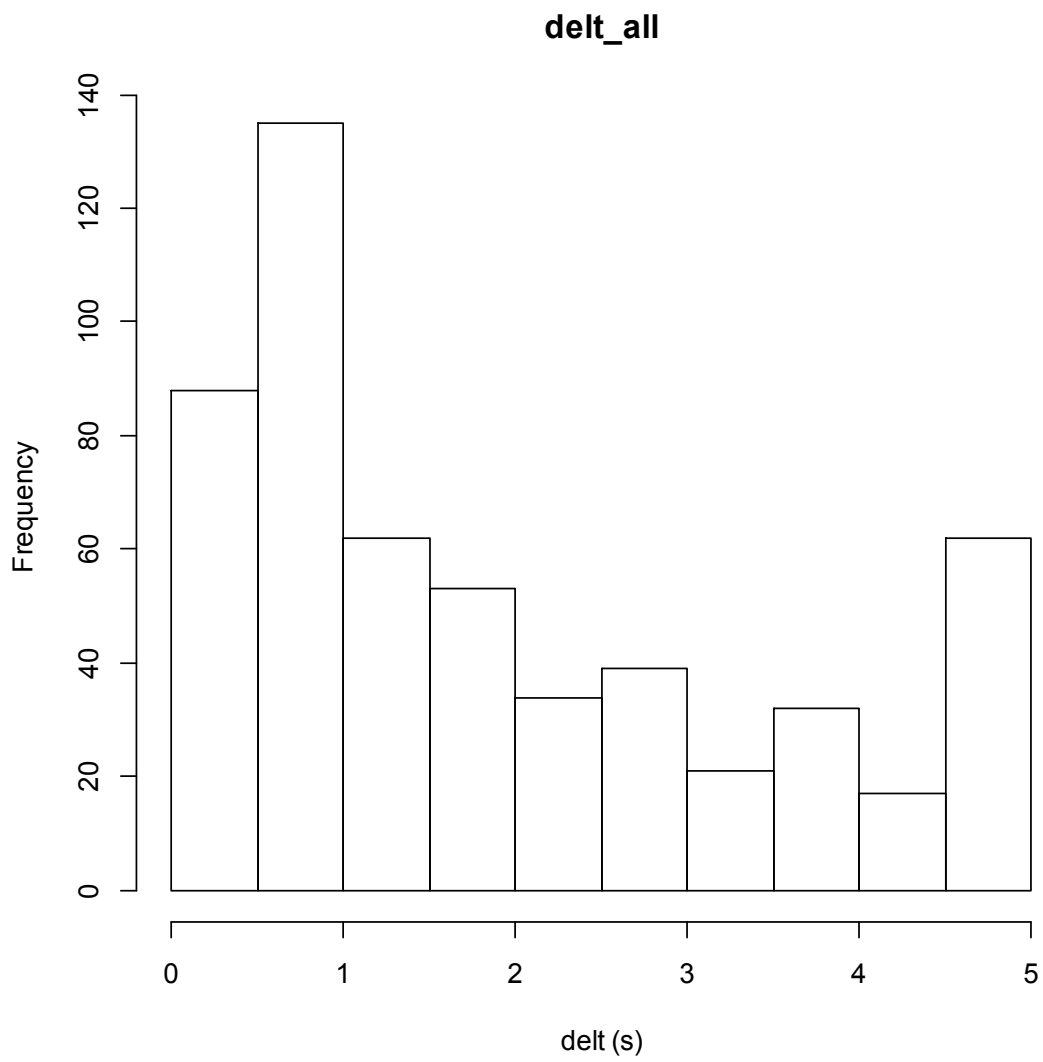


Figure 4.7.19 Cumulative frequency of Δt

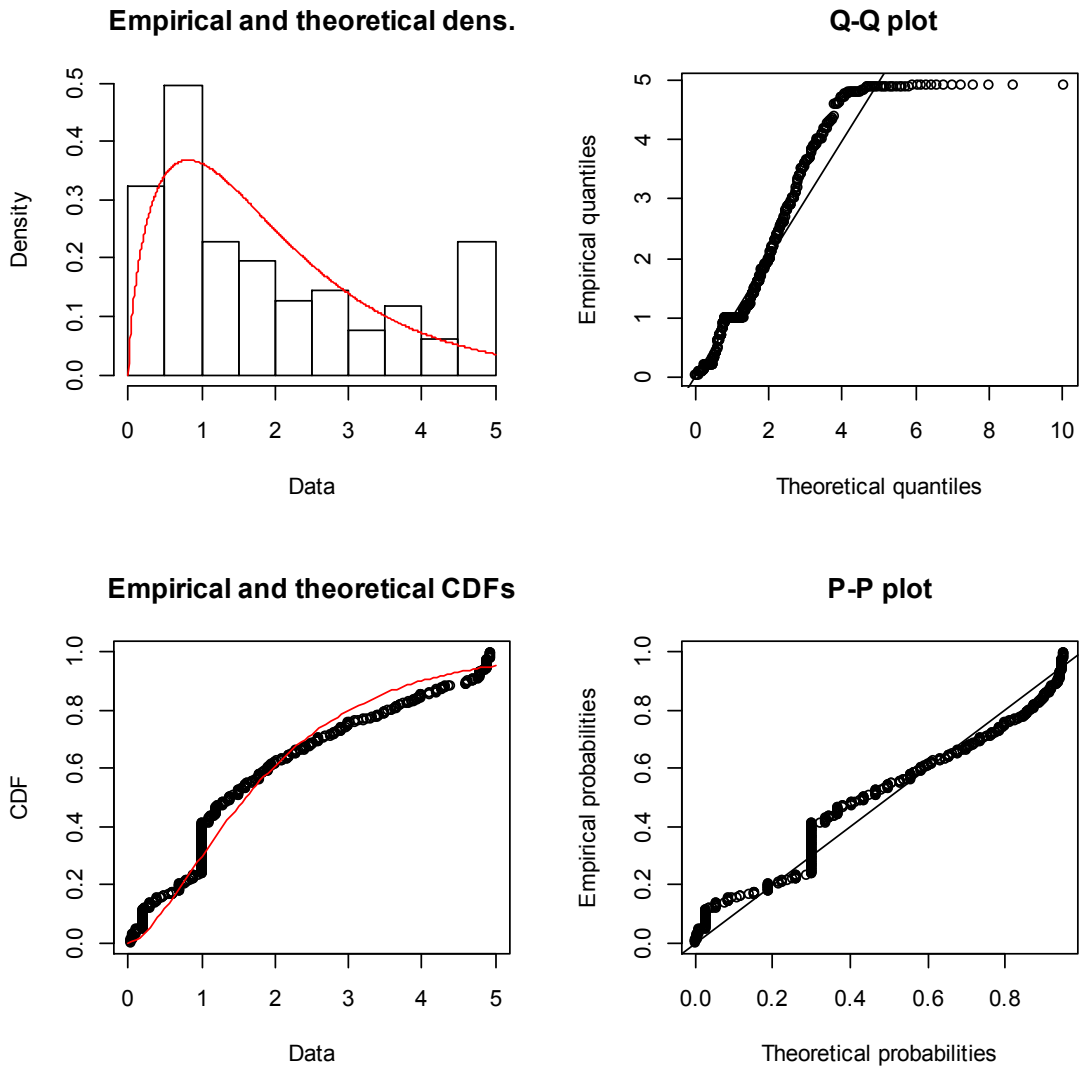


Figure 4.7.20 Distribution of Δt

These distributions of parameters are utilized in the simulation in 5.5 and the result is compared with that of the estimated parameters.

5 Simulation

A simulation of car-following behavior during congestion formation at sag section is presented in this chapter. First, the basic settings of simulation is presented in 5.1. The basic settings and scenarios are introduces in 5.2. The real and acceptable leading car behavior is tested and defined in 5.3. The validation of simulation is carried out with the indicator of congestion occurrence probability in 5.4. The simulation with car-following parameter distribution and its comparison with estimated parameters is presented in 5.5. The results in simulation are concluded in 5.6.

5.1 Simulation modeling structure

Traffic simulation is a methodology to reproduce traffic conditions by building computational models. It is especially suitable for the analysis and prediction of traffic condition resulting from complex interacting human behaviors. A simulation platform is made with the car-following model and parameters distribution obtained from field observation to reproduce the traffic condition during congestion formation and predict the probability of congestion occurrence under certain traffic demand.

The congestion formation at sag section is a result of the interaction of car-following behavior among passing vehicles. Every observed behavior and congestion condition is unique and irreproducible in field observation. Difference observation consists different driving behavior as well as traffic demand and other flow condition. Traffic simulation is used as a platform to reproduce the traffic flow condition with same set of driving behavior to analyze the interaction among drivers and its impact on congestion formation.

In traffic simulation, the car-following behavior during congestion formation is simulated with the car-following behavior model and its parameters distribution. The initial speed and leading car behavior is studied in sensitivity analysis.

A Graphical User Interface (GUI) is designed for two functions in this simulation. It makes the performance of simulation model visible so that the verification and calibration of car-following behavior is obvious and easily understandable. The other function is to show not only the congestion occurrence and vehicles behavior inside congestion, but also the temporal-spatial evolution of traffic flow condition during congestion formation.

5.2 Basic settings and input scenarios

A microscopic traffic simulation is made to simulate the car-following behavior at a single lane basic segment. Car-following model and parameter distribution are the results shown in previous chapters. The vertical layout of the road is designed as the same as the observation site on Tomei expressway (See Fig. 5.2.1).

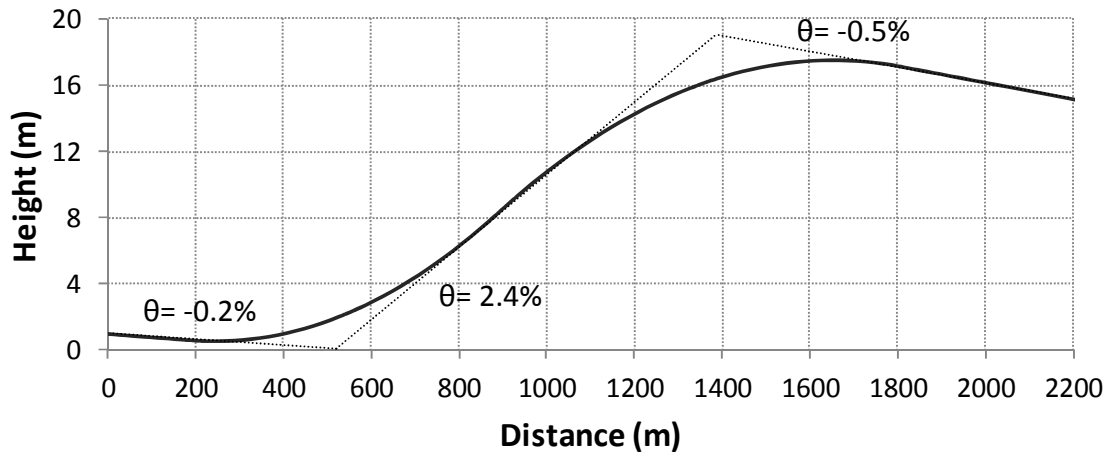


Figure 5.2.1 Vertical layout of road segment in simulation

The initial speed is 28m/s (100.8 km/h) based on the average speed of vehicles before bottleneck. Vehicles entering the road segment randomly with a headway of negative exponential distribution. The criterion for congestion is two adjacent vehicles' speed smaller than 40km/h as presented in 3.3. The independent vehicles are those with spacing bigger than 80m or headway bigger than 3s as presented in 3.3.

Initial settings are designed and studied to ensure good performance of simulation model. A feedback circle is utilized for this purpose (See Fig. 5.2.2).

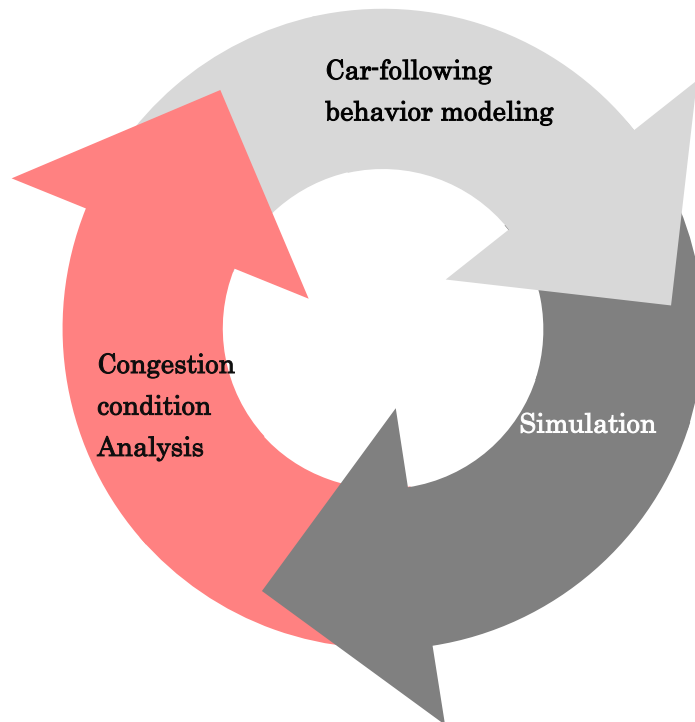


Figure 5.2.2 Feedback circle of simulation

The behavior of leading vehicle has an important affect on every following vehicle in the platoon. It is generally recognized that speed perturbation of leading vehicle amplifies to following vehicles in a platoon. It is the amplification of this speed perturbation having an obvious affect on flow condition of the platoon. So this initial speed perturbation is recognized as the key cause of congestion occurrence at sag sections. Therefore, three kind of leading vehicle's behavior were designed as function to reflect the actual deceleration of platoon leading vehicle and describe the speed perturbation at sag sections based on the observed behavior analysis in 4.6. The detailed explanation and function are shown in 5.3.

Type1. The constant sag affected driver:

The constant sag affected driver decelerates when entering into sag section and keep the constant deceleration in the sag section. The function describing the constant sag affected driver is presented as following.

Type 2. The non speed restore driver:

The non restore driver decelerates when entering into sag section and realizing the speed drop after the reaction time. The non restore driver accelerates to balance the sag effect but not trying to restore its initial speed after realizing the sag effect. The function describing the non speed restore driver is presented as following.

Type 3. The speed restore driver:

The speed restore driver decelerates when entering into sag section and realizing the speed drop after

the reaction time. The speed restore driver tries to accelerate to restore its initial speed after realizing the sag effect. The function describing the speed restore driver is presented as following. The acceleration part to restore initial speed is proposed by Newell et.,al. (Newell & Frank, 2002).

The influence of these three kinds of leading behavior is studied in 5.3.

Vehicles are design to enter simulation in equilibrium travelling state. In the car-following model, vehicles react to the speed difference and space headway with leading vehicle with a reaction time lag. If initial speed difference and acceleration of following has an initial value, it will cause change in later space headway and amplifies through car-following model. Therefore, the initial speed difference and acceleration of following vehicles were set to 0 when they entered the simulation.

The initial space headway was driven with function 1 where at the entering time of following vehicle t_1 :

$$\begin{cases} v_0(t_1) - v_1(t_1) = 0 \\ a_1(t_1) = 0 \end{cases} \quad 14$$

Therefore, initial space headway and time headway are:

$$\begin{cases} s_1^*(t_1) = \delta + \tau \cdot v_1(t_1) \\ t_{hdw} = \frac{s_1^*(t_1)}{v_0(t_1)} \end{cases} \quad 15$$

Apart from the initial entering state, vehicles will not immediately react to leading vehicle due to reaction time in car-following model. The accumulation of time lag in reaction may cause instable behaviors like collision and rapid acceleration in the platoon. To eliminate this effect, vehicles should react according to car-following model immediately after entering the sag section. The car-following model is set to function when the entering time of the leading vehicle t_0 is bigger than the entering time of the following vehicle t_1 minus reaction time Δt . The assumption is illustrated in Fig. 5.2.3).

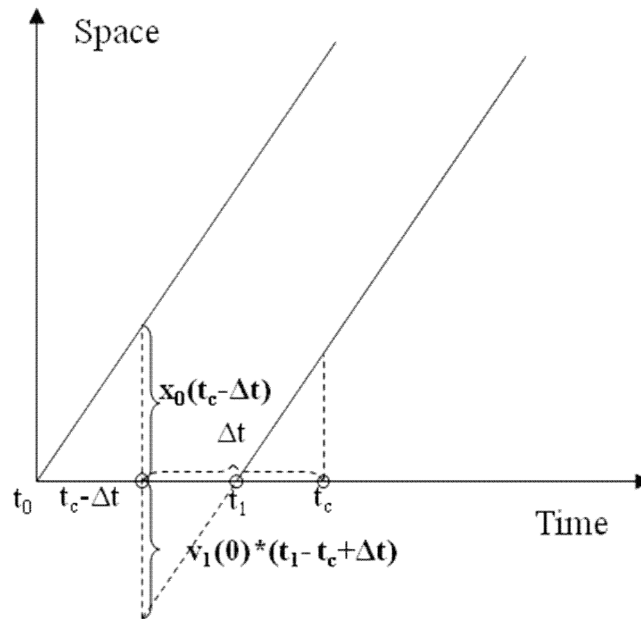


Figure 5.2.3 Calculation of car-following behavior entering simulation

The simulation is stopped under 2 circumstances: 1. If the spacing between two adjacent vehicles is smaller than 4m, which indicates a rear end collision between vehicles; 2. If the speed is zero, which indicates a sudden stop of the vehicle. Collision and sudden stop are due to the linear construction of car-following model that the parameters combination may generate some very sensitive vehicles that accelerate and decelerate too rapidly when congestion is forming. In real world, this will not happen. Vehicles will adjust to the traffic condition much more smoothly. Therefore, collision and sudden stops are recognized as aggressive behavior and excluded from analysis.

5.3 Leading car behavior

The three types of leading car are studied in simulation. The real and acceptable leading car behavior is determined based on the result. Five minutes traffic demand is input to the simulation with headways of negative exponential distribution. The lower limit of headways is 0.8s, which is equivalent to the theoretical capacity of a single lane, 4000 veh/h. The simulation iterates for a time step of 0.1 second. 500 random seeds are simulated in one scenario.

Type 1. The constant sag affected driver:

The constant sag affected driver decelerates when entering into sag section and keep the constant deceleration in the sag section. The function describing the constant sag affected driver is presented as following.

$$a_1(t + \Delta t) = \begin{cases} 0 & t < t_s \\ -\beta g[\sin \theta(t) - \sin \theta_u] & t \geq t_s \end{cases} \quad 16$$

where,

t_s – Time entering the sag section;

$\theta(t)$ – Percentage road slope;

Type 2. The non speed restore driver:

The non restore driver decelerates when entering into sag section and realizing the speed drop after the reaction time. The non restore driver accelerates to balance the sag effect but not trying to restore its initial speed after realizing the sag effect. The function describing the non speed restore driver is presented as following.

$$a_1(t + \Delta t) = \begin{cases} 0 & t < t_s \\ -\beta g[\sin \theta(t) - \sin \theta_u] & t_s \leq t < t_s + \Delta t \\ 0 & t \geq t_s + \Delta t \end{cases} \quad 17$$

Type 3. The speed restore driver:

The speed restore driver decelerates when entering into sag section and realizing the speed drop after the reaction time. The speed restore driver tries to accelerate to restore its initial speed after realizing the sag effect. The function describing the speed restore driver is presented as following. The acceleration part to restore initial speed is proposed by Newell (Newell & Frank, 2002).

$$a_1(t + \Delta t) = \begin{cases} 0 & t < t_s \\ -\beta g[\sin \theta(t) - \sin \theta_u] & t_s \leq t < t_s + \Delta t \\ [v_1(0) - v_1(t)]/\tau_0 - \beta g[\sin \theta(t) - \sin \theta_u] & t \geq t_s + \Delta t \end{cases} \quad 18$$

Some of the combinations of estimated parameters of car-following model reflecting only random driving behavior are suitable for simulation even though they have passed the calibration carried out in chapter 4. Also as mentioned in 5.1, there may be aggressive cases such as collision and sudden stop cases. Preliminary simulation is carried out to study the aggressive in car-following parameters estimated for individual drivers as well as the propagation of initial speed drop. 5-min traffic flow is generated with all the cars of the same car-following behaviors. All 543 cars are simulated.

The three types of leading car behavior reflecting three different assumptions of initial speed reduction are: 1. Constant reduction; 2. No speed restore; and 3. Speed restore.

The trajectories diagram of a simulation case with leading car behavior of type 1 is shown as Fig. 5.3.1. No congestion occurs in 5-min simulation.

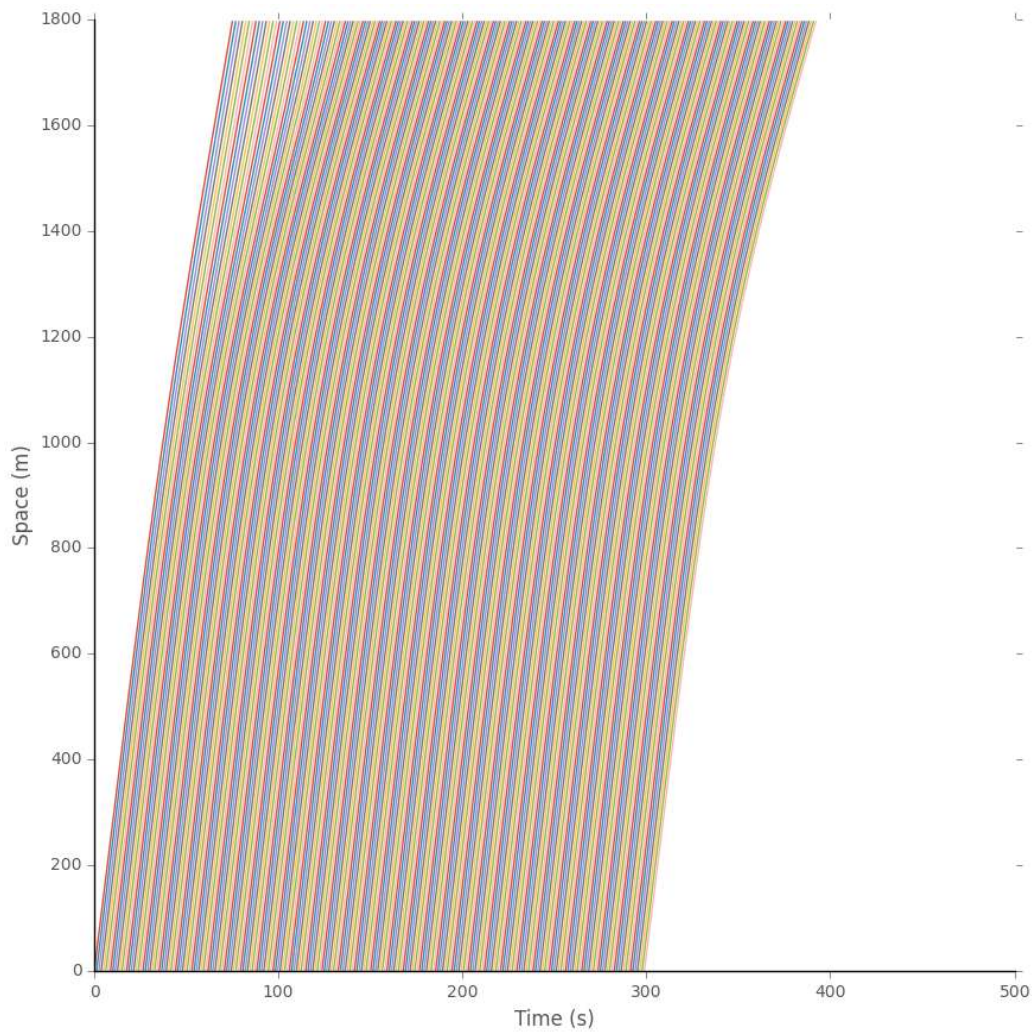


Figure 5.3.1 Trajectory of car No.28 with leading car behavior type 1

The time-speed diagram of the leading car and 9 following cars in a simulation case with leading car behavior of type 1 is shown as Fig. 5.3.2. The bold red line is leading vehicle. The time propagation of initial speed drop can be observed. Reaction time can be observed between the following vehicles. Speed drop is smaller in following cars than in leading car before 40s, which indicates this driver gently react to the initial speed drop. But in order to avoid collision, this driver decelerates more severely when it realize the constant deceleration of leading car as shown in following cars deceleration after 40s. This driver decelerates gently enough so that there is no congestion occurred in 5-min simulation.

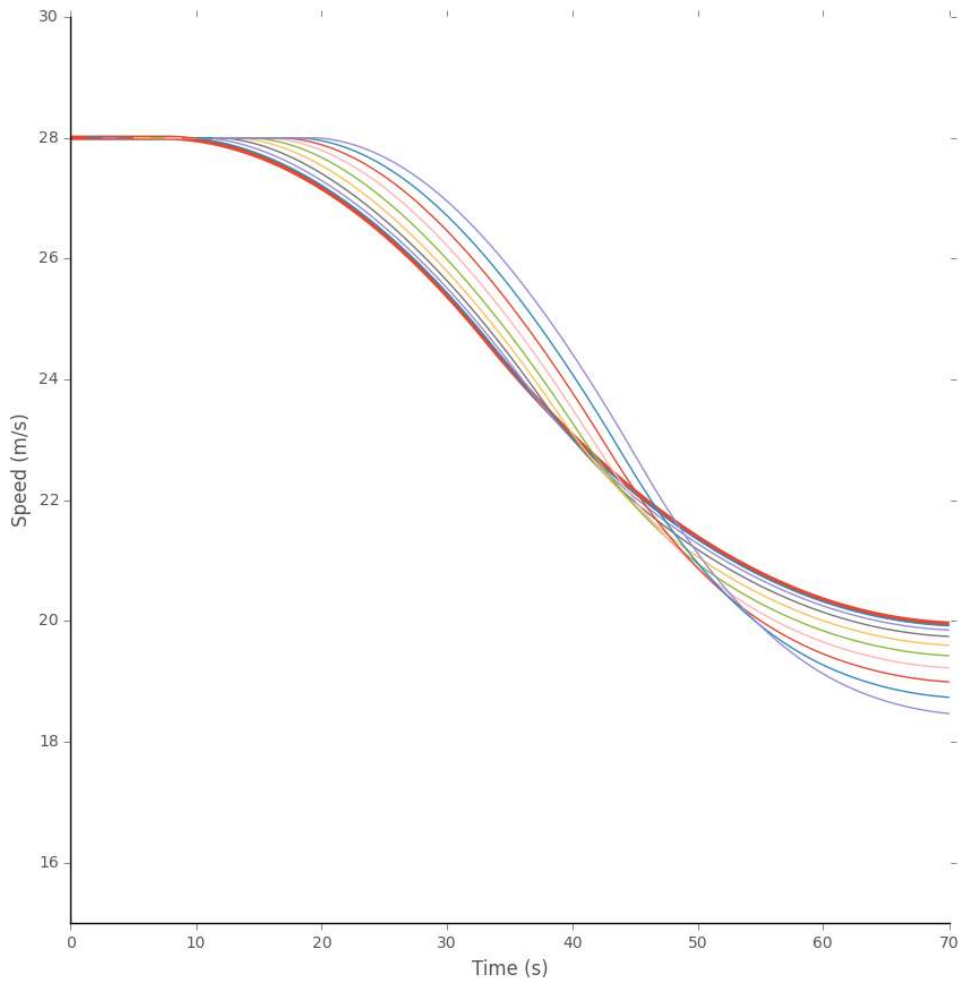


Figure 5.3.2 Time-speed diagram of car No.28 with leading car behavior type 1

The space-speed diagram of the leading car and 9 following cars in a simulation case with leading car behavior of type 1 is shown as Fig. 5.3.3. The spatial propagation of initial speed drop can be observed. The instant speed at fixed location in the sag section decreases when following cars passing.

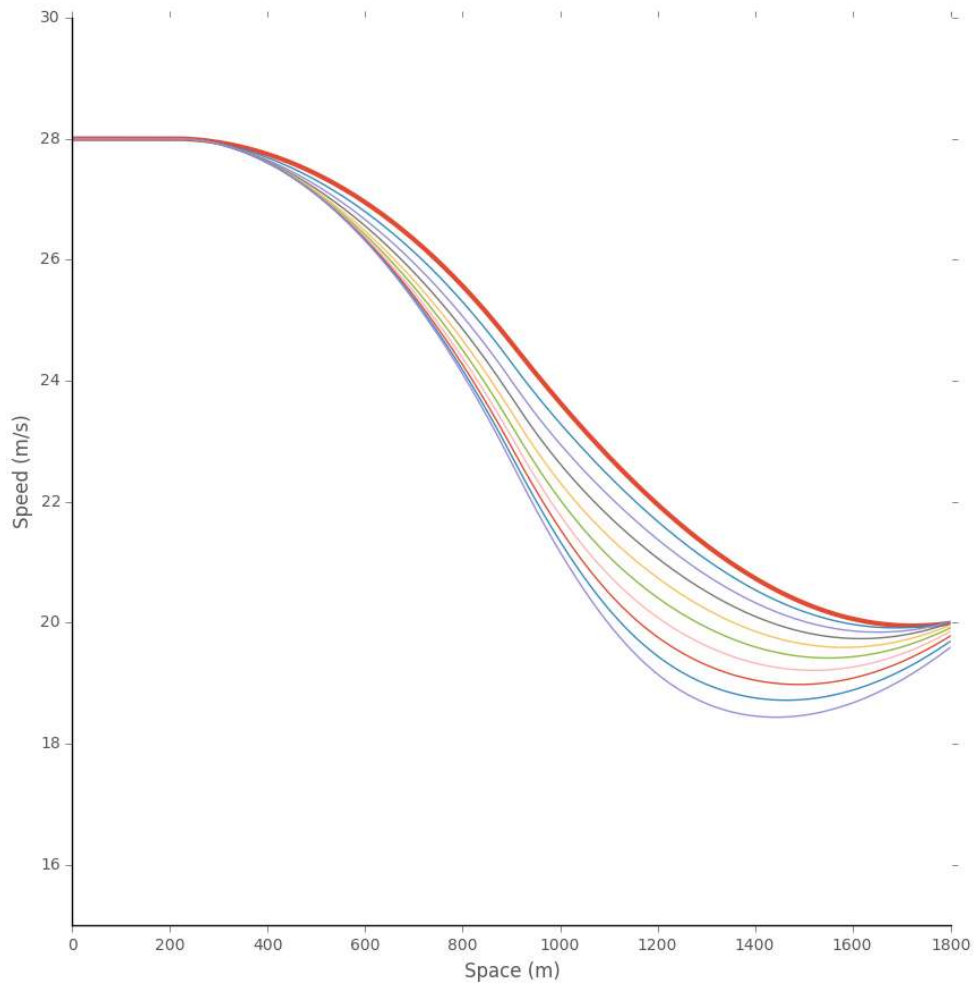


Figure 5.3.3 Space-speed diagram of car No.28 with leading car behavior type 1

The trajectories diagram of a simulation case with leading car behavior of type 2 is shown as Fig. 5.3.4. No congestion occurs in 5-min simulation.

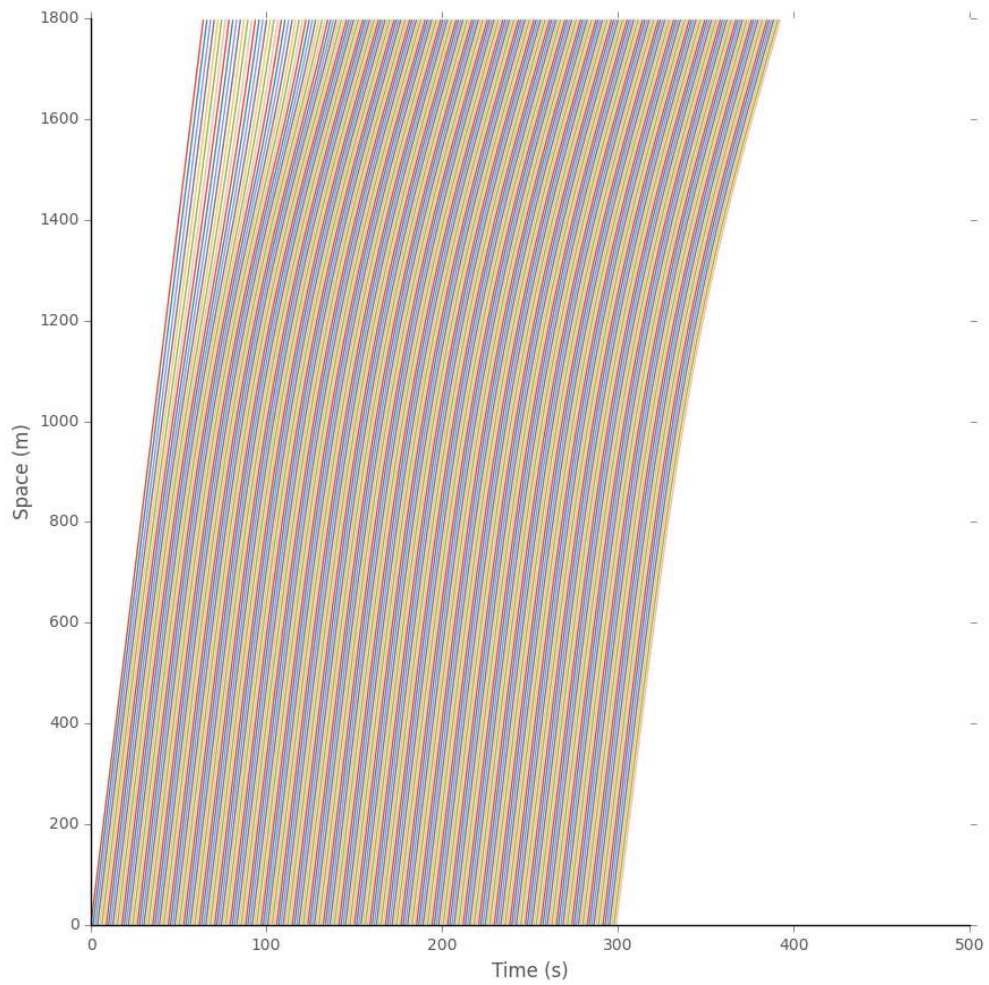


Figure 5.3.4 Trajectory of car No.28 with leading car behavior type 2

The time-speed diagram of the leading car and 9 following cars in a simulation case with leading car behavior of type 2 is shown as Fig. 5.4.5. The perturbation of initial small deceleration along cars in the platoon can be obviously observed.

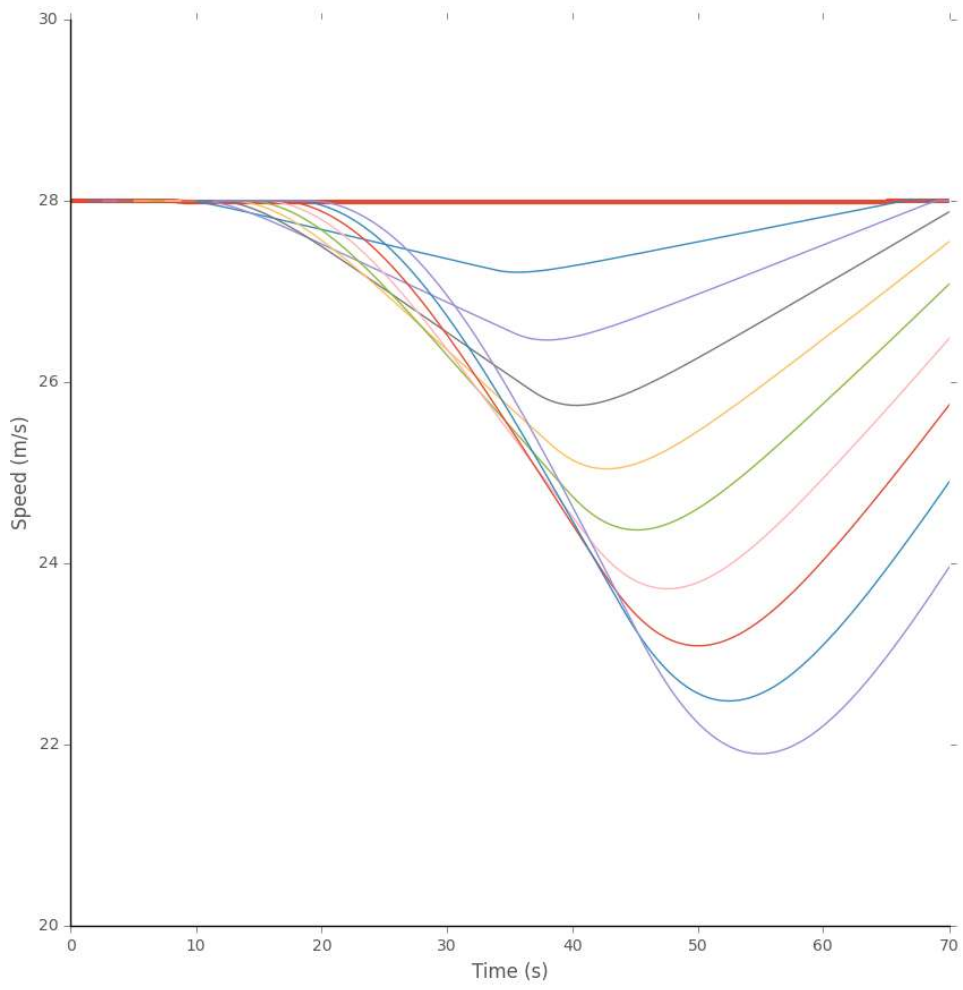


Figure 5.3.5 Time-speed diagram of car No.28 with leading car behavior type 2

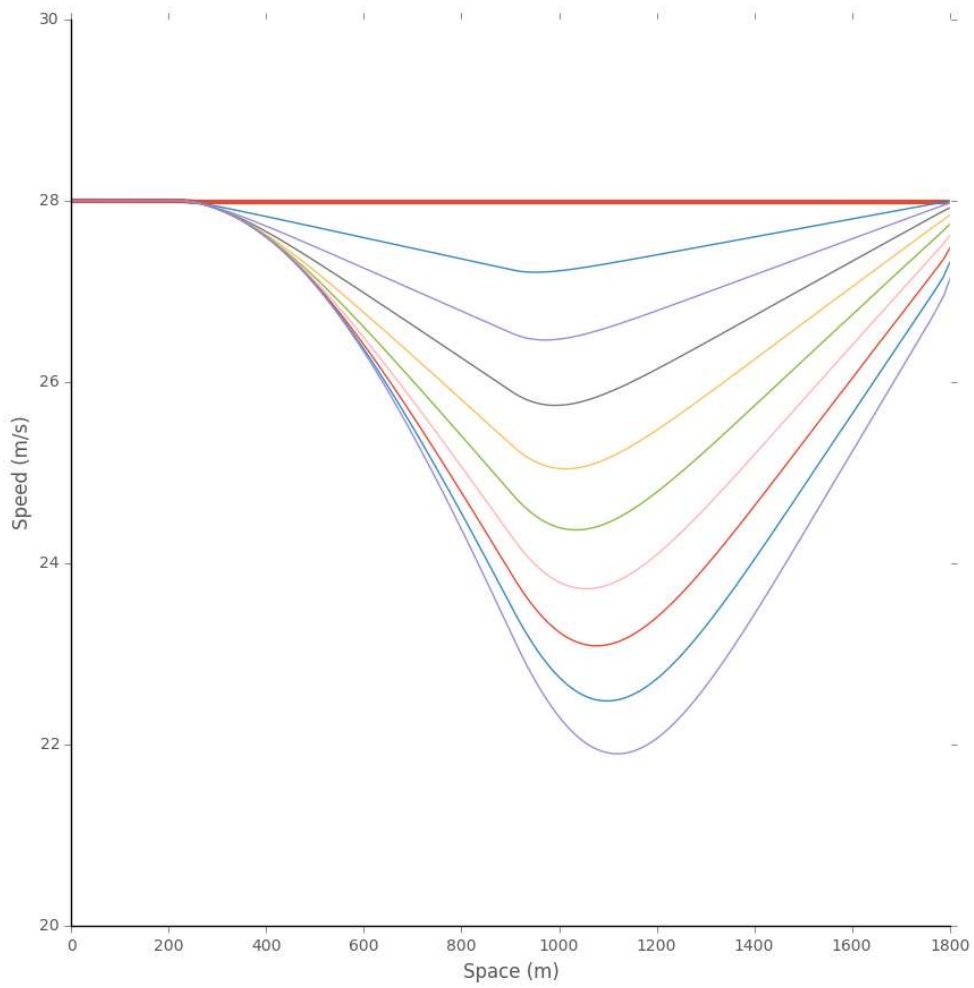


Figure 5.3.6 Space-speed diagram of car No.28 with leading car behavior type 2

The trajectories diagram of a simulation case with leading car behavior of type 3 is shown as Fig. 5.3.7. No congestion occurs in 5-min simulation.

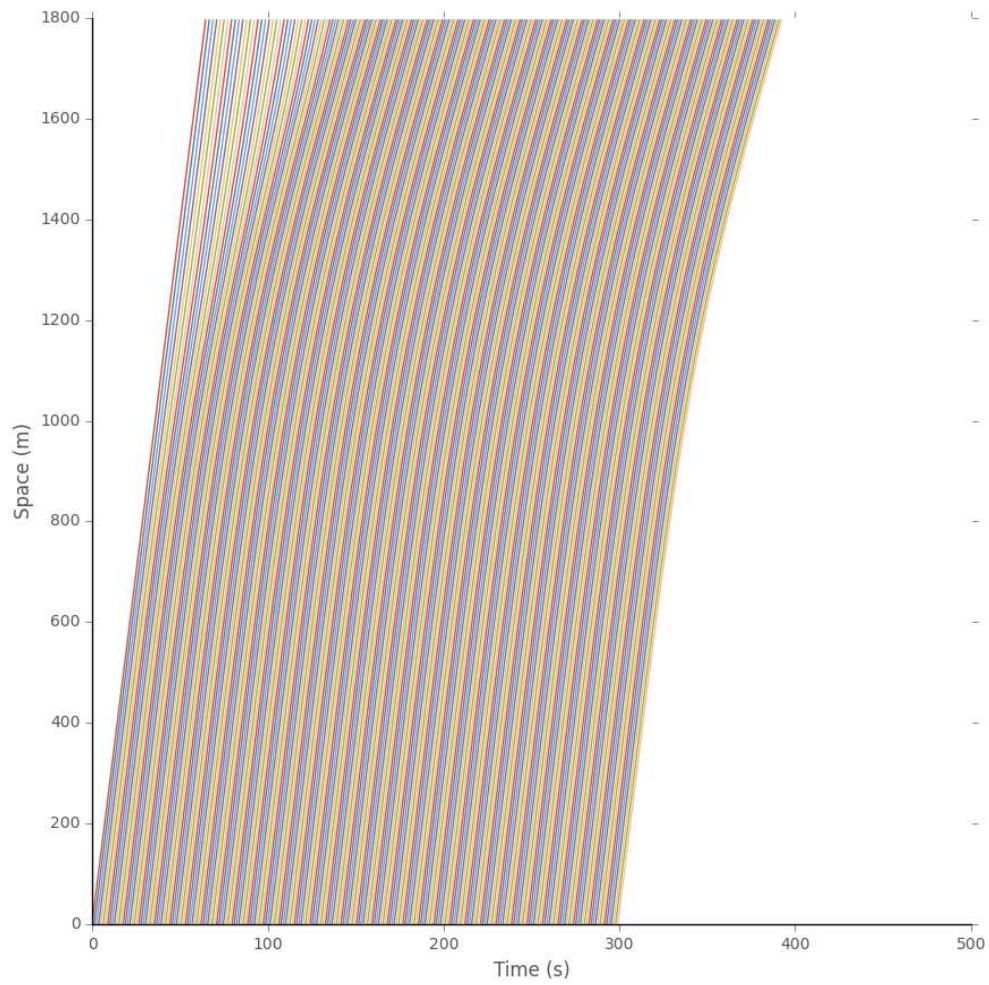


Figure 5.3.7 Trajectory of car No.28 with leading car behavior type 3

The time-speed diagram of the leading car and 9 following cars in a simulation case with leading car behavior of type 3 is shown as Fig. 5.3.8. The perturbation of initial small deceleration along cars in the platoon can be obviously observed.

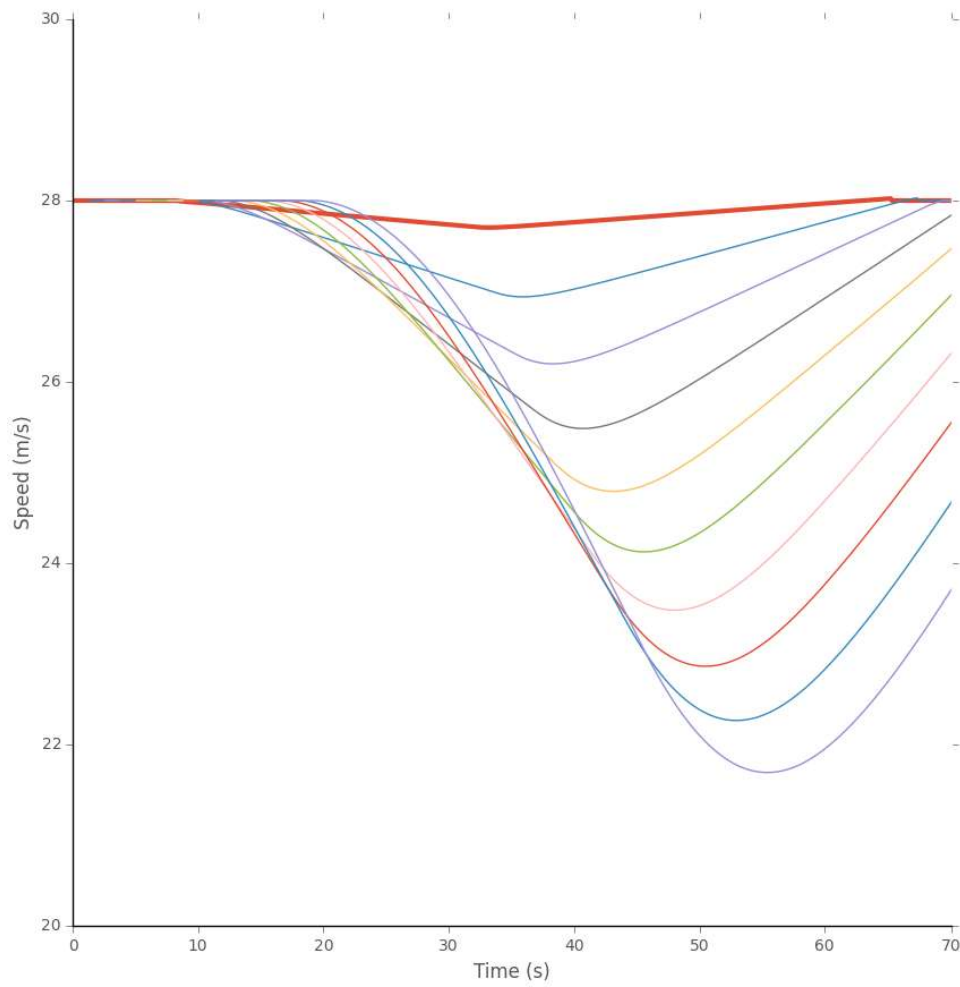


Figure 5.3.8 Time-speed diagram of car No.28 with leading car behavior type 3

The space-speed diagram of the leading car and 9 following cars in a simulation case with leading car behavior of type 3 is shown as Fig. 5.3.9.

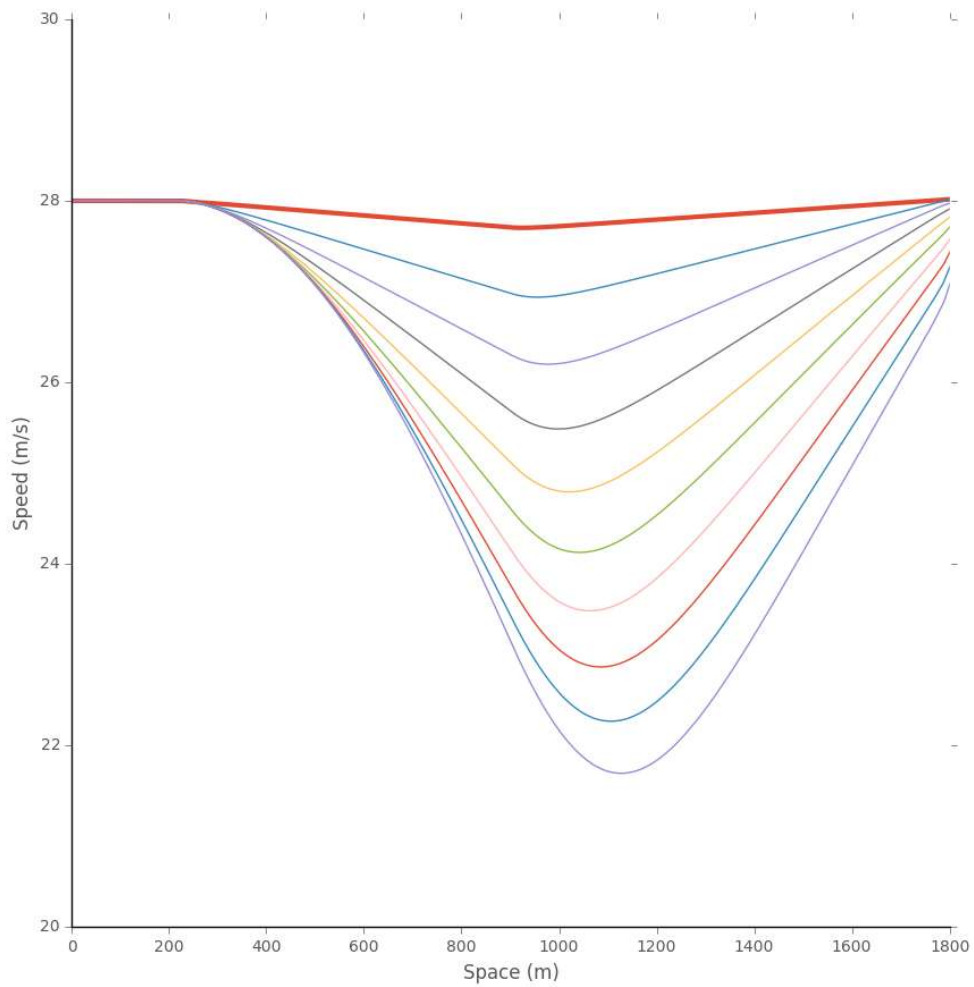


Figure 5.3.9 Space-speed diagram of car No.28 with leading car behavior type 3

Same following drivers' reaction is observed under three different leading car behaviors.

On the other hand, negligent drivers tend to cause congestion in traffic flow. The time space diagram of an example negligent driver is shown in Fig. 5.3.10.

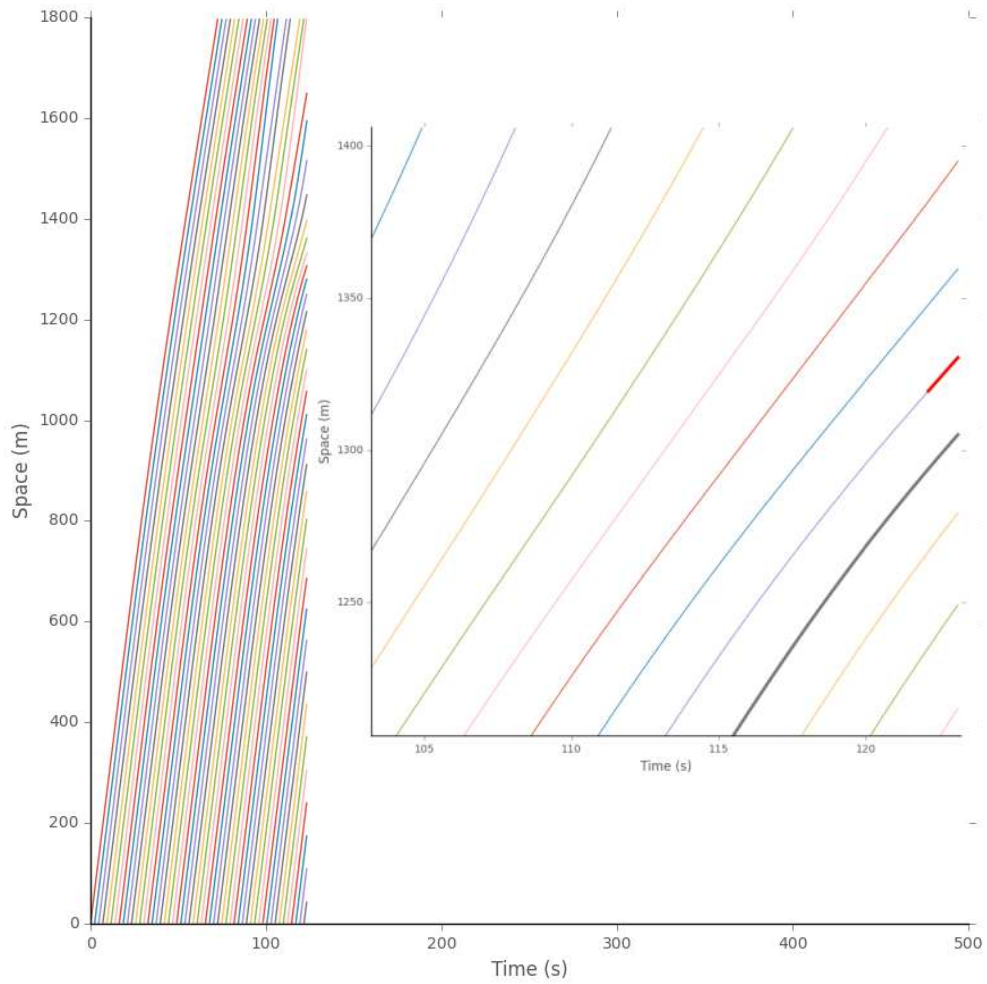


Figure 5.3.10 Example of negligent drivers

The number of aggressive cases, negligent cases and nimble cases under different leading car behavior are shown as Fig. 5.3.11.

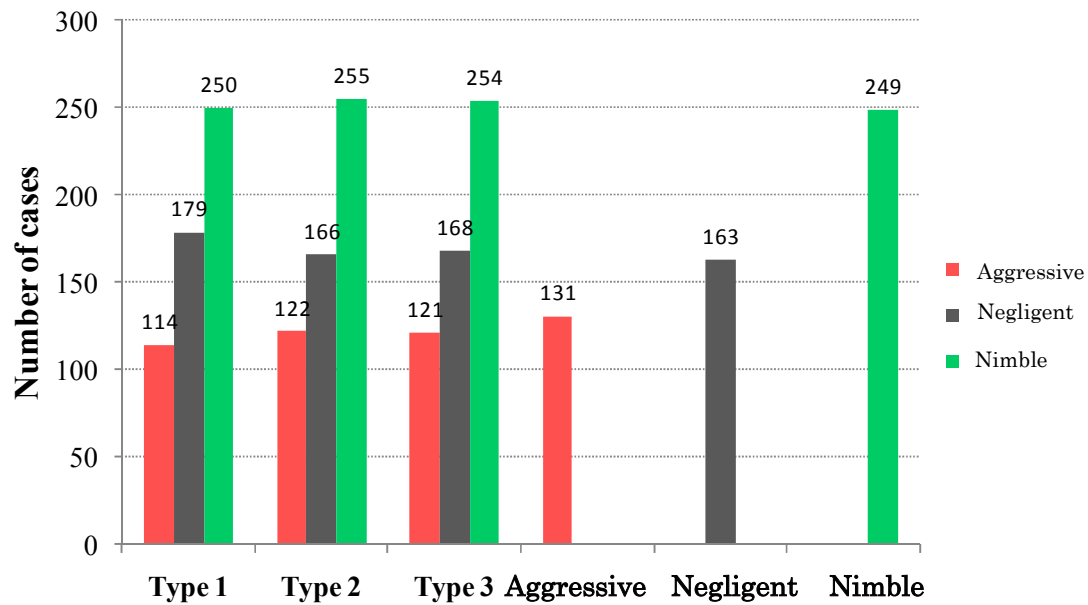


Figure 5.3.11 Number of aggressive cases, negligent cases and nimble cases under different leading car behavior

131 aggressive driving cases are excluded from further simulation study. On the other hand, the cars showing no aggressive e.g. collision and sudden stop in homogeneous platoon are not necessary non-aggressive in the platoon consisted with other cars. For example, the independent cars which do not react to the leading car may show no aggressive in homogeneous platoon because it only suffers from the same slight sag effect. But in real platoon consisted with other cars, aggressive always occur at this car no matter its position in the platoon. Another major source of aggressive is cars only reacting to the speed difference but not spacing while they have a small desired spacing. In this case, drivers have shorter time to adjust to the driving condition change of leading vehicle because of the small desired spacing, while the acceleration and deceleration is milder comparing to drivers reacting to both speed difference and spacing. The two features combined make aggressive much more likely to happen at these cases.

There are also other two kinds of drivers: negligent and nimble drivers. Speed reduction propagates and increases in 5-min platoon of negligent drivers and causes congestion occurrence as shown in Fig. 5.3.10. Speed reduction decays or increase slightly in 5-min platoon of nimble drivers and does not cause congestion.

The cumulative frequency of drivers is further studied. The δ and τ cumulative frequency of aggressive drivers and negligent drivers is evenly distributed while nimble drivers have δ and τ concentrated in $\tau=1.5\sim 2s$ and $\delta=20\sim 25m$ (See Fig. 5.3.12,13,14).

δ, τ Aggressive drivers

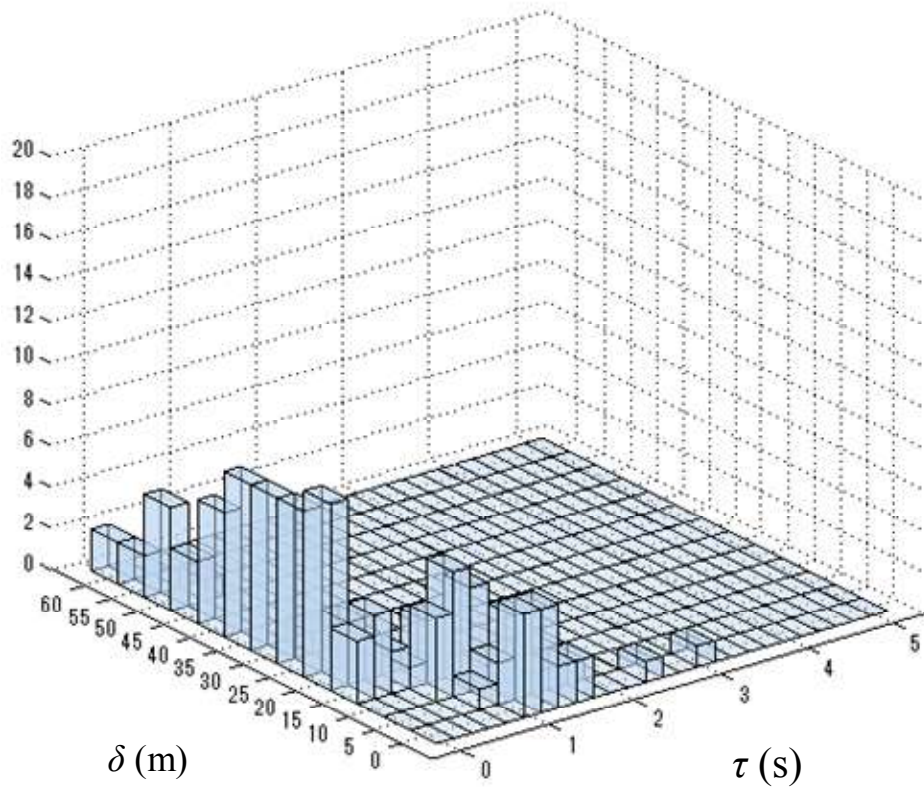


Figure 5.3.12 Joint cumulative frequency of δ and τ of aggressive drivers

δ, τ Negligent drivers

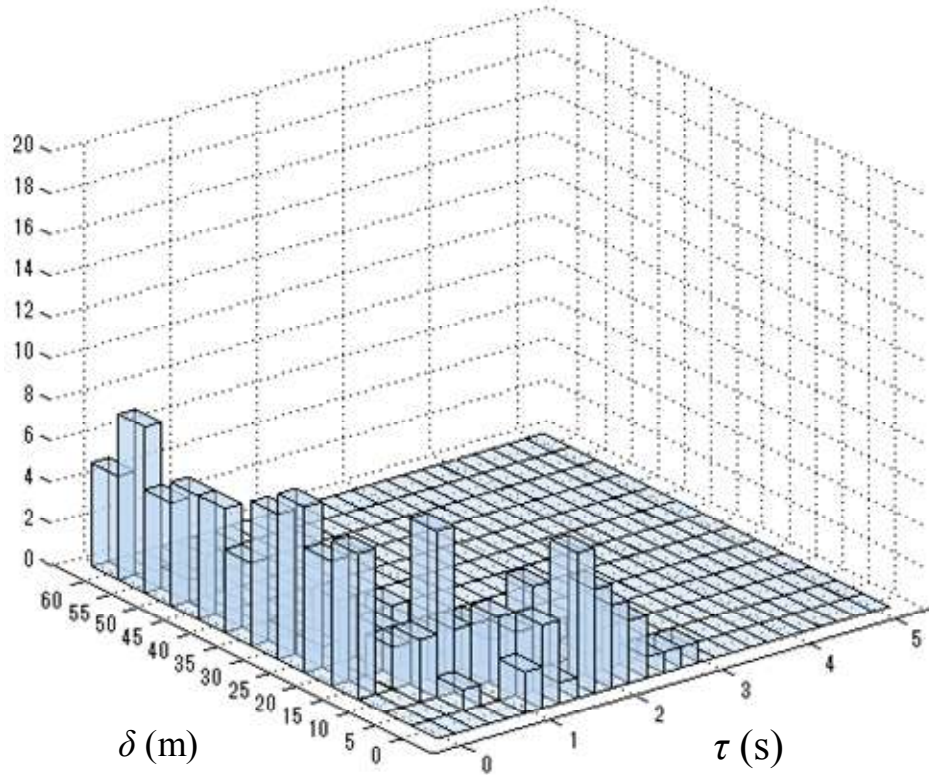


Figure 5.3.13 Joint cumulative frequency of δ and τ of negligent drivers

δ, τ Nimble drivers

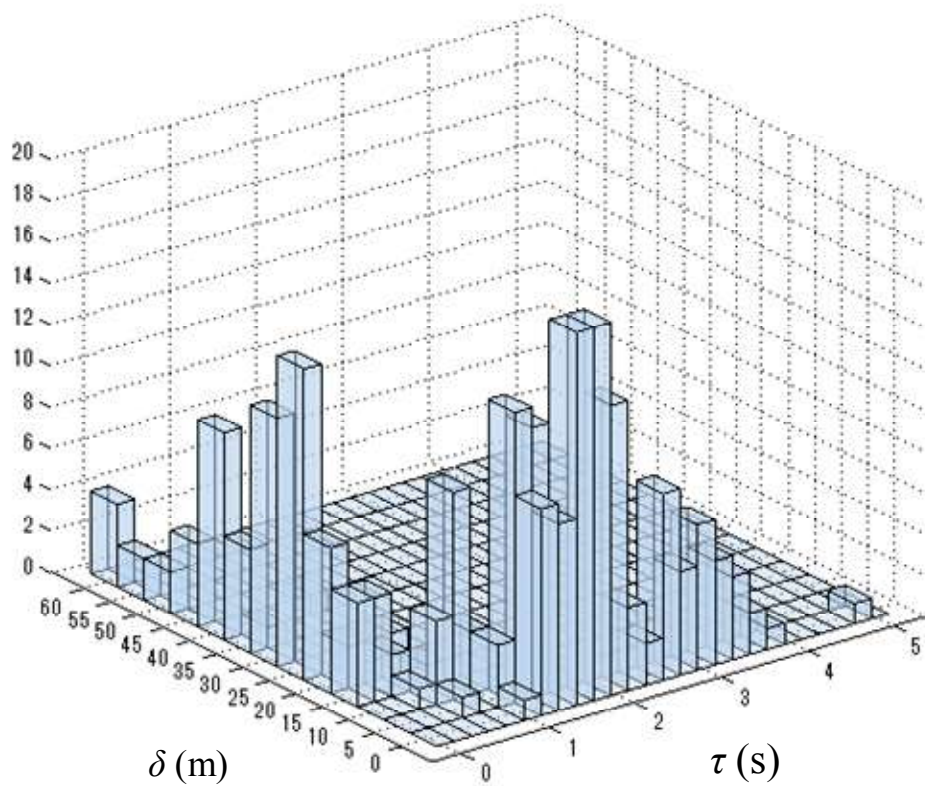


Figure 5.3.14 Joint cumulative frequency of δ and τ of nimble drivers

Most aggressive drivers have bigger α_1 than negligent and nimble drivers. The α_1 of aggressive drivers concentrates at the upper bound of estimation value range. The α_1 of nimble drivers concentrates at a small value of [0.1, 0.3] (See Fig.5.3.15, 16, 17).

α_1 Aggressive drivers

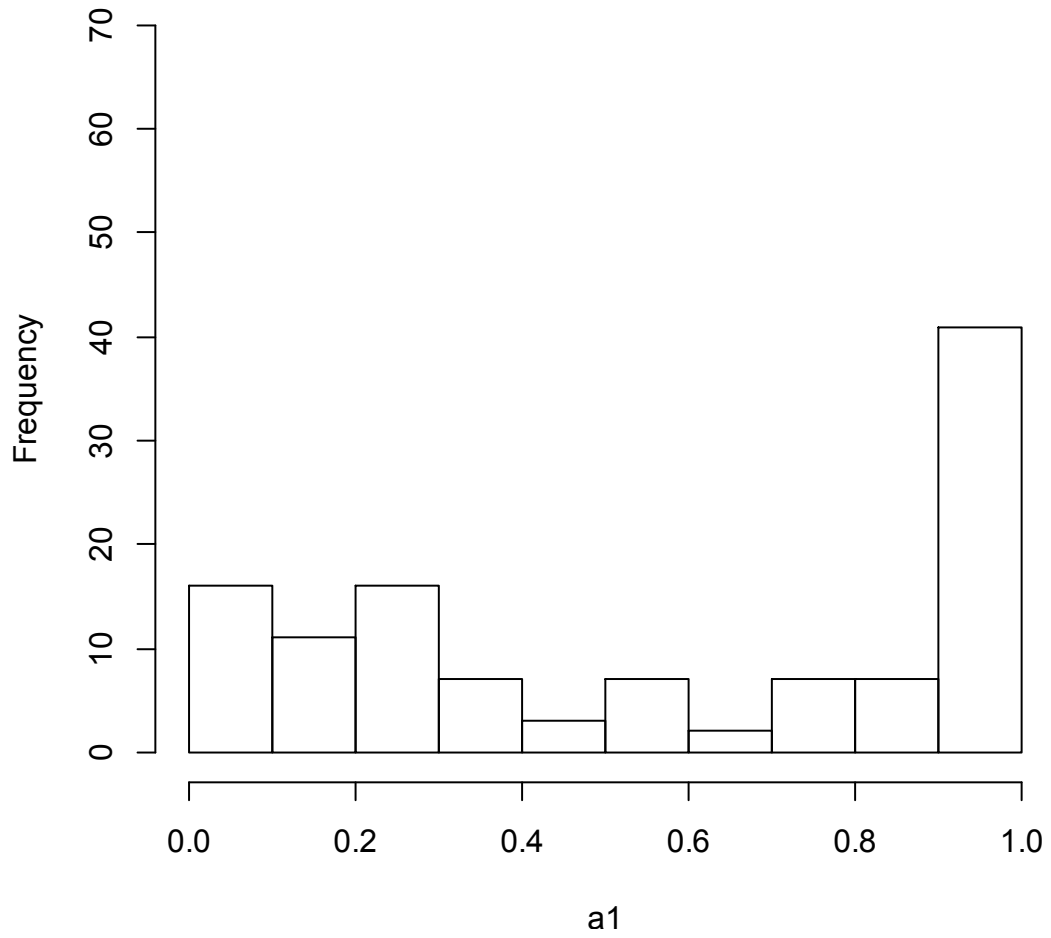


Figure 5.3.15 Cumulative frequency of α_1 of aggressive drivers

α_1 Negligent drivers

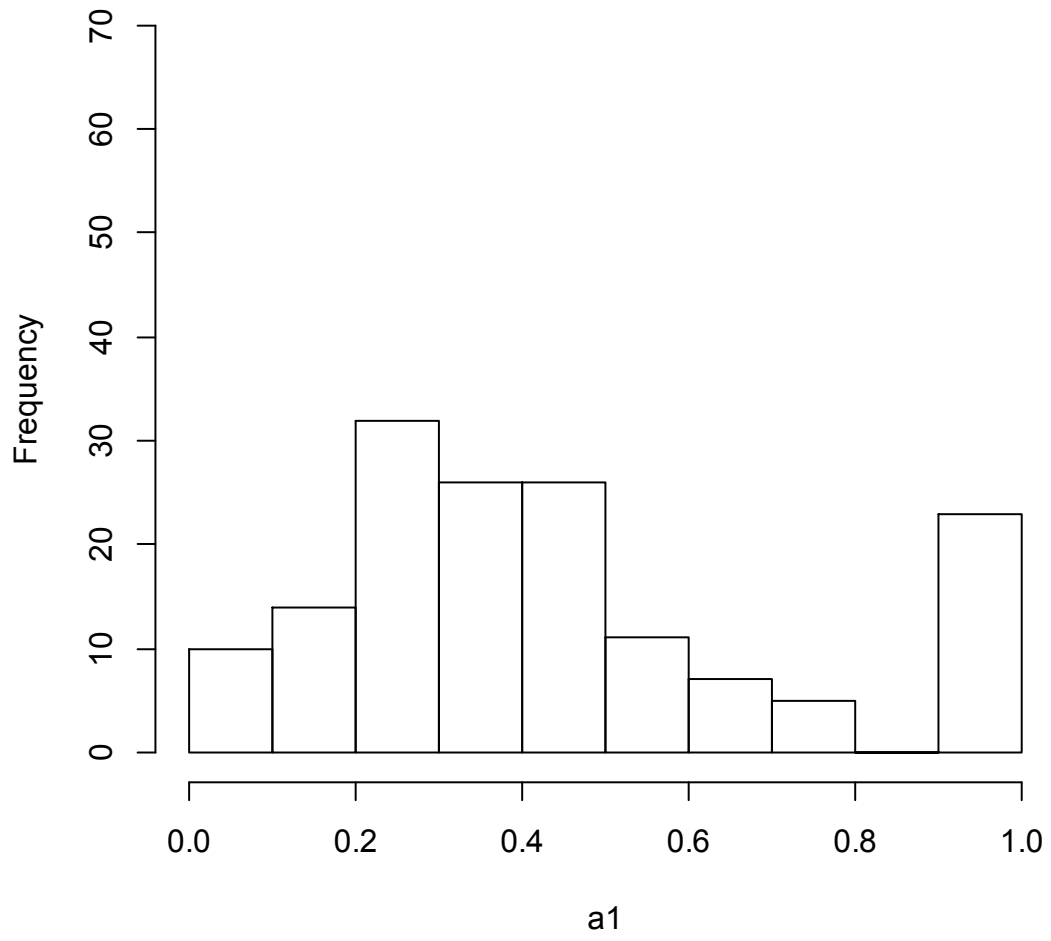


Figure 5.3.16 Cumulative frequency of α_1 of negligent drivers

α_1 Nimble drivers

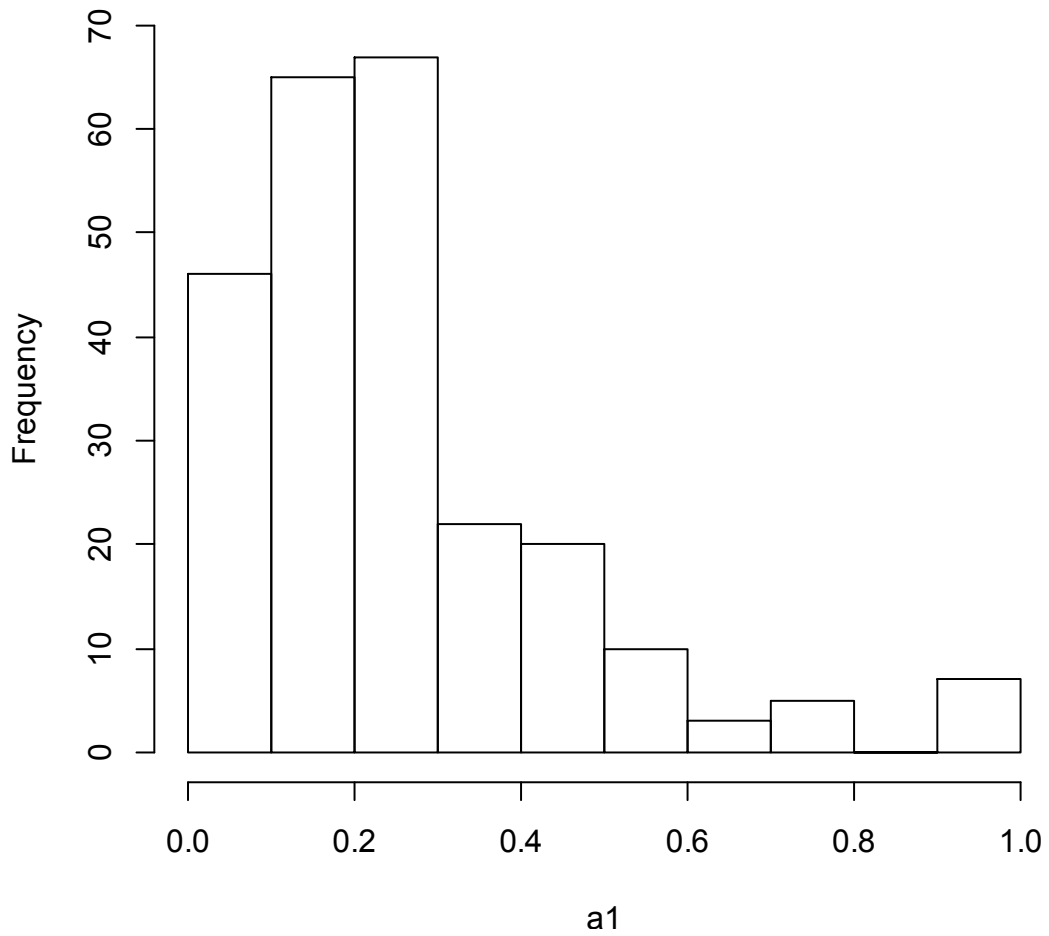


Figure 5.3.17 Cumulative frequency of α_1 of nimble drivers

Most α_2 value of negligent and nimble drivers is small and concentrate at the lower boundary, while that of aggressive drivers are evenly distributed (See Fig. 5.3.18, 19, 20).

α_2 Aggressive drivers

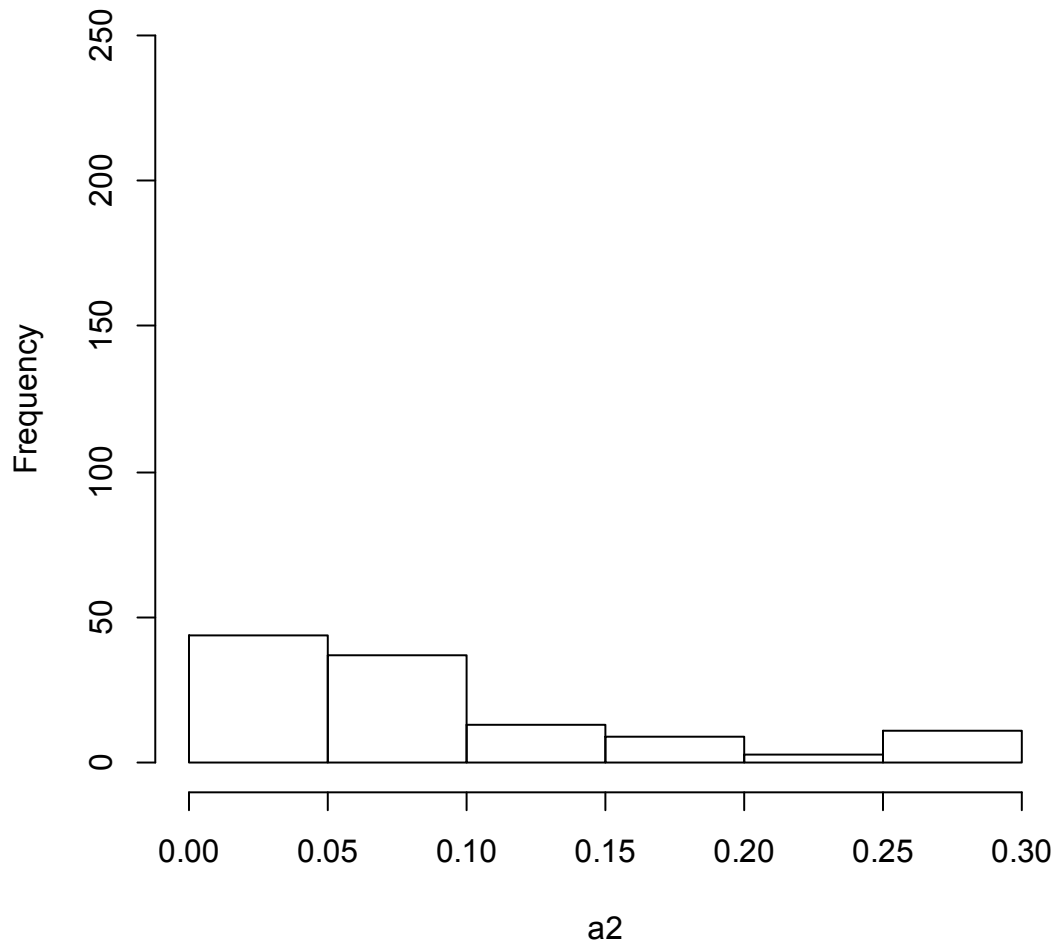


Figure 5.3.18 Cumulative frequency of α_2 of aggressive drivers

α_2 Negligent drivers

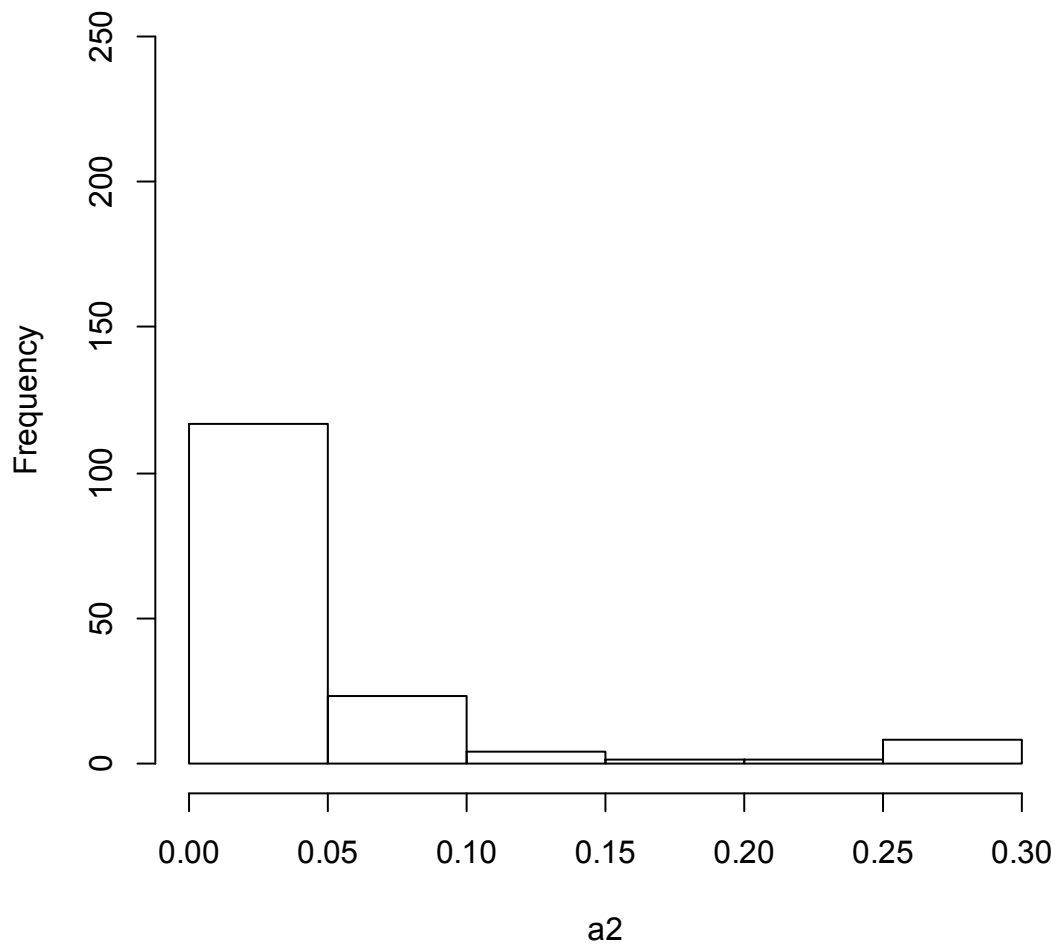


Figure 5.3.19 Cumulative frequency of α_2 of negligent drivers

α_2 Nimble drivers

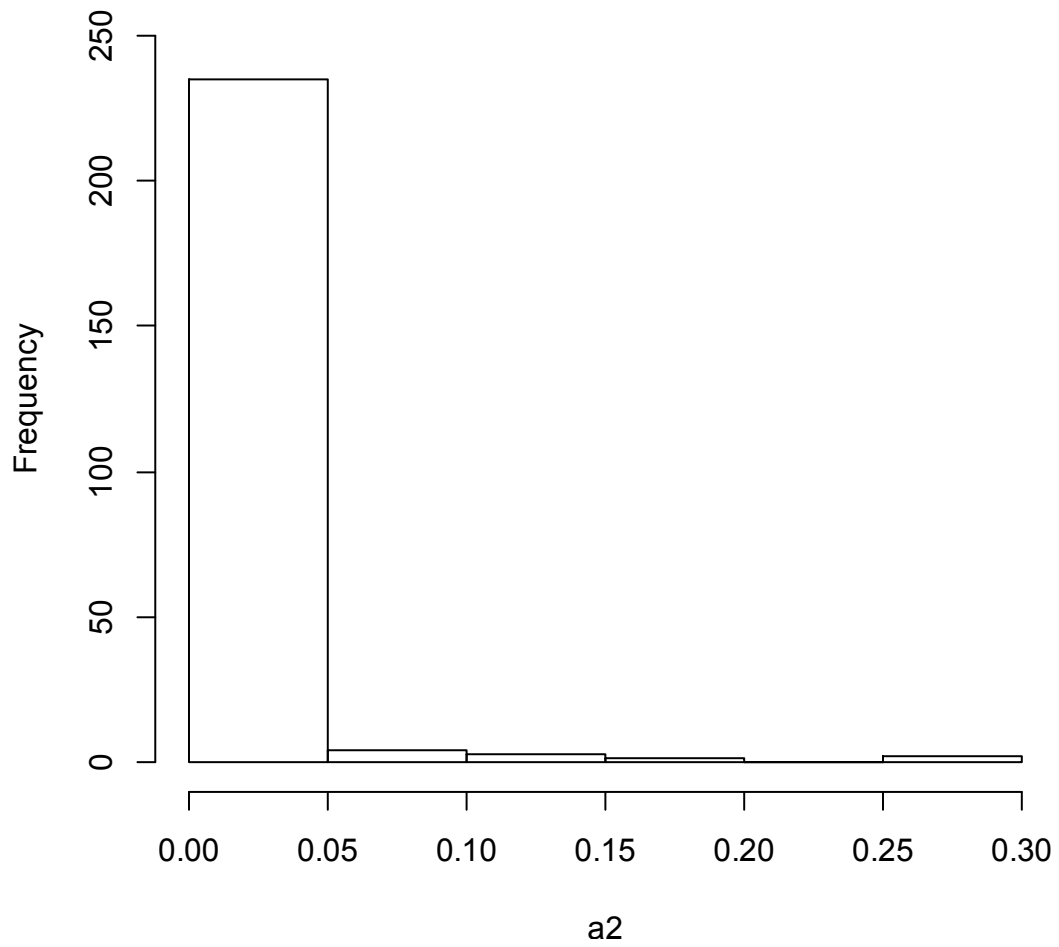


Figure 5.3.20 Cumulative frequency of α_2 of nimble drivers

The β value of negligent drivers concentrates at the upper bound of estimation value range while that of nimble drivers concentrates at the lower bound. In aggressive drivers, both types are observed (See Fig. 5.3.21, 22 , 23).

β Aggressive drivers

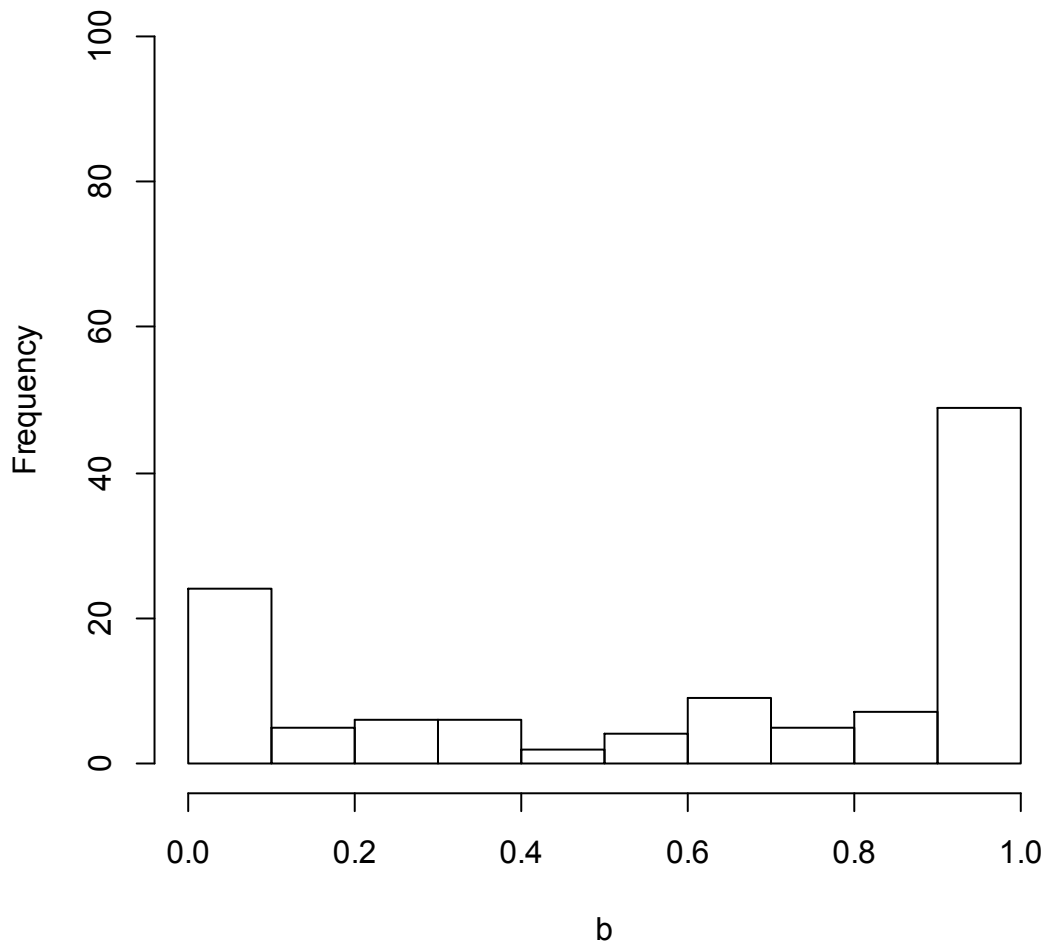


Figure 5.3.21 Cumulative frequency of β of aggressive drivers

6 Negligent drivers

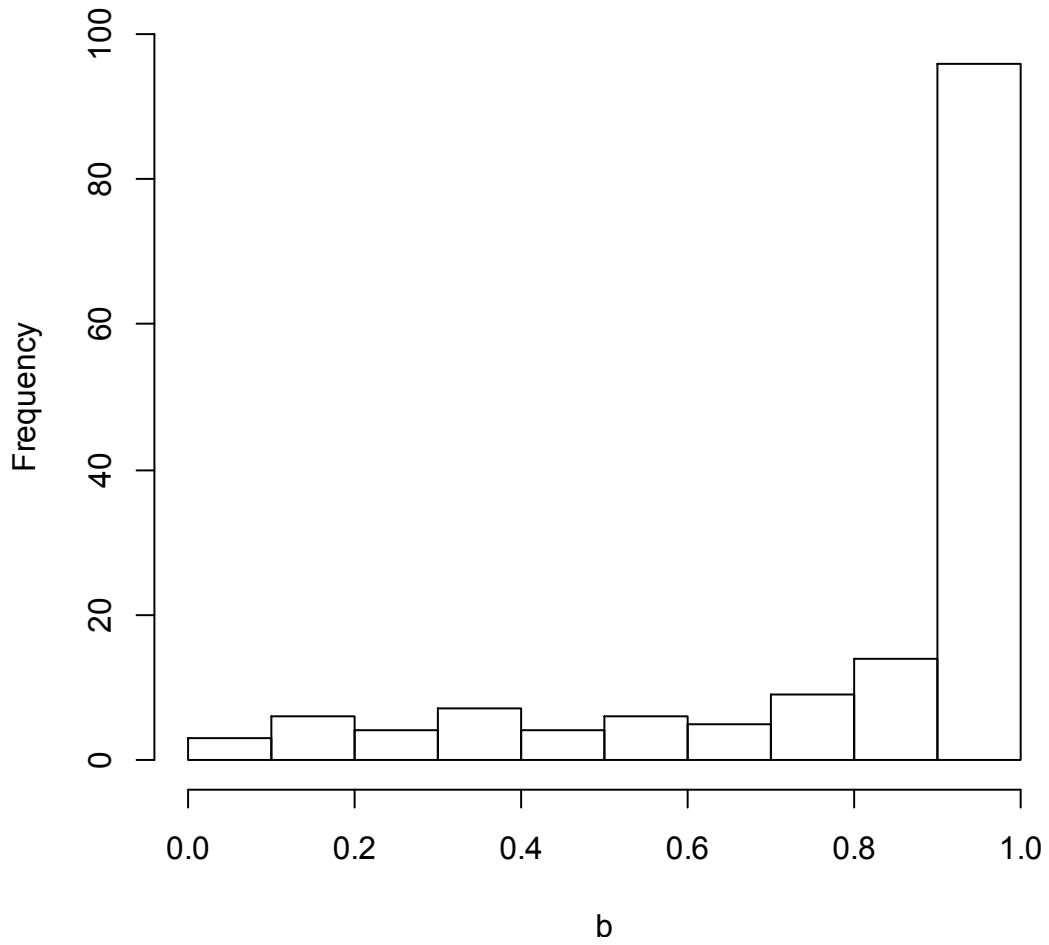


Figure 5.3.22 Cumulative frequency of β of negligent drivers

6 Nimble drivers

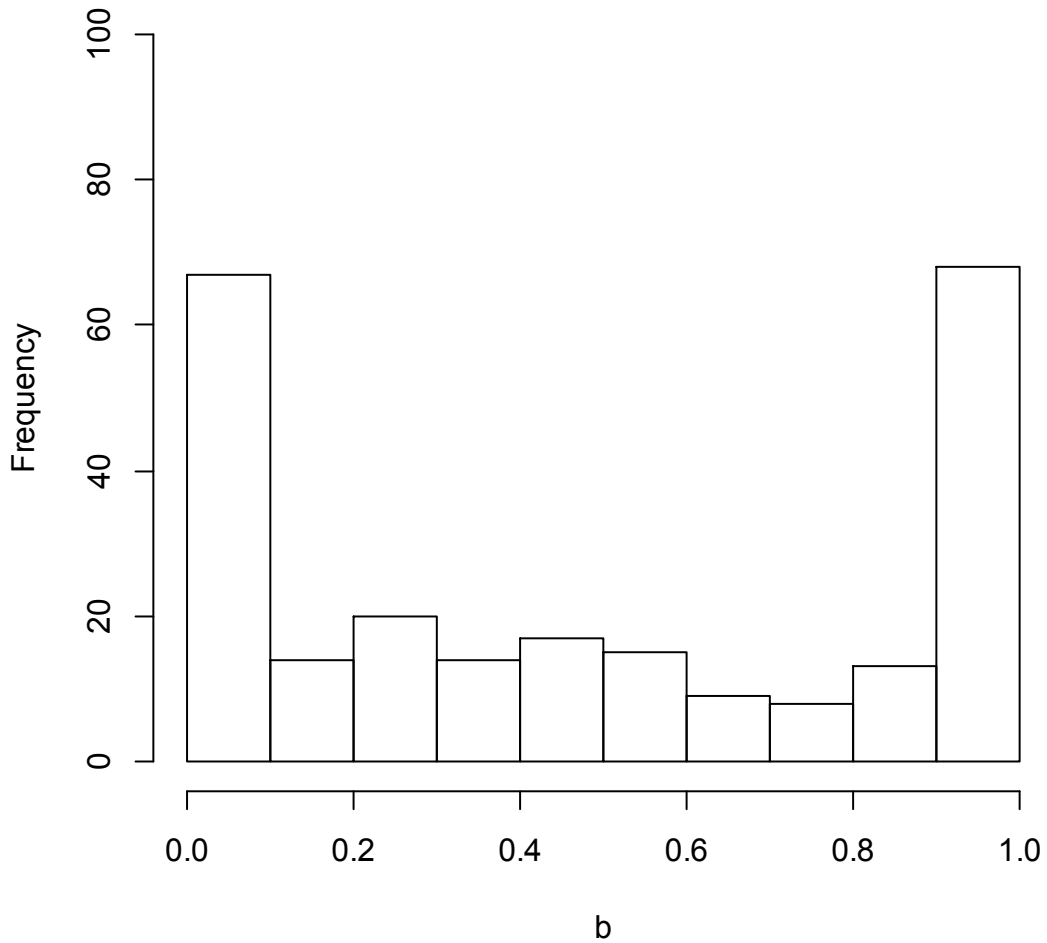


Figure 5.3.23 Cumulative frequency of β of nimble drivers

Most aggressive and negligent drivers have reaction time smaller than 1s. The reaction time of negligent drivers is slightly smaller than the aggressive drivers. Some nimble drivers have reaction time around 5s. There are also more nimble drivers have reaction time bigger than 1s (See Fig. 5.3.24, 25, 26). This indicates that a longer reaction time does not necessarily cause the congestion or it may actual help to stabilize the flow during congestion formation.

Δt Aggressive drivers

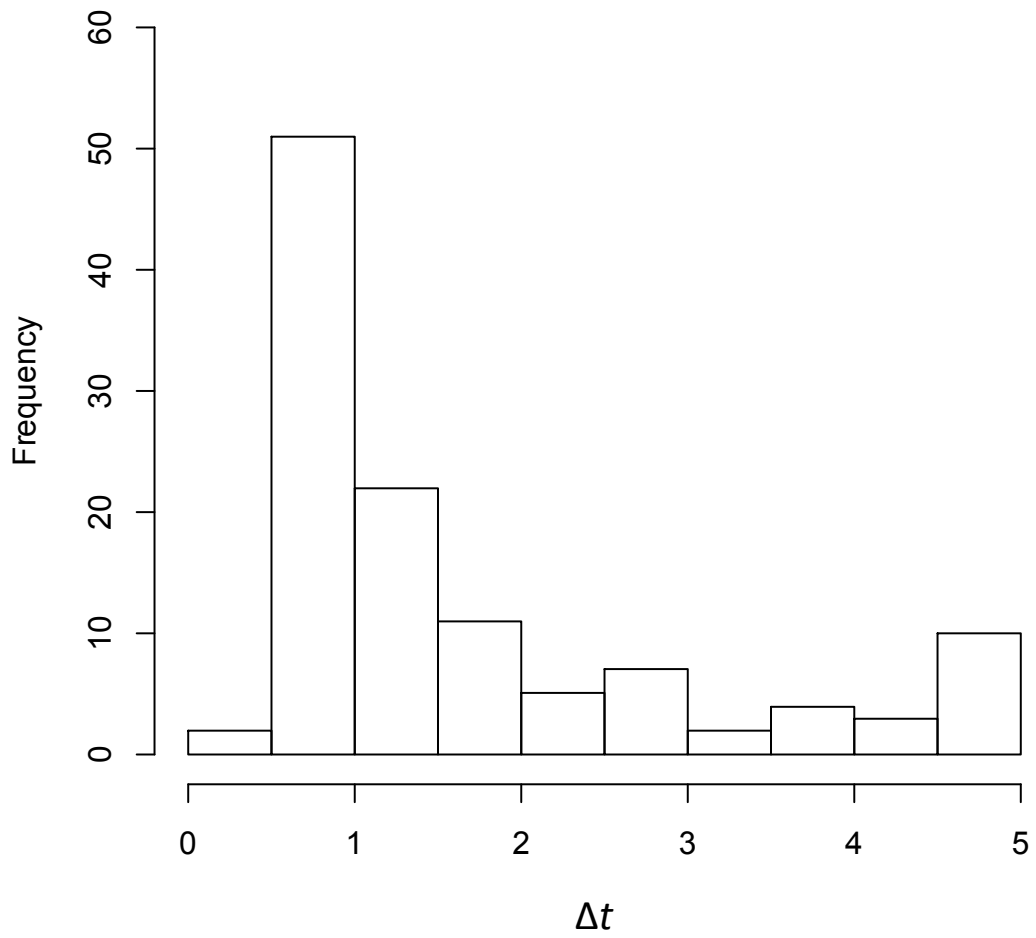


Figure 5.3.24 Cumulative frequency of Δt of aggressive drivers

Δt Negligent drivers

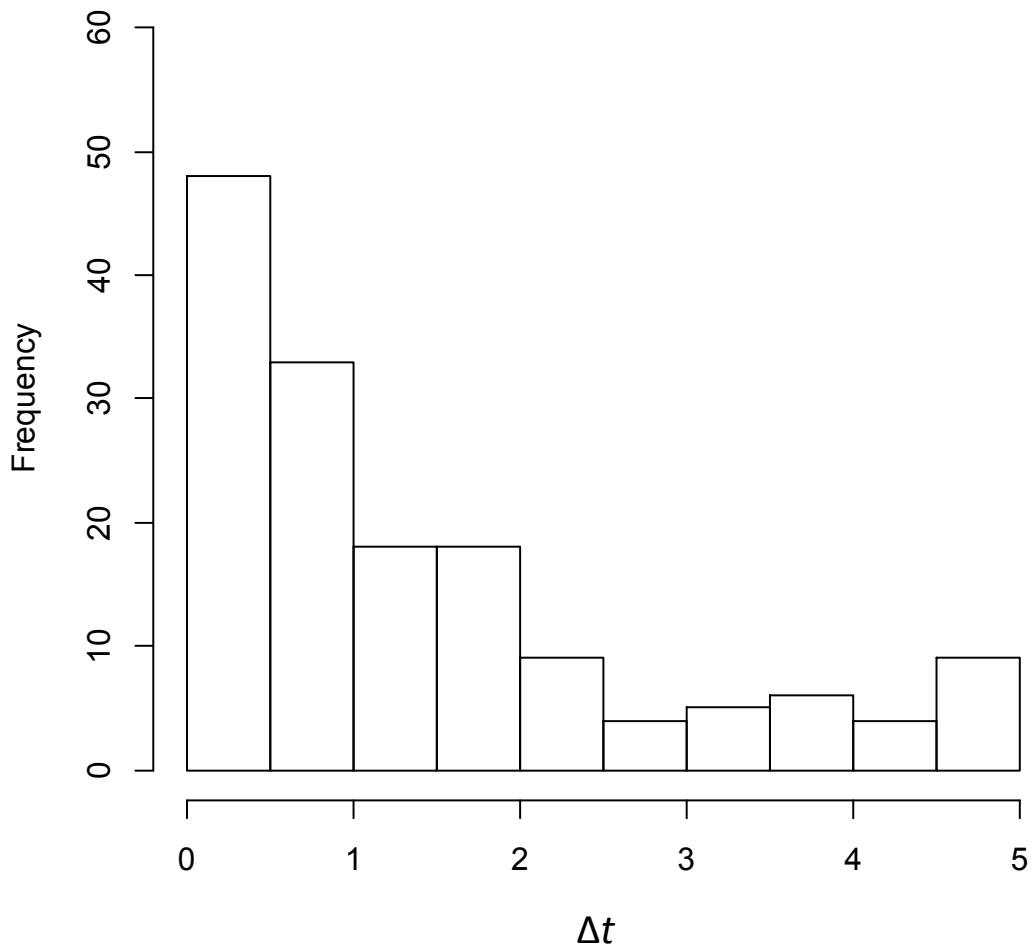


Figure 5.3.25 Cumulative frequency of Δt of negligent drivers

Δt Nimble drivers

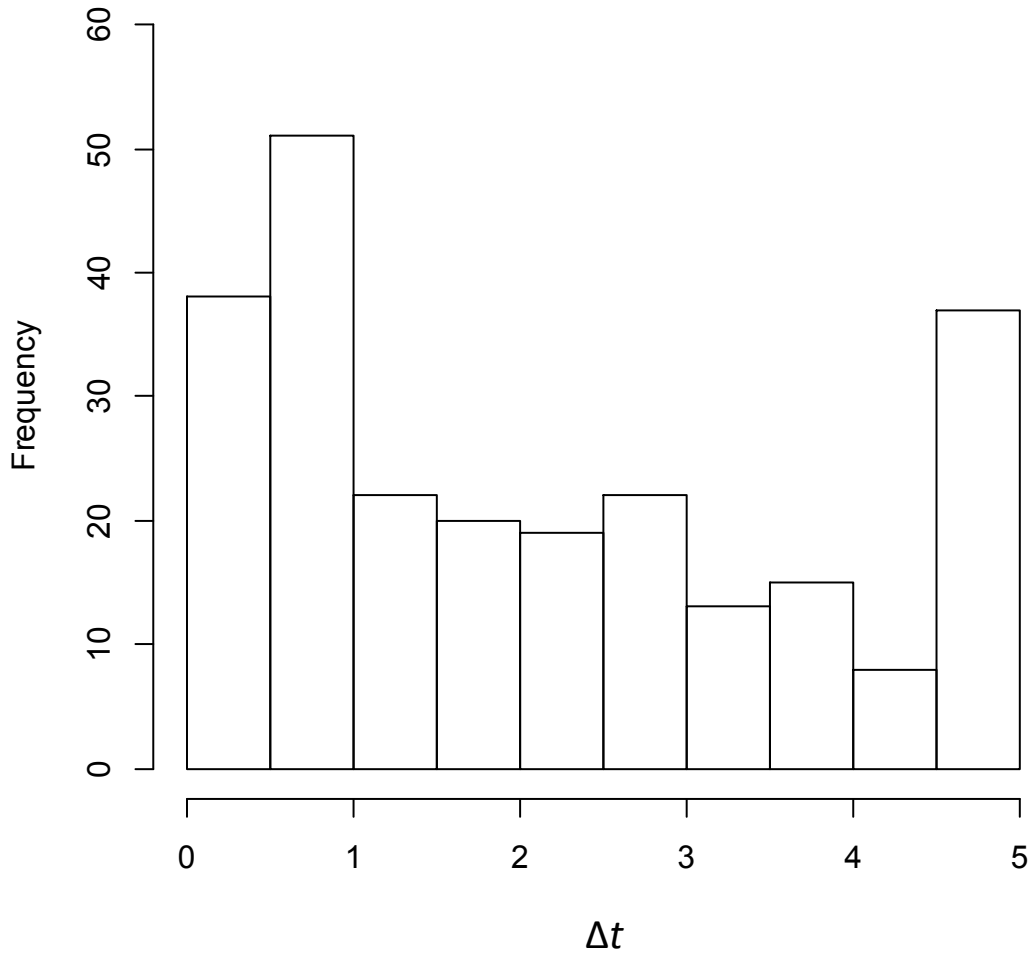


Figure 5.3.26 Cumulative frequency of Δt of nimble drivers

5.4 Congestion occurrence probability

Congestion occurrence probability is studied with simulation. 5-min platoon of certain traffic demand is generated with random entrance of vehicles. The entering headway of vehicles obeys negative exponential distribution with $\lambda = \text{mean headway}$ under certain traffic demand with a lower bound of 0.8s. The 0.8s lower bound is the mean headway under 4000 pcu/h/lane which is the theoretical capacity of a one lane expressway. No vehicle should enter the simulation with headway smaller than that.

$$\overline{t_{hdw}} = \text{Exp}(\overline{t_{hdw}})$$

$$\overline{t_{hdw}} > 0.8s$$

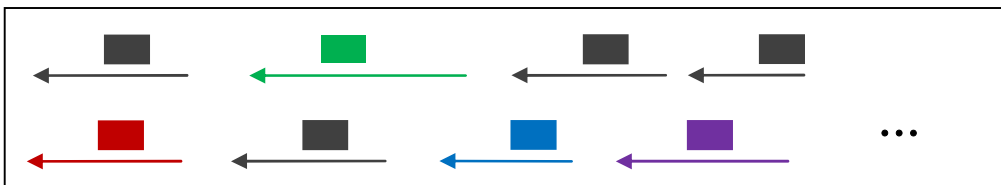
The desired headway $\begin{cases} s_1^*(t_1) = \delta + \tau \cdot v_1(t_1) \\ t_{hdw} = \frac{s_1^*(t_1)}{v_0(t_1)} \end{cases}$ of vehicles is then compared with the entering

headway. The car of the smallest absolute difference between the generated headway and its desired headway is chosen as the car in that certain position in platoon. The entering headway is change to the desired headway of the chosen car. The process is shown in Fig. 5.4.1.

Random generation of entering headway



Compare with the estimated cars' desired headway



Place the estimated car with smallest absolute difference between its desired headway and generated entering headway and change the entering headway to the desired headway.



Figure 5.4.1 choose car position based on randomly entering headway

If the generated headway of a car position in platoon is bigger than 3s, a leading car is placed in that position.

Simulation are carried out 1000 times with difference random seeds for every traffic demand level of 1250 veh/h/lane, 1500 veh/h/lane, 1750 veh/h/lane, 2000 veh/h/lane, 2250 veh/h/lane and 2500 veh/h/lane. The congestion occurrence probability is calculated with the percentage of the cases of congestion in all the valid cases in 1000 simulations. The following figures are examples of uncongested cases at sag section under 5-min traffic demand of 1,000 veh/h/lane and 2,200 veh/h/lane. The trajectories of 2,200 veh/h/lane are obvious denser than the trajectories of 1,000 veh/h/lane. It is easy to understand that there are more leading cars in a platoon of low traffic demand than in a platoon of high traffic demand.

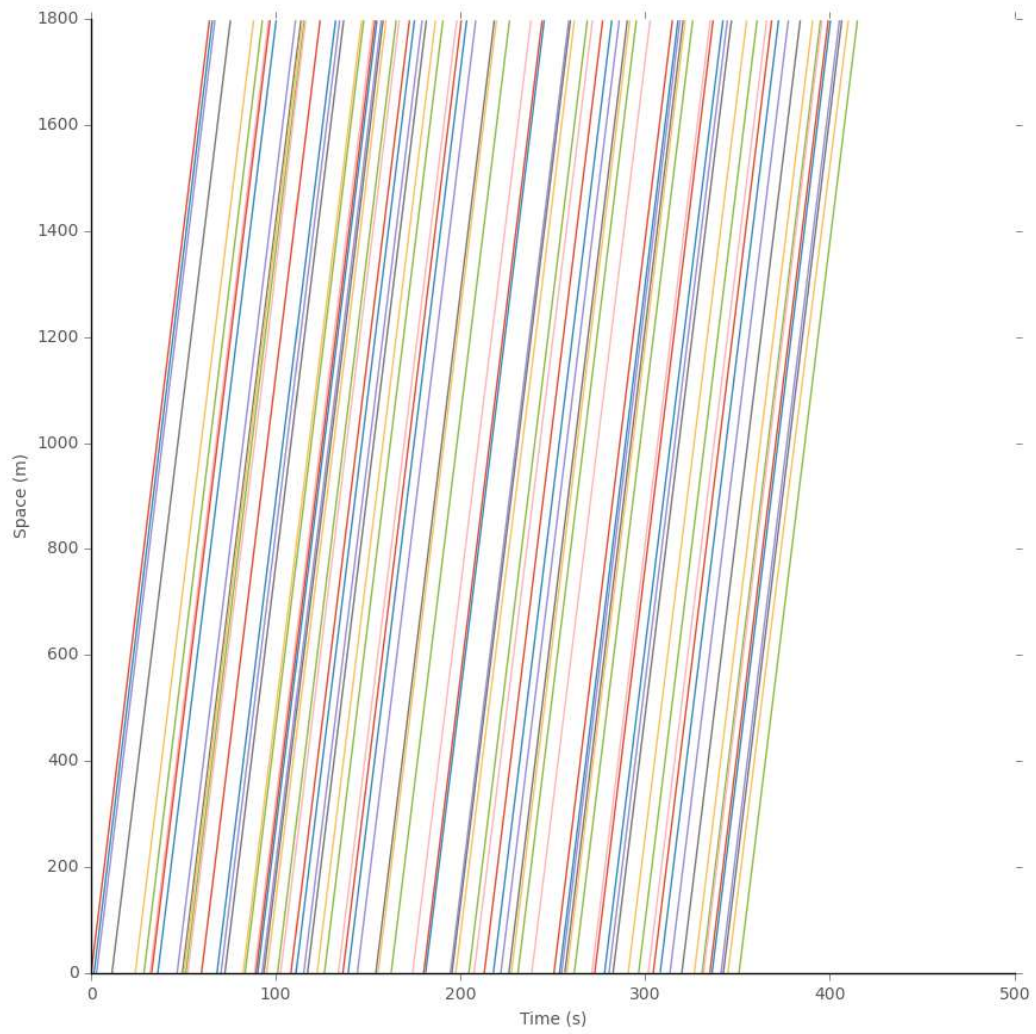


Figure 5.4.2 Trajectories under traffic demand of 1,000 veh/h/lane

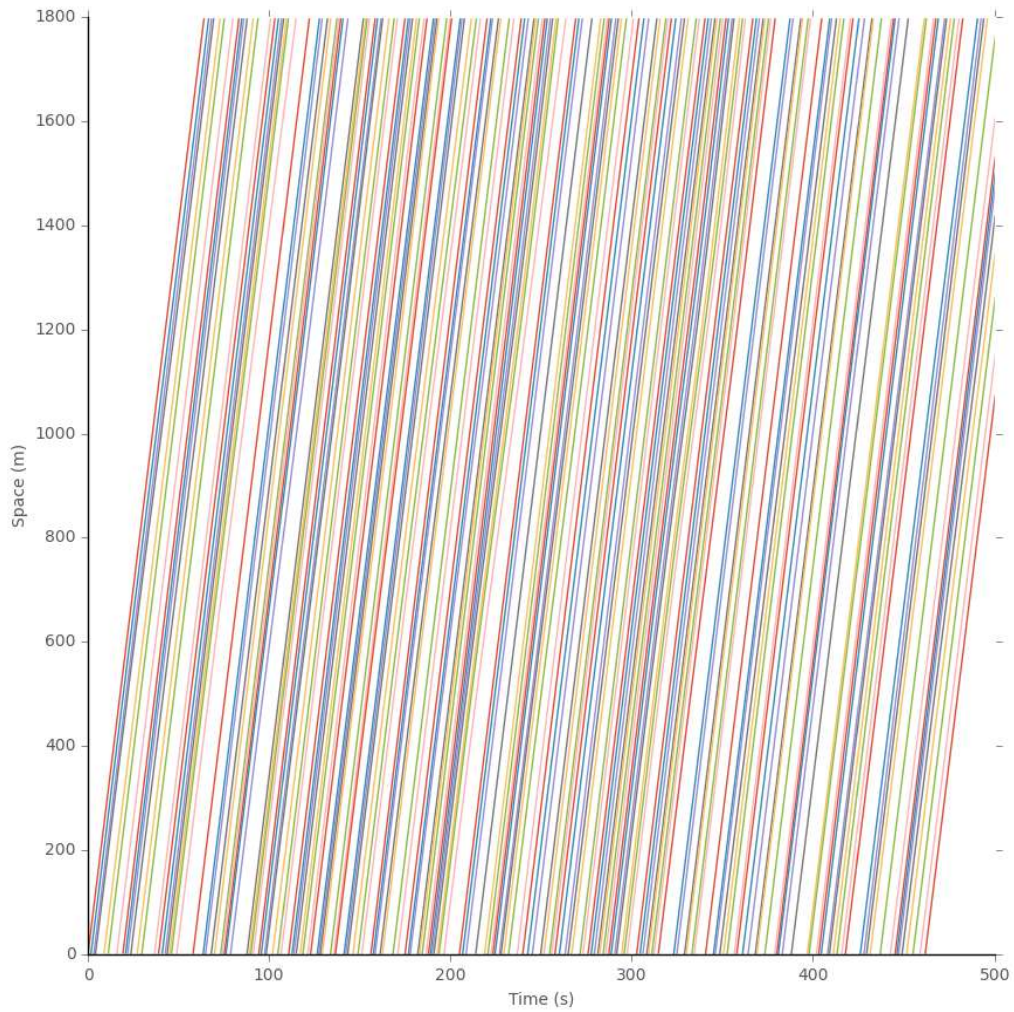


Figure 5.4.3 Trajectories under traffic demand of 2,200 veh/h/lane

Though congestion forms in field observation, Fig. 5.4.4 shows an example of all observed vehicles passing the sag section with no congestion occurrence by change their order in the platoon. This means that the position of vehicles in the platoon having influence on whether congestion occurs or not when this specific platoon passing the sag section. Congestion occurrence is probabilistic.

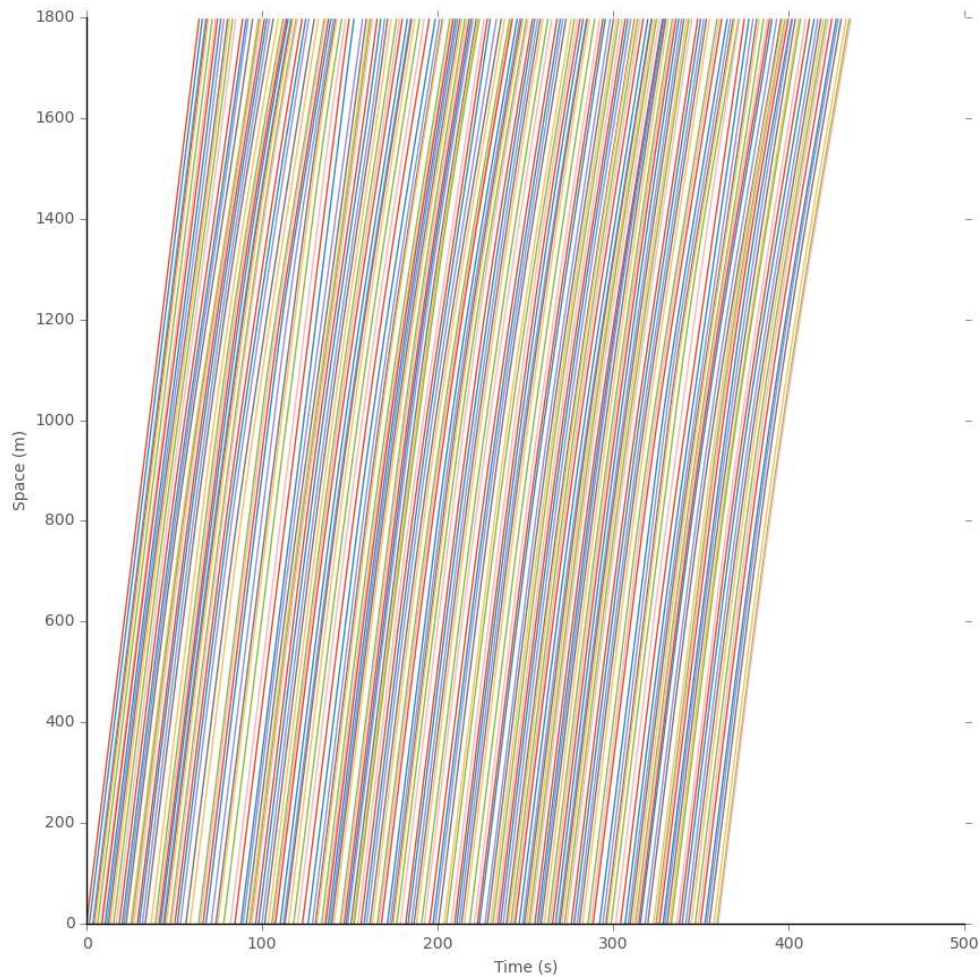


Figure 5.4.4 Example of congestion free scenario with all the observed cars

To compare the congestion occurrence probability with field observation data where the traffic demand is calculated as veh/5-min/2lane, the lane use rate under different link flow rate is used to transfer the lane base flow rate in simulation study to the link base flow rate in field observation. The function and parameters are proposed by Hong(洪性俊, 2008).

$$L_u = \exp(a_2 Q)$$

L_u – Lane use rate on outer lane;

Q – Link flow rate (veh/h);

a_2 – Constant, $-3.541e-04$ under speed limit of 100km/h;

Therefore, flow rate is calculated according to the following estimation function

$$Q_i = Q[1 - \exp(a_2 Q)]$$

Q_i – Flow rate on (veh/h);

The estimated flow rate on the outer lane and the inner lane under different link flow rate is shown as Fig. 5.4.5 .

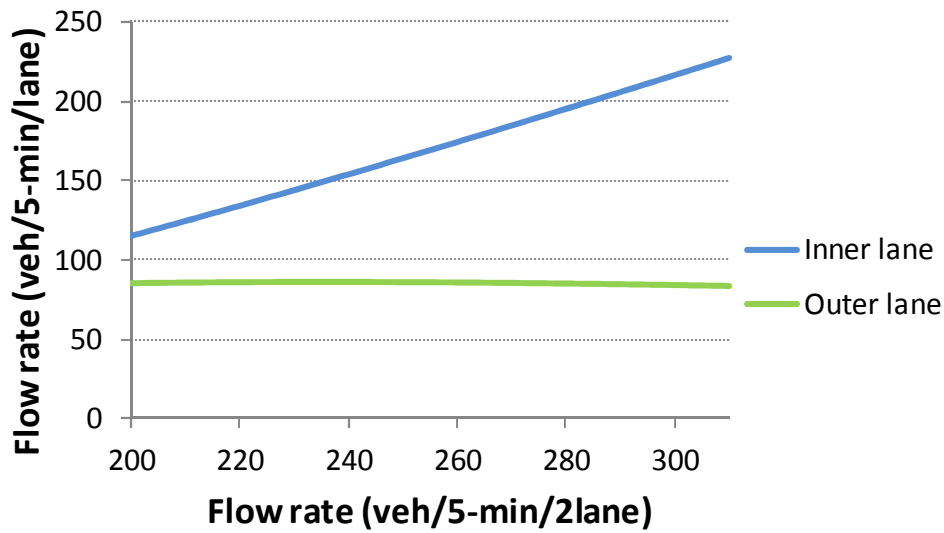


Figure 5.4.5 Relationship of 5-min link flow rate and inner/outer lane flow rate (2 lanes in 1 link)
 The congestion occurrence probability in simulation is then compared with the congestion occurrence probability observed by Oguchi (大口敬、片倉正彦、鹿田成則, 2001) at a different sag section in Japan (See Fig. 5.4.6).

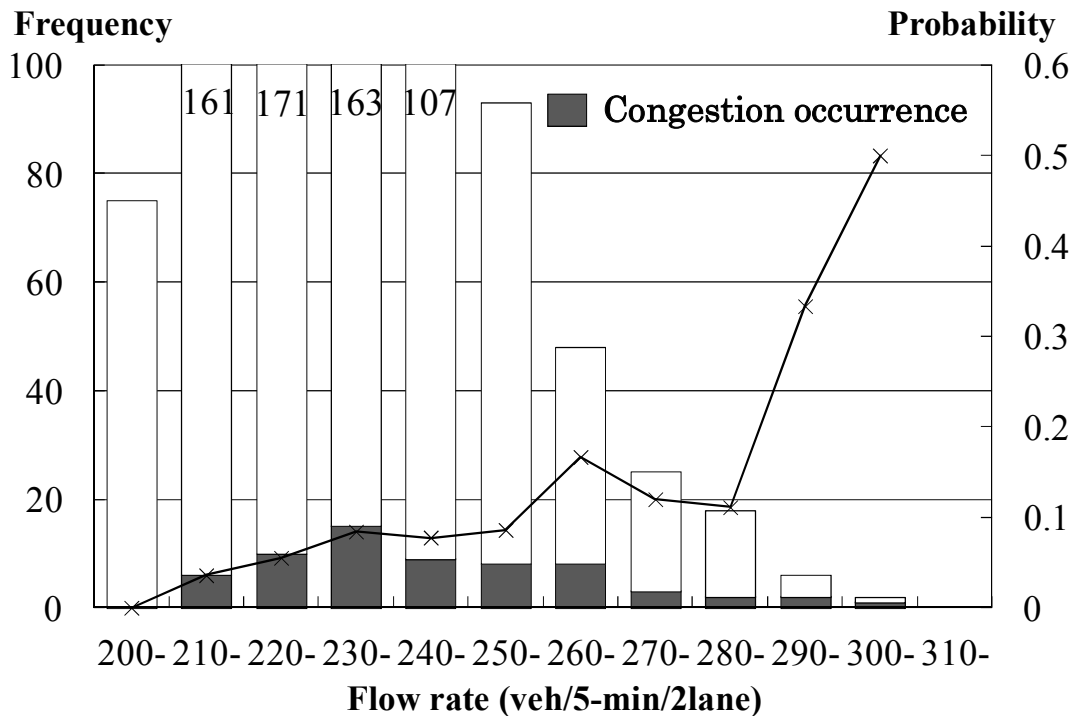


Figure 5.4.6 Congestion occurrence observed on Japanese expressway bottleneck
 The tendency of congestion occurrence probability grows with traffic demand can be observed in

both simulation with estimated car-following behaviors and field observation. Simulation with estimated car-following behavior can reproduce the congestion occurrence probability at a certain sag section. The congestion occurrence probability with car-following behaviors observed in congestion formation at Tomei yamato sag section is higher than that of the field observation when traffic demand grows. The causes of this difference are different vertical slope condition at different sag section and different observation cases.

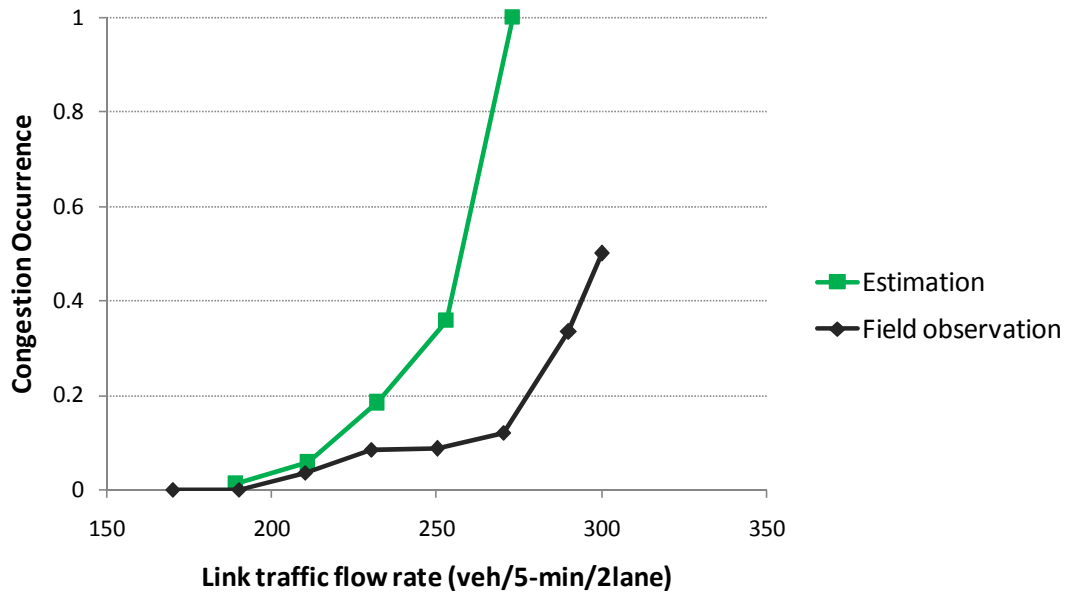


Figure 5.4.7 Comparison of congestion occurrence with estimated car-following behavior and observation at another site

5.5 Car-following parameters distribution

Simulation is also carried out with parameter values of car-following behavior generated with distribution instead of the real value. The congestion occurrence probability is compared to the simulation result of actual estimated value of parameters (See Fig. 5.5.1). The congestion occurrence probability is higher than that of the estimated value under the 5 minutes traffic demand of 210-270 veh/2lane. There are two possible causes. One is that the proportion of different kinds of drivers may not be exactly random. The other is that there exists some potential relationship between certain parameters, for example, α_1 and Δt , etc.

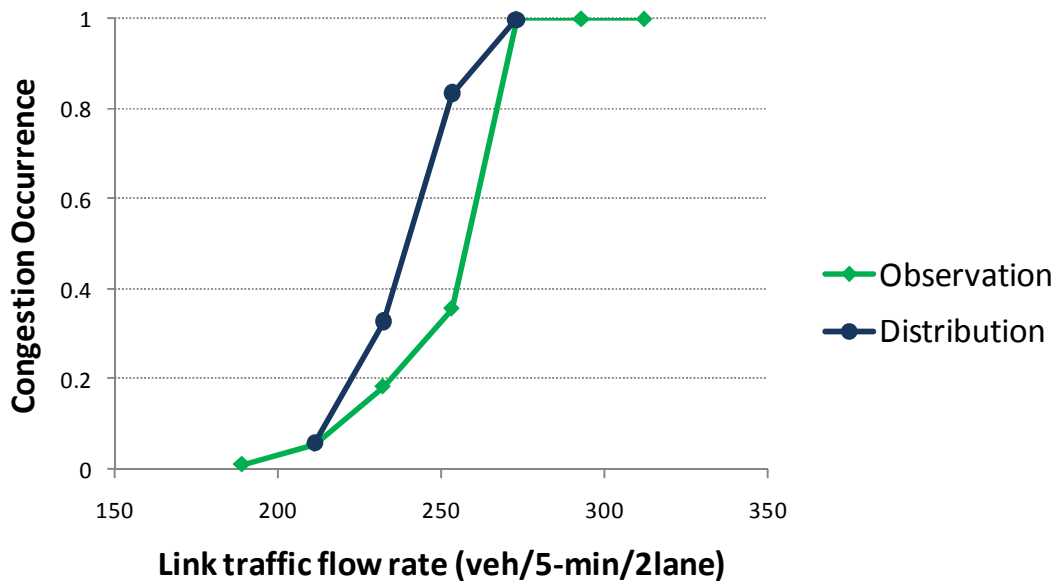


Figure 5.5.1 Congestion occurrence probability of estimated parameters values and distribution

5.6 Simulation findings

With carefully calibrated actual car-following behavior parameters, Simulation can reproduce the car-following behavior of drivers and the traffic flow condition at sag section. The 5-min traffic flow condition at the observed sag section is simulated with car-following model and parameters with a time step of 0.1s. The initial speed is 28km/h. Vehicles enter with their desired headway and react to its leader immediately after entering the simulation. Firstly, the simulation is carried out for every vehicle with 5-min homogeneous traffic consisted of the parameters only of that vehicle. Three types of leading car behavior: The constant sag affected driver, the non speed restore driver and the speed restore driver are simulated for every vehicle. The result shows little influence of leading car behavior on congestion occurrence at sag section. All three leading car behavior generates similar congestion occurrence in homogenous flow.

Different kinds of drivers have different impact on traffic flow condition at bottlenecks. The driver kinds and their impact on congestion occurrence under same traffic demand are studied in simulation. There are three kinds of drivers discovered in simulation. One is aggressive drivers that react to the driving state change of leading vehicle drastically. Sudden stop and collision can be observed in simulation of these drivers. Another one is the negligent drivers. Speed reduction propagates in 5-min platoon of negligent drivers and cause congestion occurrence. The last one is the nimble drivers. Speed reduction decays or increase slightly in 5-min platoon of nimble drivers and does not cause congestion. The cumulative frequency of parameters of

Congestion occurrence probability depends not only on the traffic flow rate but also on the composition of different types of driver in traffic flow.

6 Discussion

It is possible to further study countermeasures to prevent congestion occurrence with simulation. Apart from speed limit and input flow rate control, advanced driving aid system such as Adaptive Cruise Control (ACC) system can prevent congestion by not affected by the grade change and increase homogeneity in traffic flow. The quantitative effect of these countermeasures is evaluated in this chapter.

6.1 Car-following behavior of ACC system

One obvious countermeasure to prevent congestion at sag section is to balance the lane-use between outer lane and inner lane because this countermeasure can directly reduce the flow rate on inner lane. Another countermeasure is to make better detection of the driving condition and more sufficient driving reaction by using advanced driving aid system such as ACC system. ACC system is designed to maintain a target time gap with the leading vehicle in the car-following state. The same estimation framework was used to obtain values for the car-following parameters of the ACC system. Helly's car-following model is considered suitable for modeling car-following behavior of the ACC system because the ACC system is designed with a proportional-integral-derivative controller mechanism widely used in industrial control system where the car adjust its acceleration based on simple detection such as spacing or time gap (Kesting, Treiber, Schönhof, & Helbing, 2008)(Vahidi & Eskandarian, 2003).

In order to model the driving behavior of ACC car, a car-following experiment was conducted with a commercial ACC system on January 19–23, 2015, from 8 a.m. to 2 p.m., on a 14.2-km segment of the Tomei Expressway that includes a sag section. Congestion occurred at the sag section during the experiment. There were two vehicles involved in the experiment. One vehicle, driven by a human driver, was the leading vehicle. The other vehicle, equipped with an active commercial ACC system, was the following vehicle. The following vehicle was a one-box-type vehicle weighing 2.4 tons with a 2.4-L gasoline engine. The vehicles traveled along the route 30 times in total. The speed of the ACC system was set to 110 km/h to ensure that it remained constantly in the car-following state during the experiment. Highly accurate time and position data were acquired using a differential geographic positioning system (DGPS). Speed and acceleration data were calculated and smoothed based on the time and position.

The car-following model for ACC system is slightly different than real drivers because ACC systems control vehicle acceleration according to the real time headway with the leading vehicle. So it does

not have a reaction time in spacing difference part. The equation is:

$$a_1(t) = \alpha_1(v_0(t - \Delta t) - v_1(t - \Delta t)) + \alpha_2(x_0(t) - x_1(t) - s_1^*) \quad 20$$

$$s_1^* = \delta + \tau v_1(t)$$

The estimated ACC car-following behavior is:

$$a_1(t) = 0.113 \cdot (v_0(t - 4.4) - v_1(t - 4.4)) + 0.024 \cdot (x_0(t) - x_1(t) - 1.7 \cdot v_1(t) - 5) \quad 21$$

The dynamic performance of the ACC system was first analyzed with simulation. The time step was 0.1s. The initial speed of the leading vehicle was 28 m/s. A deceleration of $a_0 = -1 \text{ m/s}^2$ occurred during an interval of 15–20s. The following vehicle followed the leading vehicle with an initial headway of $\delta/v_{ini} + \tau$, where the initial speed v_{ini} was the same for both the following and the leading vehicle. Two schemes were tested: one in which only one following vehicle followed the leading vehicle, to assess the local reaction to perturbation; and another in which five succeeding following vehicles followed the leading vehicle, to assess the reaction to perturbation in the vehicle platoon. The same two schemes were tested using a commercial ACC vehicle. When vehicles formed a platoon following one another, the commercial ACC vehicle platoon absorbed the perturbation in the platoon with an amplification of the perturbation (see Fig. 6.1.1), whereas some human-driven vehicles performed better at absorption of perturbation without further amplification in the platoon (see Fig. 6.1.2): 28.83% of actual drivers managed to stabilize the initial perturbation.

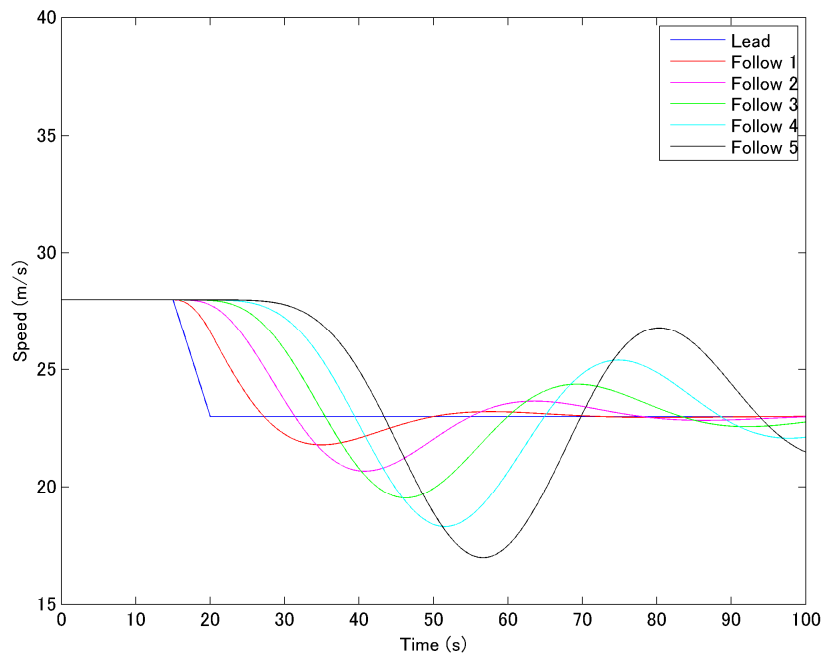


Figure 6.1.1 Dynamic performance of ACC system

The car-following parameters of the example in Fig. 6.1.2 is: $\alpha_1 = 0.498$, $\alpha_2 = 0.015$, $\Delta t = 0.3 \text{ s}$, $s_1^* = 1.2078 \cdot v_1(t) + 5$. It can also be observed that the stabilizing vehicle had a very large α_1 and a very small Δt value compared to those of the ACC system.

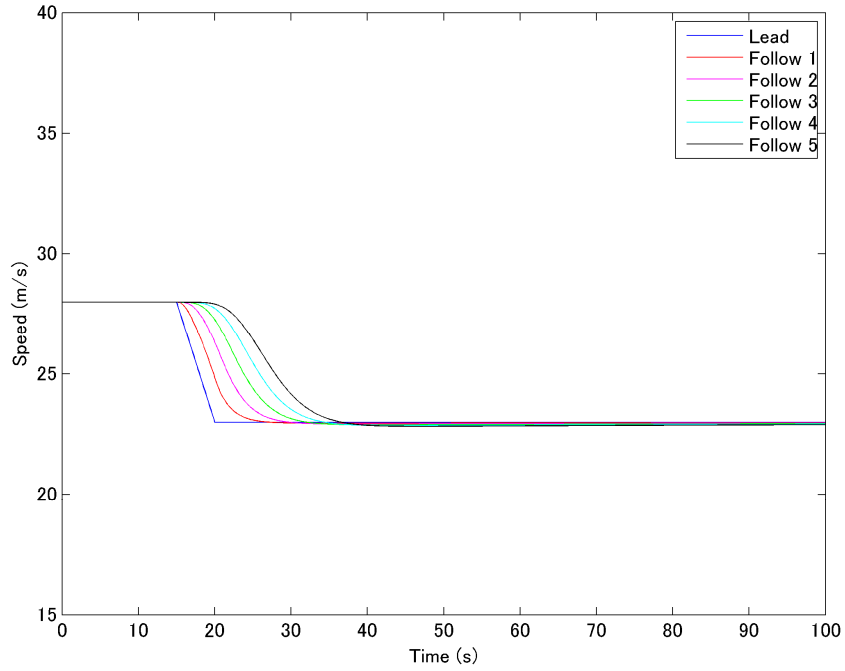


Figure 6.1.2 Dynamic performance of a human driver

The performance of ACC is also studied for the sag section in the simulation. The leading car behavior is type 1, the constant sag affected driver, where $\beta=1$:

$$a_1(t + \Delta t) = \begin{cases} 0 & t < t_s \\ -g[\sin \theta(t) - \sin \theta_u] & t \geq t_s \end{cases} \quad 22$$

The following cars are all the same ACC car (100% homogeneous ACC car platoon). 5-min traffic flow was generated to pass the sag section. All the other settings are the same as in chapter 5. The time space diagram is shown in Fig. 6.1.3, the time speed diagram is shown in Fig. 6.1.4 and the space speed diagram is shown in Fig. 6.1.5.

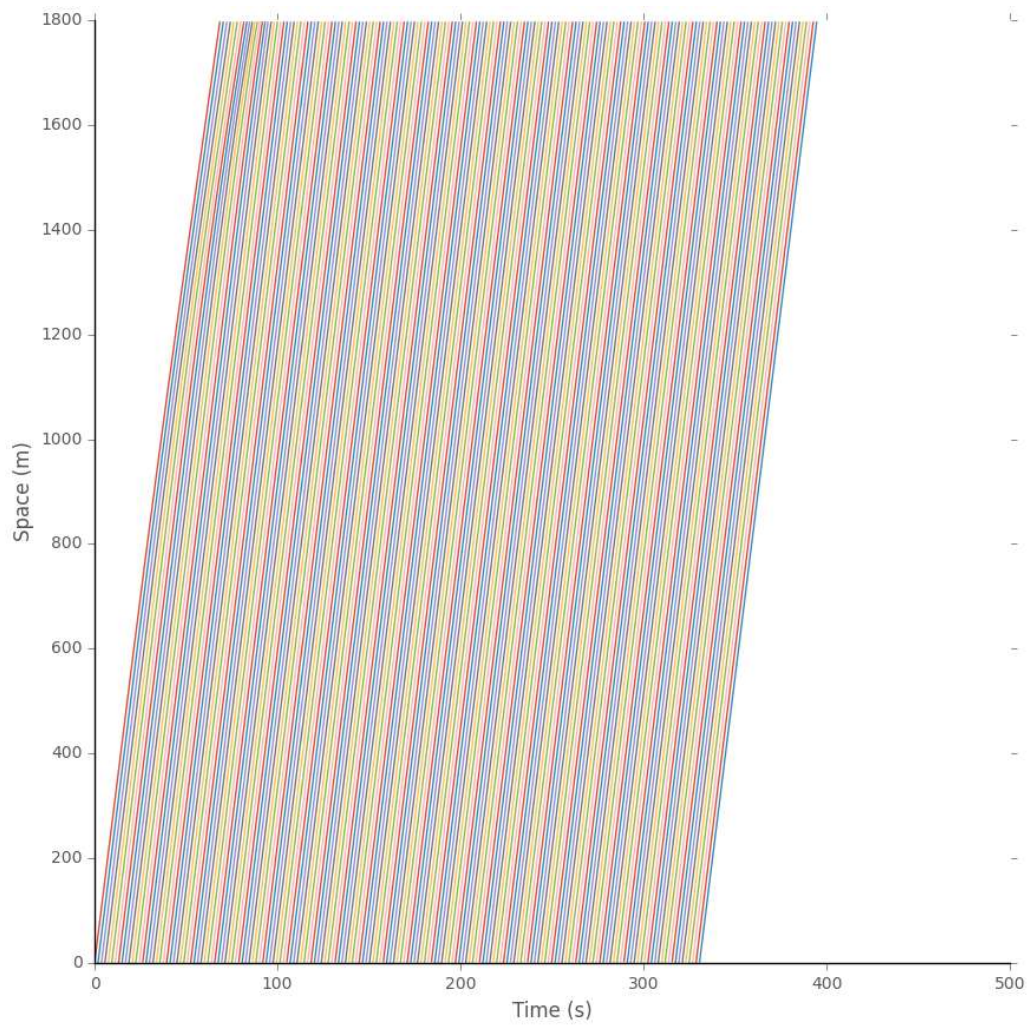


Figure 6.1.3 Time space diagram of ACC platoon

It can be observed that ACC cars absorb the perturbation slowly with little increase in perturbation. Also, the perturbation propagates upstream in both time speed diagram and space speed diagram. The front line of the severest speed reduction is gradually moving out of the sag section where initial perturbation occurs so that it can recover outside the bottleneck.

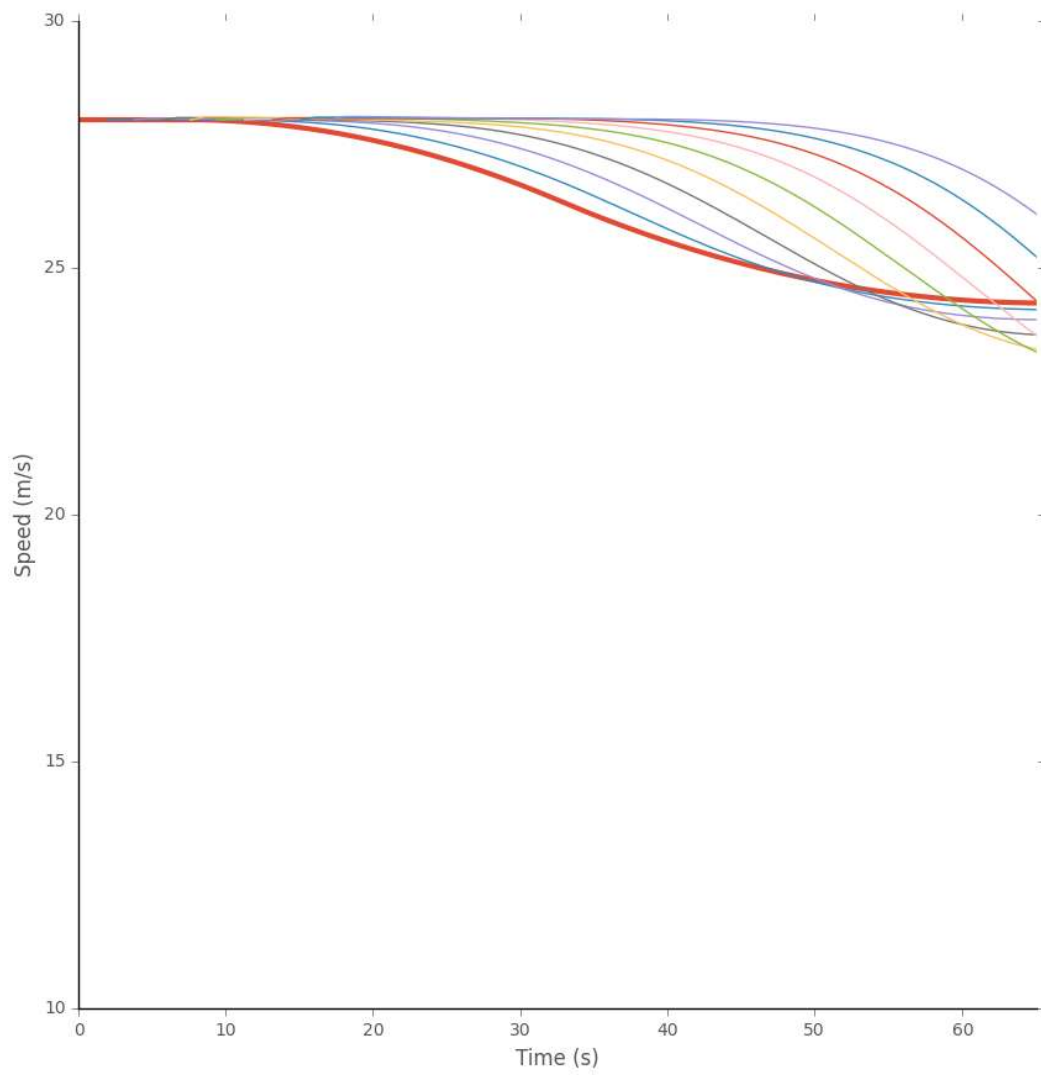


Figure 6.1.4 Time speed diagram of ACC platoon

It can be observed from Fig. 6.1.5 that speed reduction increase along the driving direction in the platoon.

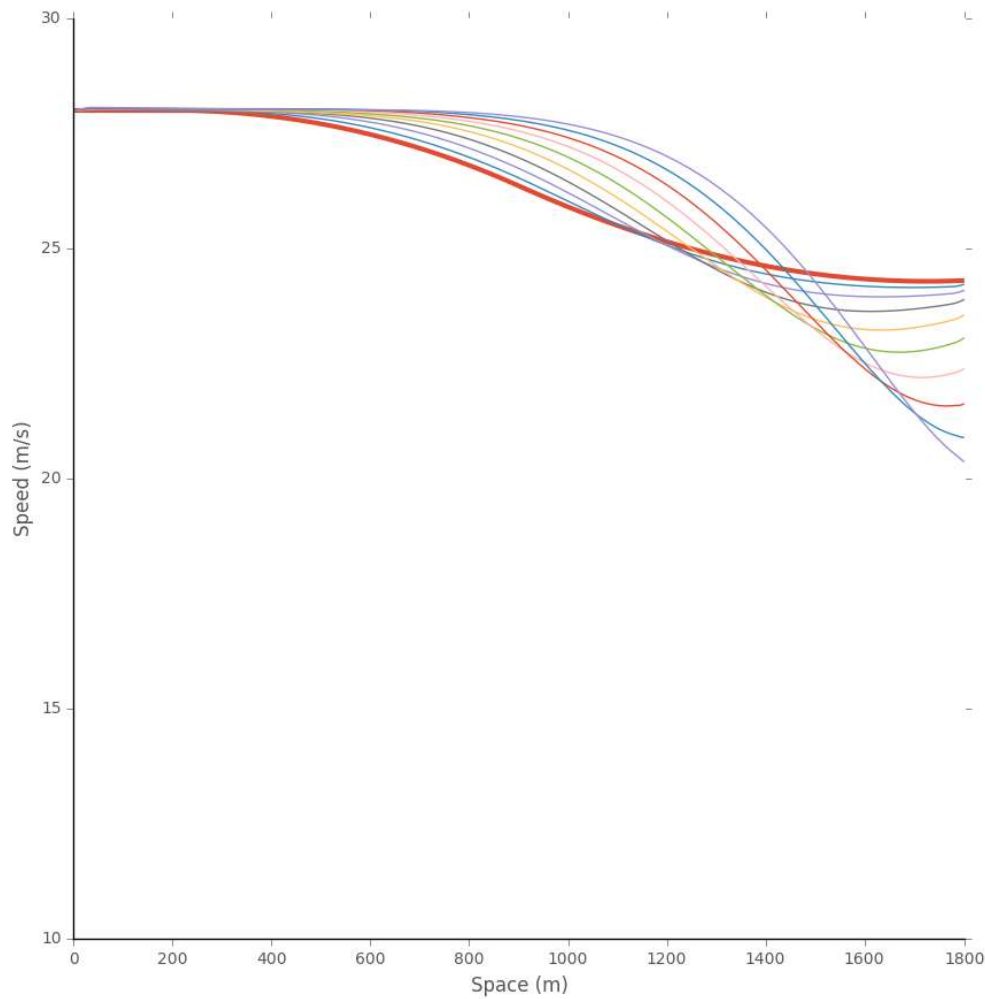


Figure 6.1.5 Space speed diagram of ACC platoon

With a very long reaction time of 4.4 seconds, the perturbation in platoon propagates upstream instead of conventionally propagates downstream. On the other hand, this long reaction time may cause drastic reaction during deceleration.

6.2 ACC system introduction to prevent congestion occurrence at sag section

In order to further study the impact of ACC in actual traffic flow, 5-min traffic demand is generated with estimated car-following parameters and a part of them is randomly replaced with the parameters of ACC systems. 1000 time simulation with different random seed is carried out for the ACC replacement rate of 25%, 50% and 75%. Figure 6.2.1 shows the congestion occurrence probability under different traffic demands with certain ACC penetration rate.

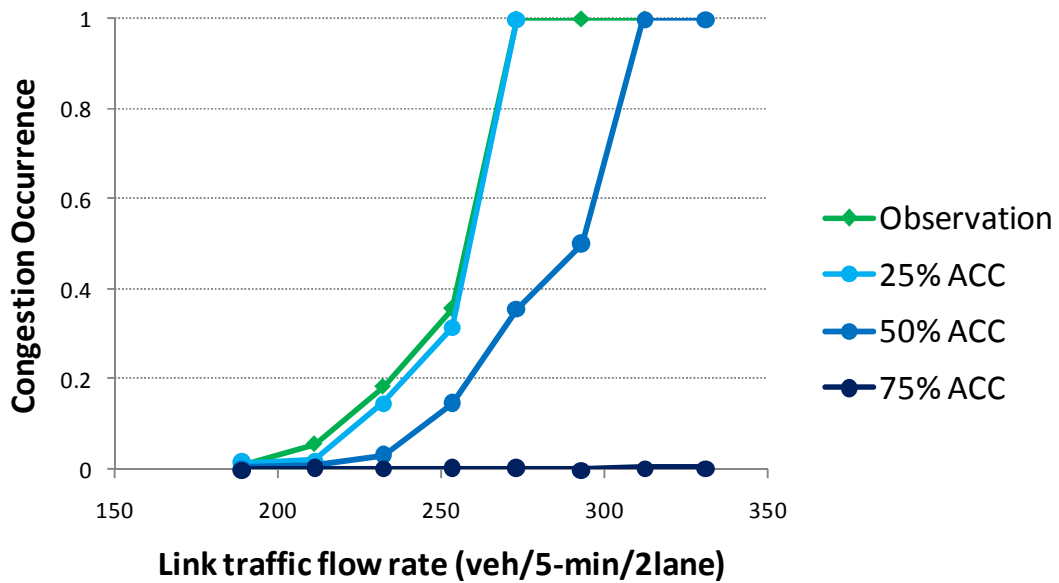


Figure 6.2.1 Congestion occurrence probability with different ACC penetration rate (1)

It can be observed that 25% ACC penetration rate makes small difference to congestion occurrence, which means a low ACC penetration rate has little contribution to congestion prevention. 50% ACC penetration is effective in reduce congestion occurrence. Figure 6.2.2 is a transformation of Figure 6.2.1. On which it can be observed that replacing 50% of human driving vehicles randomly with ACC system reduces 50% of congestion occurrence probability under moderate to high traffic demand. Replacing 75% of vehicles with ACC stabilize the flow and reduce the congestion occurrence to almost zero. Note that the headway of 100% ACC cars is $1.7+5/v_i$, which is 1.88s with the initial speed of 100km/h. The corresponding flow rate is 246 veh/5-min/2lane, where the congestion occurrence probability in simulation with estimated car-following behavior is lower than 40% (See Fig. 6.2.1).

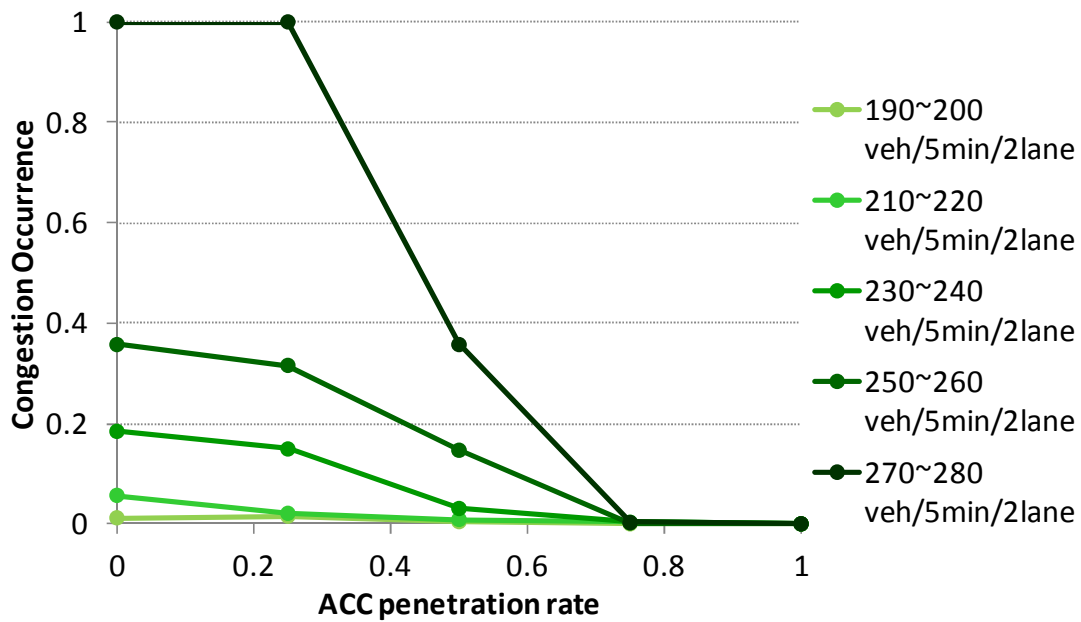


Figure 6.2.2 Congestion occurrence probability with different ACC penetration rate (2)

Another way of ACC introduction which is intentionally introduce ACC system to replace a part of drivers in the three kinds of drivers is also studied in simulation. Note that while the random introduction of ACC system simply replace a certain percentage of human driver car-following behavior, the intentional introduction of ACC replace a certain percentage of human driver car-following behavior in a certain drivers kind while keep the other two kinds of drivers' parameters unchanged, which means the total number of intentional introduction of ACC is always smaller than that of random ACC introduction.

Random introduction of 25% ACC cars in traffic flow has little influence in congestion occurrence. But intentional introduction of 25% ACC cars in negligent and nimble drivers increases the congestion occurrence probability (See Fig. 6.2.3). Especially when the traffic demand is relatively high, the congestion occurrence probability increases more obviously. This may because that the relatively small desired spacing of ACC cars may increase the probability of perturbation amplification when they happen to replace the drivers with bigger desired spacing.

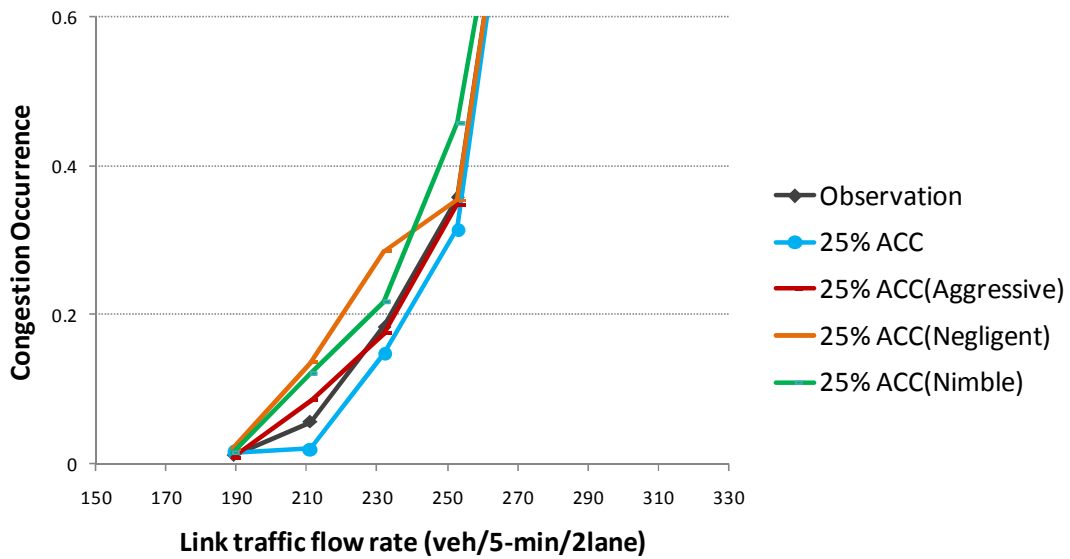


Figure 6.2.3 Congestion occurrence probability of intentional introduction of ACC system (25%)
 Intentional introduction of 50% ACC cars in aggressive and negligent drivers reduce the congestion occurrence probability obviously when traffic demand is high (around 250 veh/h), while the introduction in nimble drivers increases the congestion occurrence probability (See Fig. 6.2.4).

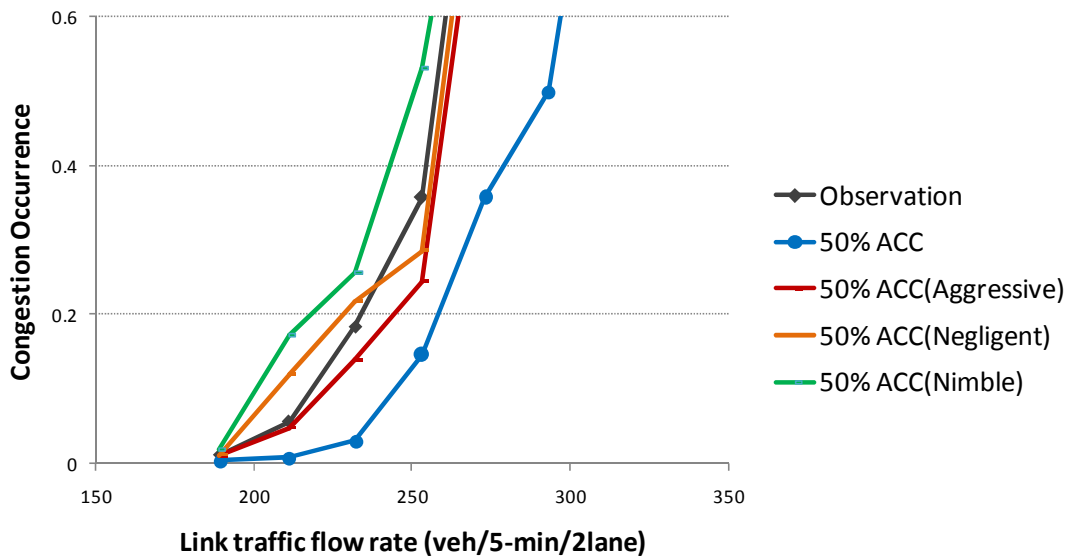


Figure 6.2.4 Congestion occurrence probability of intentional introduction of ACC system (50%)
 Intentional introduction of 75% ACC cars in aggressive drivers reduces congestion occurrence probability, especially when traffic demand is high the probability is reduced to half. Intentional introduction of 75% ACC cars in negligent drivers reduce congestion occurrence probability when traffic demand is relatively high. Intentional introduction of 75% ACC cars in nimble driver reduces congestion occurrence probability when traffic demand is low, but makes no difference when traffic

demand is high.

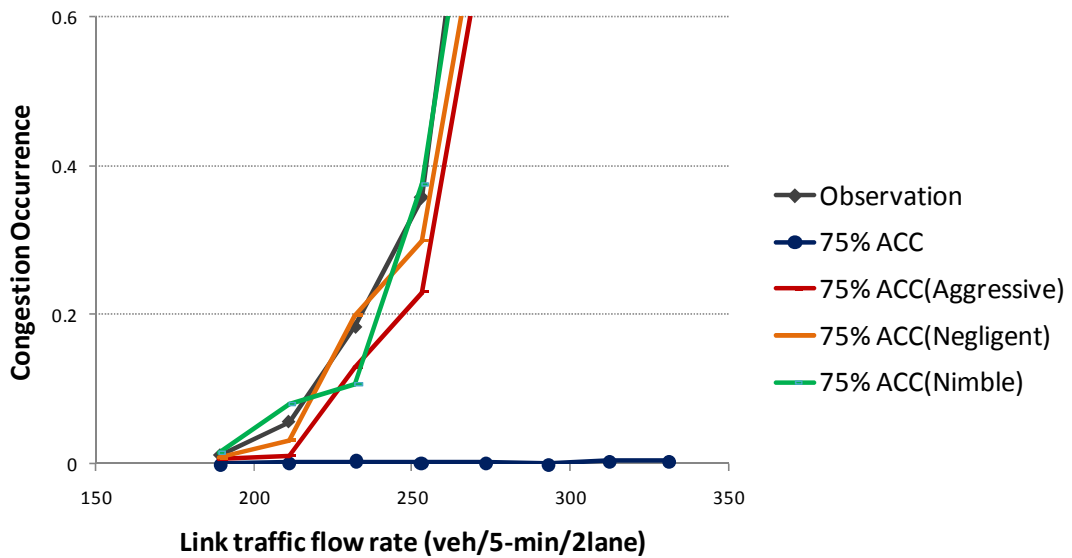


Figure 6.2.5 Congestion occurrence probability of intentional introduction of ACC system (75%)

The tendency of congestion occurrence probability reduction grows when traffic demand grows is more obvious in intentional introduction of 100% ACC cars in aggressive drivers. This can be also observed in intentional introduction of 100% ACC cars in negligent drivers. But even all the nimble drivers are replaced with ACC cars, the congestion occurrence probability does not change when traffic demand is high.

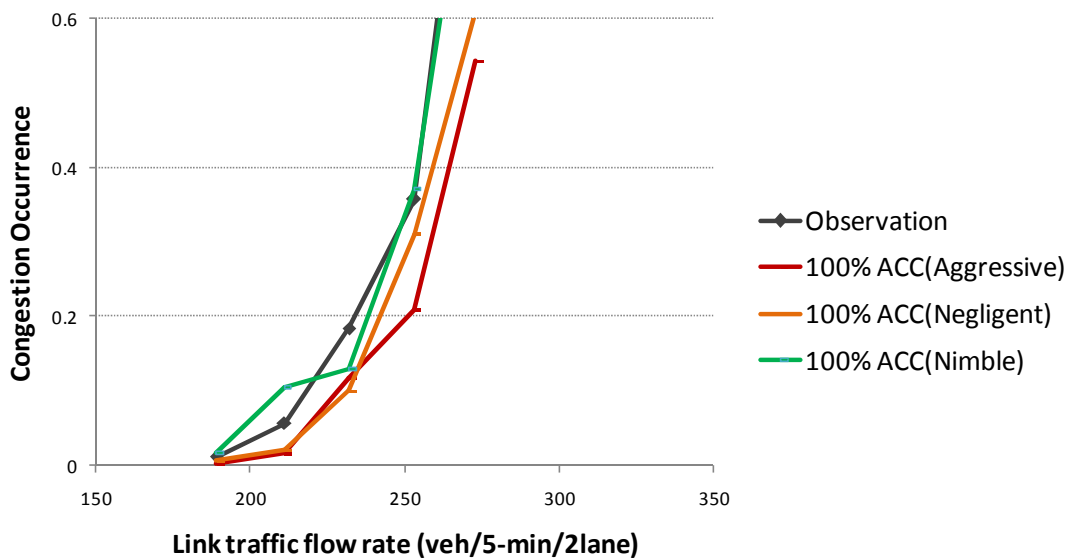


Figure 6.2.6 Congestion occurrence probability of intentional introduction of ACC system (100%)

Random introduction of ACC system with a penetration rate higher than 50% can obviously reduce congestion occurrence probability at sag section. When more than 75% drivers use ACC system at

sag section, the congestion caused by vertical slope effect in car-following behavior can be eliminated. Intentional introduction of ACC system in aggressive and negligent drivers can reduce congestion occurrence probability while intentional introduction of ACC system in nimble drivers shows little effect.

Apart from the possible potential relationship between parameter values in estimated car-following behavior, it should also be noted that the randomness in simulation as well as the changing of the composition of different drivers in traffic flow may also be the cause of small fluctuation in congestion occurrence rate when traffic demand is low.

7 Conclusion and future work

This research presents a simulation study of probabilistic congestion occurrence at expressway basic segment bottlenecks well known as sag section in Japan with individual variations in car-following behavior obtained from an actual sag section. A sag section is a road segment on an expressway in which the vertical slope increases at a small but constant rate. Through many previous researches, it is found impossible to predict congestion directly from detector data because the only observable flow condition changes happen right at the time congestion occurs. The propagation of unnoticed deceleration due to the vertical slope increase has long been researched as the cause of congestion. Perturbation amplifies in dense vehicle platoon consisted with drivers of varying car-following behavior. In this research, a car-following behavior model considering both the intra-driver variations and inter-driver variations is utilized and calibrated with field observation data. The variations are described with parameter distribution of car-following model. A simulation to reproduce traffic condition with the estimated parameters is thus proposed and validated in order to predict the probability of congestion occurrence at basic segment bottlenecks as well as test possible countermeasures to prevent and alleviate bottleneck congestion.

Two datasets containing all together 875 trajectories during congestion formation at the tomei yamato sag section are used in car-following behavior modeling. Trajectories of independent vehicles which do not react to the driving behavior of preceding vehicle and vehicles already involved in congestion are excluded from analysis. A car-following model considering both the intra-driver variations and inter-driver variations is utilized. The car-following model is based on a classic simple linear model which is found to be suitable for describing driving behavior during congestion formation at sag section. It is consisted of speed difference and spacing difference to its desired spacing with a time lag as well as an unnoticed deceleration caused by the vertical grade change at sag section. The intra-driver variations are described with a sag section part in car-following model to reflect the unnoticed deceleration caused by vertical slope. The inter-driver variations are described by different car-following parameter values for every individual driver. The combination of direct estimation of observable parameters and heuristic search method for unobservable parameters are present for obtaining well-fitted and reasonable car-following model parameters distribution. Apart from the objective function of relative spacing error, performance indicators of the root mean square error of spacing, speed and acceleration are also examined to ensure the performance of estimated parameter values. The relationships between different parameters are studied and no cross correlations excepted for the two parameters to determine desired speed are found.

A simulation platform which describes individual trajectory reflecting the variations in the distributed parameter values is proposed. The platform is designed to reproduce the probabilistic nature of traffic congestion occurrence at a bottleneck of sag section including the effect of vertical slope increase. It was carefully validated with different initial settings to make sure its capability of accurately reproducing the real condition. It provides a platform for analyze how different key components of the driving behavior, leading car behavior affecting the probability of congestion occurrence as well as a tool to quantify the effect of countermeasure like Adaptive Cruise Control (ACC) system. An interactive user interface was made to visualize the congestion formation progress. It reproduces congestion occurrence by changing the order of vehicles within the same platoon, which will help us to analyze the parameters of vehicles tending to cause congestion. It enables us to study the range of car-following parameters that causes propagation and amplification of speed reduction. Three kinds of drivers are observed in simulation: aggressive, negligent and nimble drivers. Collision and sudden stop occurs in 5-min platoon of aggressive drivers. Congestions occur in 5-min traffic flow consisted with negligent drivers, while no congestion occurs in 5-min traffic flow consisted with nimble drivers at sag section. It successfully reproduces the tendency that the congestion occurrence probability grows with traffic demand. A higher traffic demand will cause higher probability of congestion occurrence at sag section, which is the same in reality. Congestion occurrence probability is higher in simulation with parameter values generated from distribution than in simulation with actual estimated value.

The effect of introducing ACC system was also studied in simulation platform. Apart from the ACC penetration rate, two different ACC introduction schemes of 1) Random introduction and 2) Intentional introduction by replacing vehicles with certain features, e.g. negligent drivers and nimble drivers, is simulated and compared. Random introduction of ACC system with a penetration rate higher than 50% can obviously reduce congestion occurrence probability at sag section. When more than 75% drivers use ACC system at sag section, the congestion caused by vertical slope effect in car-following behavior can be eliminated. Intentional introduction of ACC system in aggressive and negligent drivers can reduce congestion occurrence probability while intentional introduction of ACC system in nimble drivers shows little effect.

There are some issues remain for future study. Two major issues among them are the potential relationship with parameters in distribution and the estimation of composition of drivers at sag section. For the first one, parameters distribution of different types of drivers can be estimated and compared with the overall parameter distribution. Simulations can also be carried out. For the second one, simulations can be carried out with different composition of drivers and results compared with the result obtained from all the parameters to determine the most realistic composition of drivers in real traffic flow.

More schemes can be tested for both random introduction and intentional introduction of ACC system. Especially for the intentional introduction, schemes with penetration in two kinds drivers at the same time can be tested, like 50% penetration rate in aggressive drivers and 50% penetration rate in negligent drivers at the same time.

Acknowledgement

The author wish to express her sincere gratitude for providing precious data by several researchers and institutes. Vehicle trajectory data extracted and processed by multiple video cameras are kindly offered by Professor Hirokazu Akahane of Chiba Institute of Technology. The vehicle trajectory data used for model validation are provided through the collaborative research activity between Professor Takashi Oguchi (supervisor) of the University of Tokyo and Intelligent Transport System Division of National Institute for Land and Infrastructure Management (lead by Mr. Hiroshi Makino). The source of road geometry data of expressways is based on the collaborative research activity between Professor Oguchi and former Japan Highway Research Institute of Japan Highway Public Corporation (dissolved in 2005).

I can never thank my supervisor Prof. Oguchi enough for his kind and patient guide on my research. I appreciate Prof. Iryo and Prof. Wada for their kind help and advice on my research. This research will never be like this without their advice. I thank all the staff in my lab and all the OBs and OGs who helped to make our lab a great working space. Without the nice working condition and fast computers I cannot spend nights running simulation and preparing for presentation.

I thank my university and the MEXT for providing me a scholarship to support my life here so that I can concentrate on my research. I thank all the staff in my department, my university and Ochanomizu University for providing my dorm room and constantly supporting my life in this three years.

I thank my dearest friends and lab mates. Mrs. Yasuko Sagara, you are the best friend I can ever imagine. Sandy, we've had so much nice talks. You've always been the greatest and kindest friend. I thank the precious companionship offered by my dear lab mates. My other friends who have been with me along this way and heading to new directions, thank you for the joys and fun we had together. I wish you all the best and I'm looking forward to seeing you again soon.

This work will not exist without my parents' constant support and encouragement for me to explore this world on my own. Thank you for being proud of me.

No human can live in this world without the kindness of others. There certainly are names I forgot to mention and kindness I haven't thanked. Please let me hereby thank you all for helping to build a part of my life. Words can never express how thankful I am for the kindness I have received during this time.

References

- Bando, M., Hasebe, K., Nakanishi, K., Nakayama, A., Shibata, A., & Sugiyama, Y. (1995). Phenomenological study of dynamical model of traffic flow. *Journal de Physique I*, 5(11), 1389-1399.
- Banks, J. H. (1990). Flow processes at a freeway bottleneck. *Transportation Research Record*(1287).
- Brackstone, M., & McDonald, M. (1999). Car-following: a historical review. *Transportation Research Part F: Traffic Psychology and Behaviour*, 2(4), 181-196.
- Brackstone, M., & Waterson, B. (2009). Determinants of following headway in congested traffic. *Transportation Research Part F*, 131-142.
- Chandler, R. E., Herman, R., & Montroll, E. W. (1958). Traffic dynamics: studies in car following. *Operations research*, 6(2), 165-184.
- Department for Transport and Driver and Vehicle Standards Agency, U. (2007). *The Highway Code*.
- Gazis, D. C., Herman, R., & Rothery, R. W. (1961). Nonlinear follow-the-leader models of traffic flow. *Operations research*, 9(4), 545-567.
- Gipps, P. G. (1981). A behavioural car-following model for computer simulation. *Transportation Research Part B: Methodological*, 15(2), 105-111.
- Goñi Ros, B., Knoop, V. L., van Arem, B., & Hoogendoorn, S. P. (2012). Reducing congestion at uphill freeway sections by means of a Gradient Compensation System. *Intelligent Vehicles Symposium (IV), 2012 IEEE*, (pp. 191-198).
- Helly, W. (1959). Simulation of bottlenecks in single lane traffic flow. *International Symposium on the Theory of Traffic Flow*.
- Hoogendoorn, S. (2008). *Calibrating car-following models using microscopic trajectory data*.
- Hoogendoorn, S. P., & Ossens, S. (2006). Empirical Analysis of Two-Leader Car-Following Behavior *. *European Journal of Transport and Infrastructure Research*, 6(3), 229-246.
- Kesting, A., & Treiber, M. (2008). Calibrating Car-Following Models using Trajectory Data: Methodological Study. *Transportation Research Record*, 2088(6), 148-156.
- Kesting, A., Treiber, M., & Helbing, D. (2010). Enhanced intelligent driver model to access the impact of driving strategies on traffic capacity. *Philosophical Transactions of the Royal Society of London A: Mathematical, Physical and Engineering Sciences*, 368(1928), 4585-4605.
- Kesting, A., Treiber, M., Schönhof, M., & Helbing, D. (2008). Adaptive cruise control design for active congestion avoidance. *Transportation Research Part C: Emerging Technologies*, 16(6), 668-683.
- Kometani, E., & Sasaki, T. (1961). Dynamic behaviour of traffic with a non-linear spacing-speed relationship. *Theory of TRAFFIC FLOW, PROCEEDINGS*, 105-119.

- Koshi, M., Kuwahara, M., & Akahane, H. (1992). Capacity of Sags and Tunnels on Japanese Motorways. *i* (May), 17-22.
- Muto, N., & Akahane, H. An Analysis of Bottleneck Phenomena at a Sag Based on Precision Observations of Vehicle Trajectories. *IP conference*, 40.
- National Institute for Land and Infrastructure Management. (n.d.). *Research on traffic smoothing in expressway sag sections through road-to-vehicle cooperation*. Retrieved 8 12, 2015, from National Institute for Land and Infrastructure Management: http://www.nilim.go.jp/lab/qcg/japanese/0frame/index_c.htm
- Newell, & Frank, G. (2002). A simplified car-following theory: a lower order model. *Transportation Research Part B: Methodological*, 195-205.
- Oguchi, T., & Konuma, R. (2009). Comparative study of car-following models for describing breakdown phenomena at sags. *Proceedings of the 19th ITS World Congress, Stockholm, Sweden*.
- Ossen, S., & Hoogendoorn, S. (2005). Car-Following Behavior Analysis from Microscopic Trajectory Data. *Transportation Research Record*, 1934(1), 13-21.
- Pasanen, E., & Salmivaara, H. (1993). Driving speeds and pedestrian safety in the city of Helsinki. *Traffic Engineering and Control*, 308-310.
- Patire, A. D., & Cassidy, M. J. (2011). Lane changing patterns of bane and benefit: Observations of an uphill expressway. *Transportation research part B: methodological*, 45(4), 656-666.
- Rubinstein, R. (1999). The cross-entropy method for combinatorial and continuous optimization. *Methodology and computing in applied probability*, 1(2), 127-190.
- TRB. (2000). *Highway Capacity Manual*. Washington, D.C.
- Treiber, M., & Kesting, A. (2012). *Traffic Flow Dynamics: Data, Models and Simulation*. Springer Science & Business Media.
- Vahidi, A., & Eskandarian, A. (2003). Research advances in intelligent collision avoidance and adaptive cruise control. *Intelligent Transportation Systems, IEEE Transactions on*, 4(3), 143-153.
- Vogel, K. (2002). What characterizes a "free vehicle" in an urban area? *Transportation Research Part F*, 15-29.
- Xing Jian、越正毅. (1996). 高速道路のサグにおける渋滞現象と車両追従挙動の研究. *土木学会論文集*, 45-55.
- Xing, J., Tsuru, M., Ishida, T., & Muramatsu, E. (2010). An Analysis of the Characteristics of Vehicle Platoons Resulting in the Occurrence of Traffic Congestion on Expressways. *42th Infrastructure Planning Conference*.
- Yoshida, Y., Koshi, M., & Yasui, K. (1997). Effectiveness of adaptive cruise control for increasing sag capacities. *Proceedings of Infrastructure Planning*, 307-310.
- Yoshizawa, R., Shiomi, Y., Uno, N., Iida, K., & Yamaguchi, M. (2012). Analysis of car-following behavior on sag and curve sections at intercity expressways with driving simulator. *International Journal of Intelligent Transportation Systems Research*, 10(2), 56-65.
- 大口敬. (1995). 高速道路サグにおける渋滞の発生と道路線形との関係. *土木学会論文集*,

69-78.

大口敬. (2000). 高速道路単路部渋滞発生解析-追従挙動モデルの整理と今後の展望. 土木学会論文集, 39-51.

大口敬、片倉正彦、鹿田成則. (2001). 高速道路単路部をボトルネックとする渋滞発生特性に関する実証的研究. *高速道路と自動車*, Vol44.

福島賢一、Xing Jian、瀬戸稔和、佐藤久長. (2008). 潜在的ボトルネック交通容量の推定及び交通容量の確率分布を用いた年間の渋滞予測検討. *土木計画学研究・講演集*.

洪性俊. (2008). *高速道路における交通性能評価手法の開発*. 首都大学東京.

渋谷公佑、大口敬、洪性俊. (2013). ACC 車両の追従挙動に対する追従挙動モデルの比較分析. *土木計画学研究・講演集*.

尾崎晴男. (2003). 交通流 高速道路における自動車交通流のあい路現象. *日本流体力学会誌「ながれ」*, 123-129.

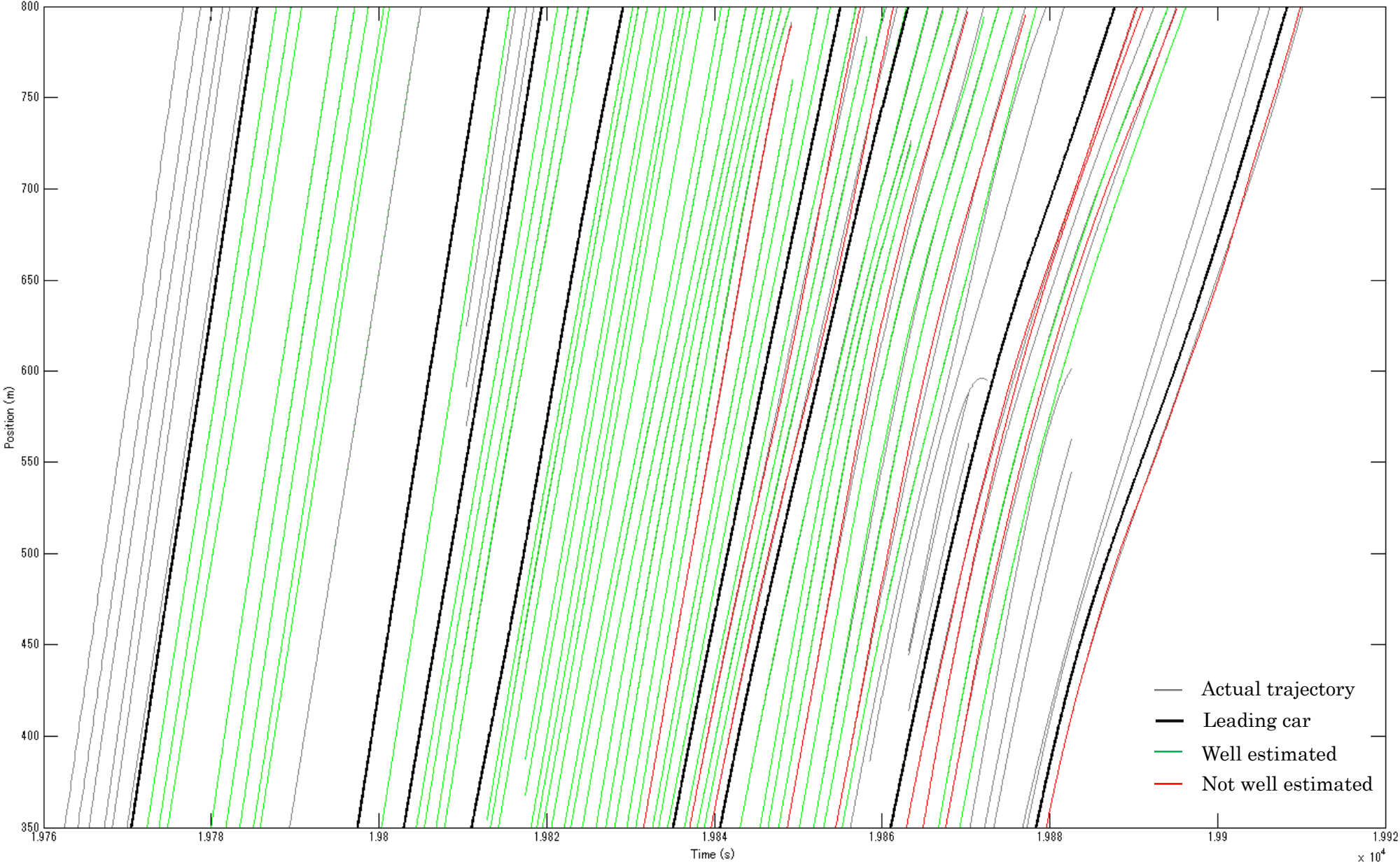
越正毅. (1986). 高速道路のボトルネック容量. *土木学会論文集*, 1-7.

越正毅、桑原雅夫、赤羽弘和. (1993). 高速道路のトンネル、サグにおける渋滞現象に関する研究. *Japan Society of Civil Engineers*, 65-71.

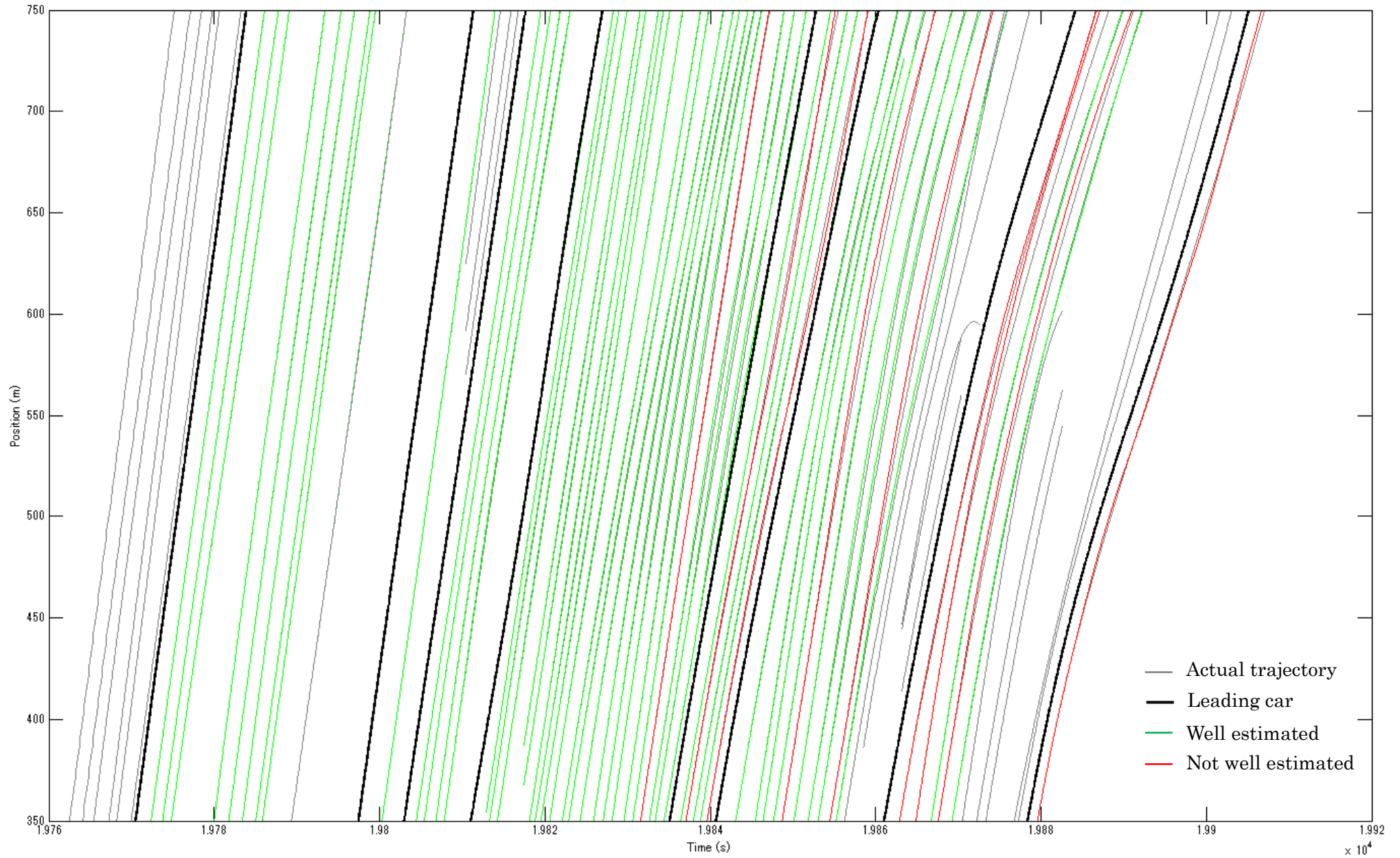
Appendix 1

Initial and estimated trajectories of dataset 1

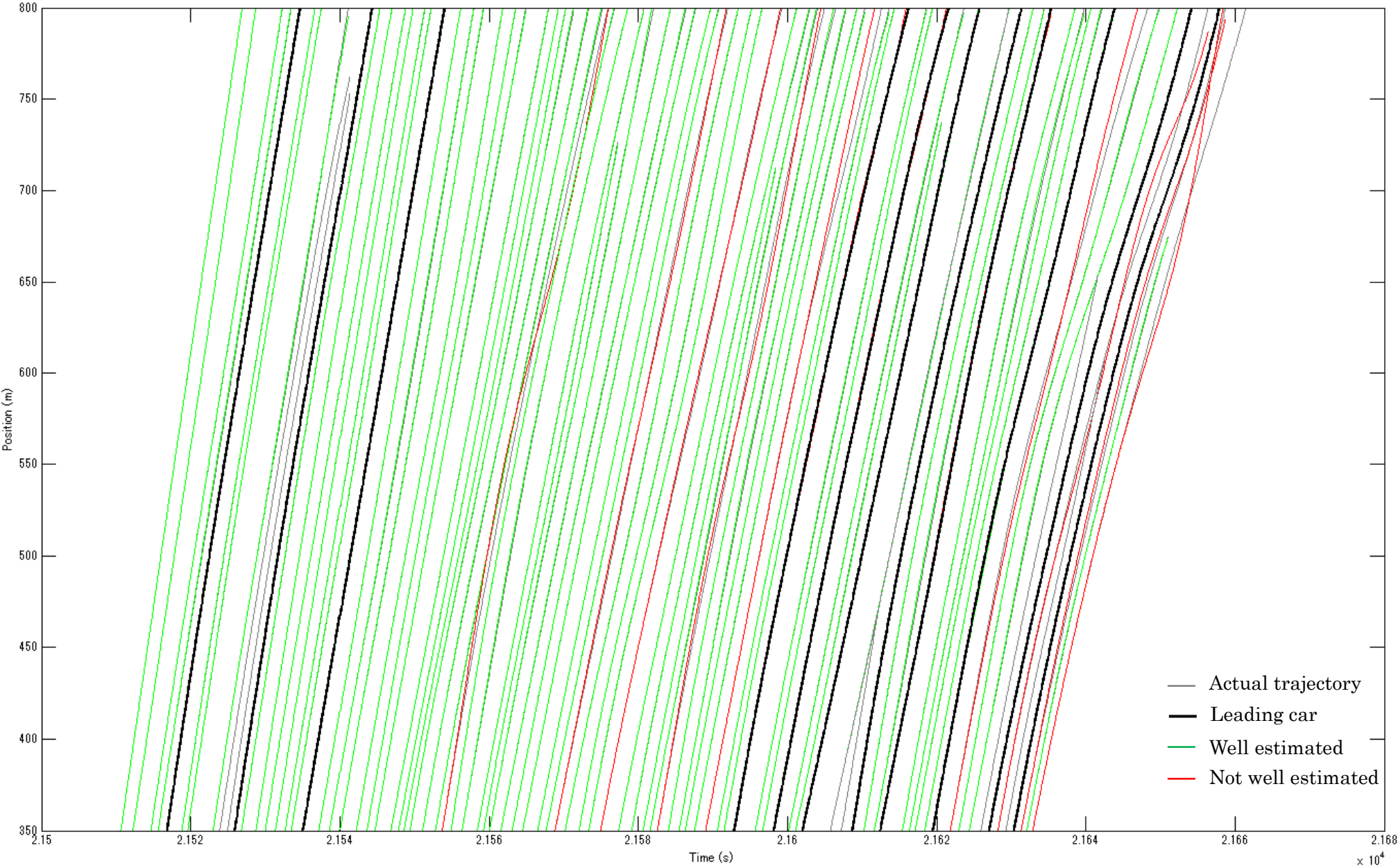
Observation and estimation of dataset1 at Jul. 15, 2006 (Error not accumulated)



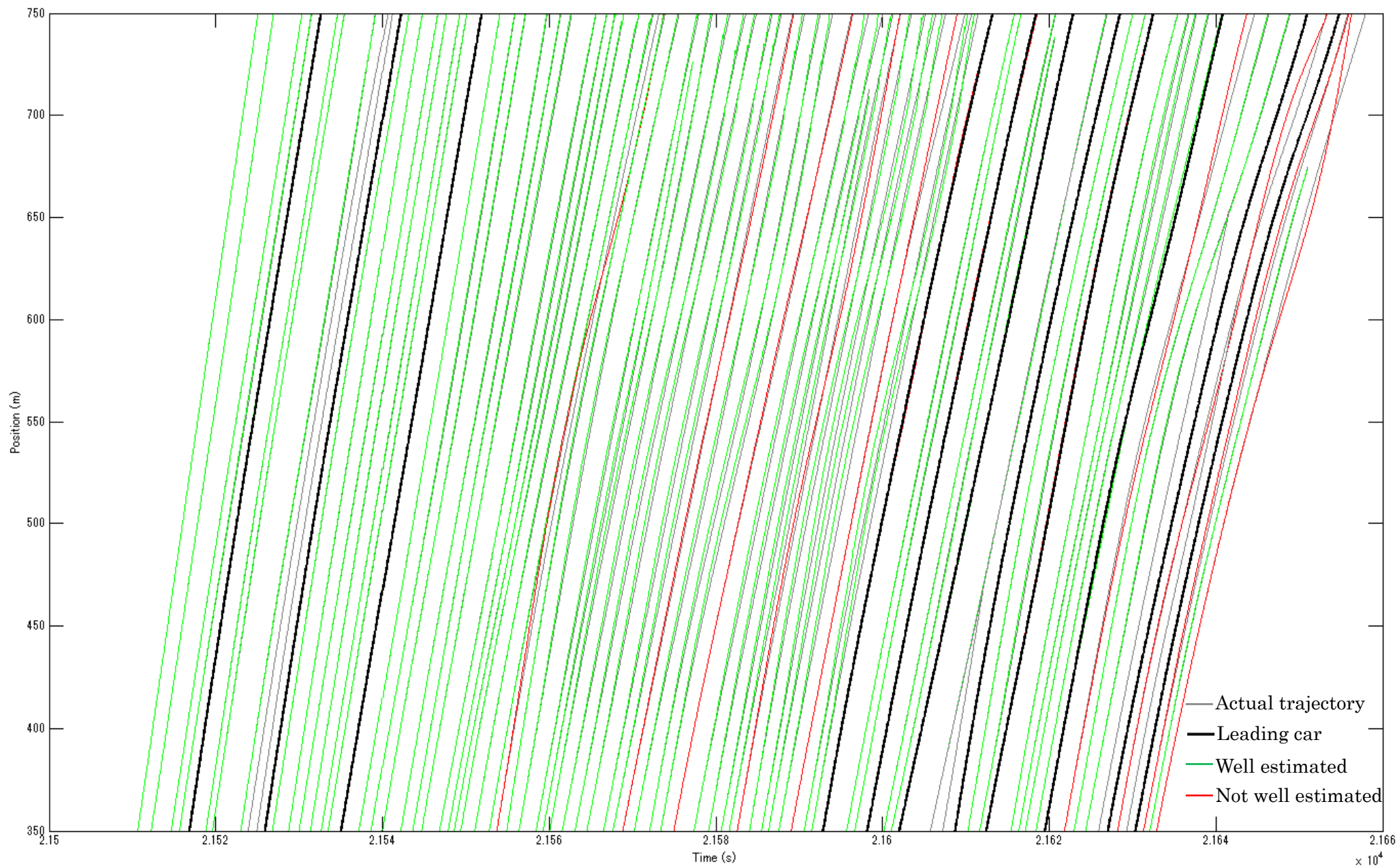
Observation and estimation of dataset1 at Jul. 15, 2006 (Error accumulated)



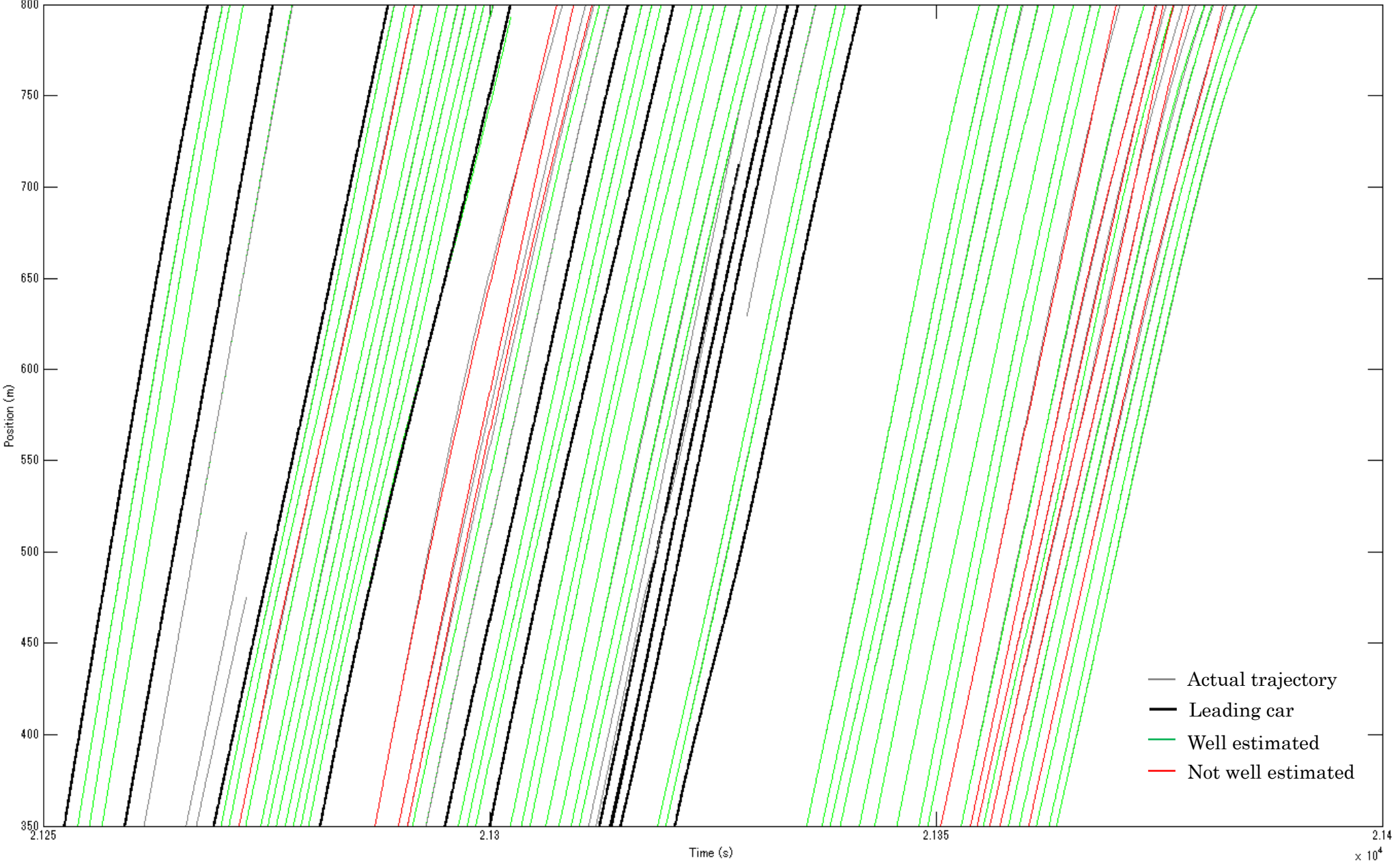
Observation and estimation of dataset1 at Jul. 22, 2006 (Error not accumulated)



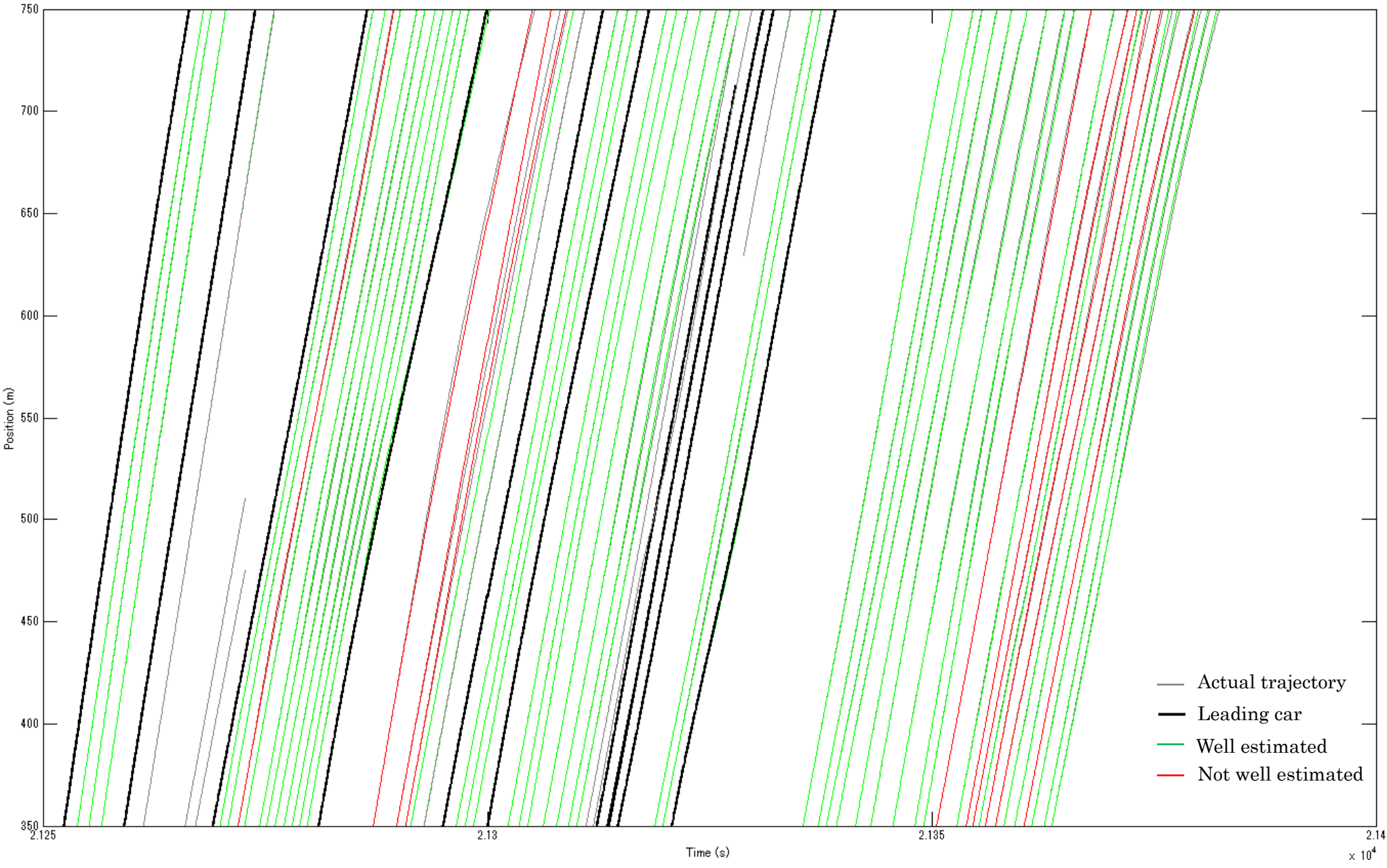
Observation and estimation of dataset1 at Jul. 22, 2006 (Error accumulated)



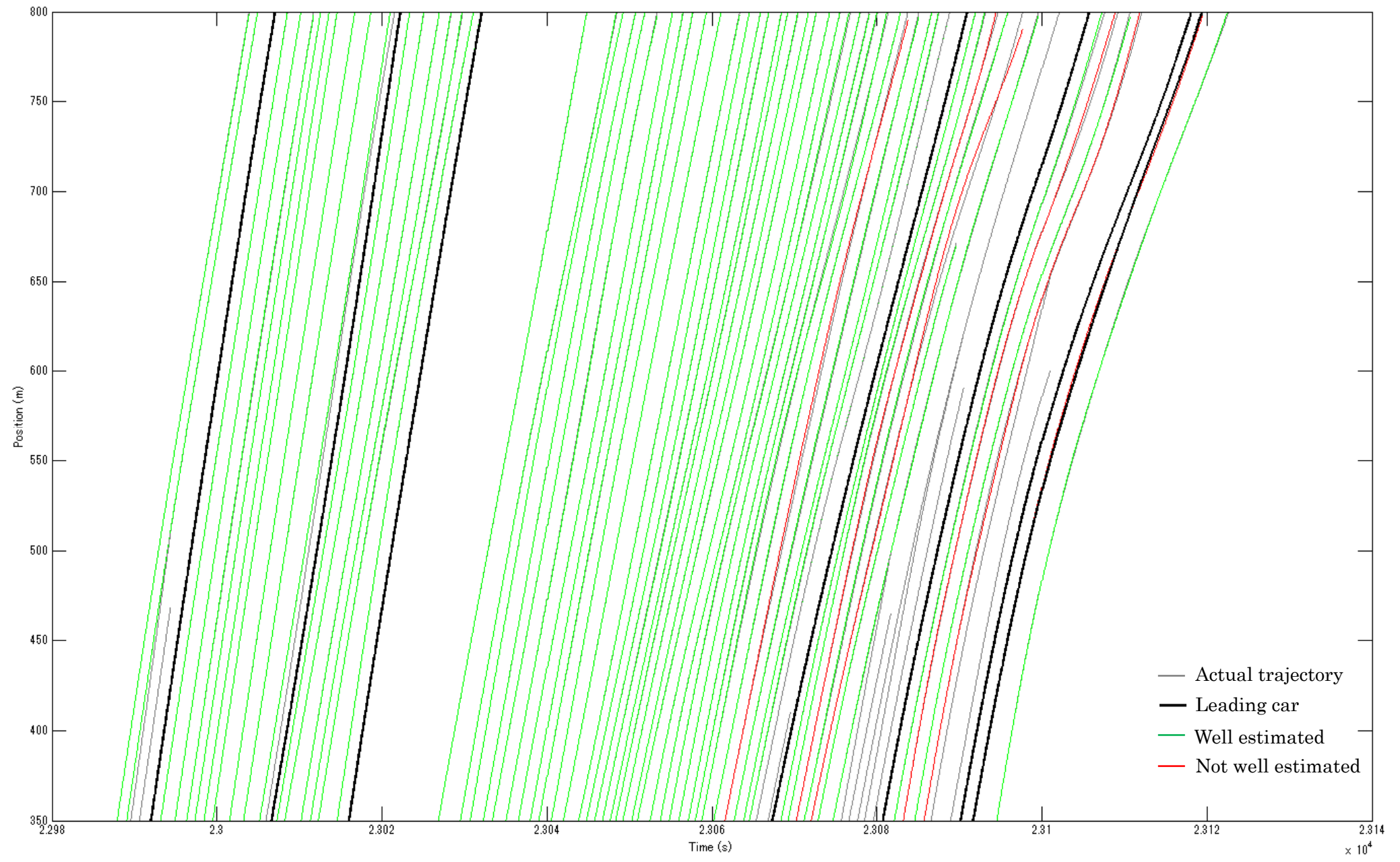
Observation and estimation of dataset1 at Jul. 29, 2006 (Error not accumulated)



Observation and estimation of dataset1 at Jul. 29, 2006 (Error accumulated)



Observation and estimation of dataset1 at Aug. 4, 2006 (Error not accumulated)



Observation and estimation of dataset1 at Aug. 4, 2006 (Error accumulated)

